

# FrontISTR Tutorial Guide

FrontISTR Commons

October 5, 2020

## Contents

<b>1</b>	<b>FrontISTR Tutorial Guide</b>	<b>2</b>
1.1	Manuals . . . . .	3
1.2	List of description on this manual . . . . .	3
1.3	Static Analysis (Elasticity) . . . . .	4
1.3.1	Analysis target . . . . .	4
1.3.2	Analysis contents . . . . .	4
1.3.3	Analysis results . . . . .	5
1.4	Static Analysis (Elasticity, Parallel) . . . . .	6
1.5	Static Analysis (Hyperelasticity, Part 1) . . . . .	6
1.5.1	Analysis target . . . . .	6
1.5.2	Analysis content . . . . .	7
1.5.3	Analysis results . . . . .	7
1.6	Static Analysis (Hyperelasticity, Part 2) . . . . .	8
1.6.1	Analysis target . . . . .	8
1.6.2	Analysis content . . . . .	9
1.6.3	Analysis results . . . . .	10
1.7	Static Analysis (Elastoplastic, Part 1) . . . . .	10
1.7.1	Analysis target . . . . .	10
1.7.2	Analysis content . . . . .	11
1.7.3	Analysis results . . . . .	11
1.8	Static Analysis (Elastoplastic, Part 2) . . . . .	12
1.8.1	Analysis target . . . . .	12
1.8.2	Analysis content . . . . .	13
1.8.3	Analysis results . . . . .	14
1.9	Static Analysis (Elastoplastic, Part 2) . . . . .	15
1.9.1	Analysis target . . . . .	15
1.9.2	Analysis content . . . . .	15
1.9.3	Analysis results . . . . .	16
1.10	Static Analysis (Viscoelasticity) . . . . .	17
1.10.1	Analysis target . . . . .	17
1.10.2	Analysis content . . . . .	17
1.10.3	Analysis results . . . . .	17
1.11	Static Analysis (Creep) . . . . .	18
1.11.1	Analysis target . . . . .	18
1.11.2	Analysis content . . . . .	18
1.11.3	Analysis results . . . . .	19
1.12	Contact Analysis (Part 1) . . . . .	20
1.12.1	Analysis target . . . . .	20
1.12.2	Analysis content . . . . .	20
1.12.3	Analysis results . . . . .	21
1.13	Contact Analysis (Part 2) . . . . .	21
1.13.1	Analysis target . . . . .	21
1.13.2	Analysis content . . . . .	22
1.13.3	Analysis results . . . . .	23
1.14	Contact Analysis (Part 3) . . . . .	24

1.14.1 Analysis target . . . . .	24
1.14.2 Analysis contents . . . . .	24
1.14.3 Analysis results . . . . .	24
1.15 Linear Dynamic Analysis . . . . .	25
1.15.1 Analysis target . . . . .	25
1.15.2 Analysis contents . . . . .	26
1.15.3 Analysis results . . . . .	27
1.16 Non-Linear Dynamic Analysis . . . . .	27
1.16.1 Analysis target . . . . .	27
1.16.2 Analysis content . . . . .	27
1.16.3 Analysis results . . . . .	28
1.17 Non-Linear Contact Dynamic Analysis . . . . .	29
1.17.1 Analysis target . . . . .	29
1.17.2 Analysis content . . . . .	30
1.17.3 Analysis Results . . . . .	31
1.18 Eigenvalue Analysis . . . . .	31
1.18.1 Analysis target . . . . .	31
1.18.2 Analysis content . . . . .	31
1.18.3 Analysis results . . . . .	32
1.19 Heat Conduction Analysis . . . . .	32
1.19.1 Analysis target . . . . .	32
1.19.2 Analysis content . . . . .	33
1.19.3 Analysis results . . . . .	34
1.20 Frequency Response Analysis . . . . .	34
1.20.1 Analysis target . . . . .	34
1.20.2 Analysis content . . . . .	35
1.20.3 Analysis results . . . . .	36
1.21 Verification by Simple-Shaped Model . . . . .	36
1.21.1 Elastic static analysis . . . . .	36
1.21.2 Non-linear static analysis . . . . .	42
1.21.3 Contact analysis (1) . . . . .	44
1.21.4 Contact analysis (2): Hertz contact problem . . . . .	45
1.21.5 (3) Eigenvalue analysis . . . . .	47
1.21.6 (4) Heat conduction analysis . . . . .	49
1.21.7 (5) Linear dynamic analysis . . . . .	53
1.21.8 (6) Frequency response analysis . . . . .	57
1.22 Actual Model Examples for Elastic Static Analysis . . . . .	59
1.22.1 Analysis Model . . . . .	59
1.22.2 Analysis results . . . . .	61
1.23 Actual Model Examples for Eigenvalue Analysis . . . . .	66
1.23.1 Analysis model . . . . .	66
1.23.2 Analysis Results . . . . .	67
1.24 Actual Model Examples for Heat Conduction Analysis . . . . .	70
1.24.1 Analysis model . . . . .	70
1.24.2 Analysis Results . . . . .	72
1.25 Actual Model Examples for Linear Dynamic Analysis . . . . .	73
1.25.1 Analysis model . . . . .	73
1.25.2 Analysis results . . . . .	74

## 1 FrontISTR Tutorial Guide

This software is the outcome of “Research and Development of Innovative Simulation Software” project supported by Research and Development for Next-generation Information Technology of Ministry of Education, Culture, Sports, Science and Technology. We assume that you agree with our license agreement of “MIT License” by using this software either for the purpose of profit-making business or for free of charge. This software is protected by the copyright law and the other related laws, regarding unspecified issues in our license agreement and contact, or condition without either license agreement or contact.



Item	Content
Name of Software	FrontISTR
Version	5.1
License	MIT License
Corresponding Clerks	FrontISTR Commons2-11-16 Yayoi, Bunkyo-ku, Tokyo/o Institute of Engineering Innovation, School of EngineeringE-mail support@frontistr.com

## 1.1 Manuals

- Introduction
- How to install
- Theory
- User's manual
- Tutorial
- FAQ

This manual describes the analysis implementation guidelines using a large-scale structural analysis program using the finite element method FrontISTR based on examples.

## 1.2 List of description on this manual

- PDF
- Tutorials:
  - Static Analysis (Elasticity)
  - Static Analysis (Elasticity, Parallel)
  - Static Analysis (Hyperelasticity Part 1)
  - Static Analysis (Hyperelasticity Part 2)
  - Static Analysis (Elastoplasticity Part 1)
  - Static Analysis (Elastoplasticity Part 2)
  - Static Analysis (Viscoelasticity)
  - Static Analysis (Creep)
  - Contact Analysis (Part 1)
  - Contact Analysis (Part 2)
  - Contact Analysis (Part 3)
  - Linear Dynamic Analysis
  - Nonlinear Dynamic Analysis
  - Nonlinear Contact Dynamic Analysis
  - Eigenvalue Analysis
  - Heat Conduction Analysis
  - Frequency Response Analysis
- Example Verification:
  - Verification by Simple Geometric Model
  - Example of Actual Model for Elastic Static Analysis
  - Example of Actual Model for Eigenvalue Analysis
  - Example of Actual Model for Heat Conduction Analysis
  - Example of Actual Model for Linear Dynamic Analysis

### 1.3 Static Analysis (Elasticity)

This analysis uses the data of tutorial /01\_elastic\_hinge.

#### 1.3.1 Analysis target

The target of this analysis is a hinge part whose shape and mesh data are shown in Figs. 4.1.1 and 4.1.2, respectively. The mesh is a tetrahedral secondary element with 49871 elements and 84056 nodes.

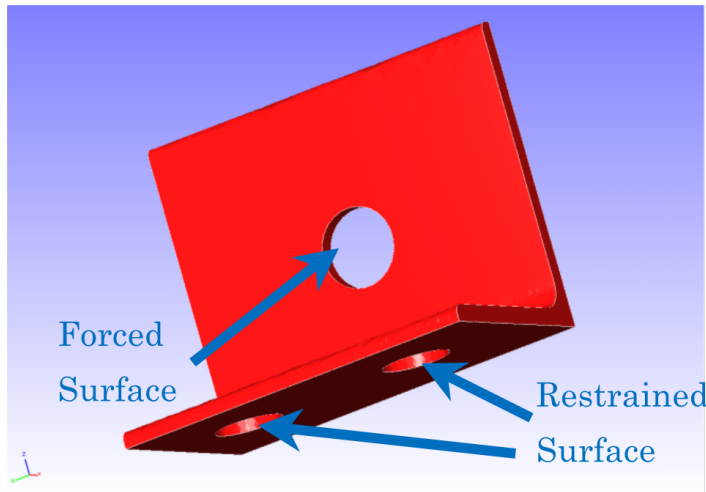


Fig. 4.1.1 : Shape of the hinge part

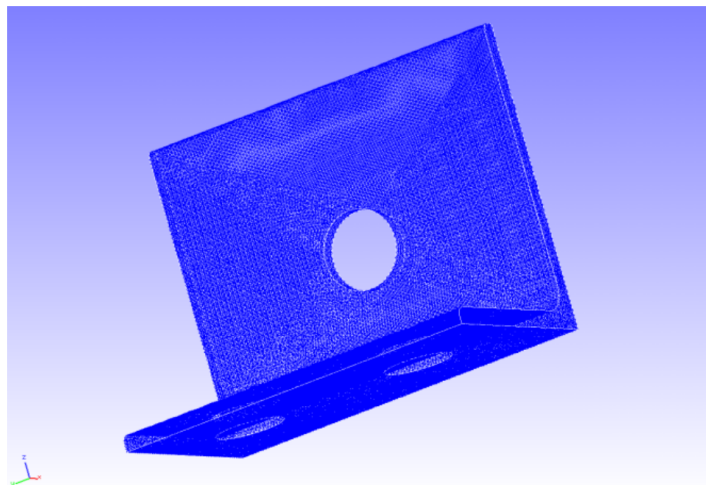


Fig. 4.1.2 : Mesh data of the hinge part

#### 1.3.2 Analysis contents

In this stress analysis, the displacement of the constrained surface shown in Fig. 4.1.1 is restrained, and a concentrated load is applied to the forced surface. The analysis control data are presented below.

```
# Control File for FISTR
## Analysis Control
!VERSION
      3
!SOLUTION, TYPE=STATIC
!WRITE,RESULT
!WRITE,VISUAL
## Solver Control
### Boundary Condition
!BOUNDARY
  BND0, 1, 3, 0.000000
```

```

!BOUNDARY
BND1, 1, 3, 0.000000
!CLOAD
CL0, 1, 1.000000
### Material
!MATERIAL, NAME=STEEL
!ELASTIC
210000.0, 0.3
!DENSITY
7.85e-6
### Solver Setting
!SOLVER,METHOD=CG,PRECOND=1,ITERLOG=YES,TIMELOG=YES
10000, 2
1.0e-8, 1.0, 0.0

```

### 1.3.3 Analysis results

The contour diagram of a Mises stress created with REVOCAP\_PrePost is shown in Fig. 4.1.3. Furthermore, a part of the log files of the analysis results is shown below as numerical data of the analysis.

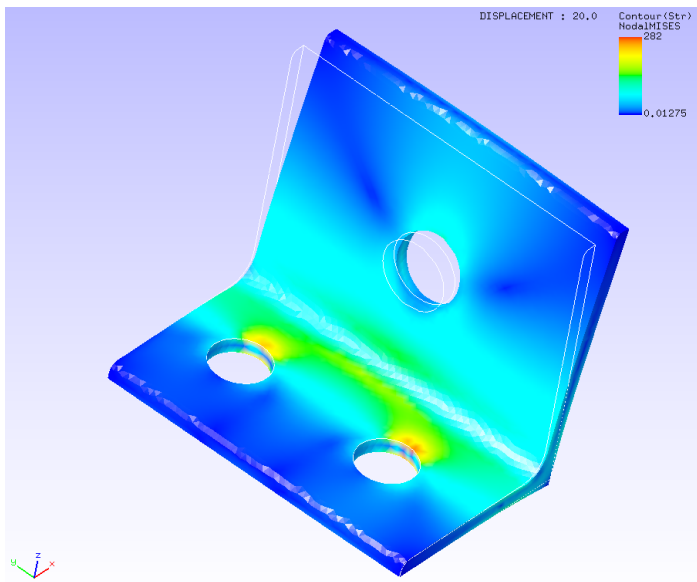


Fig. 4.1.3 : Analysis results of Mises stress

```

##### Result step= 1
##### Local Summary @Node :Max/IdMax/Min/IdMin#####
//U1 3.9115E+00 82452 -7.1083E-02 65233
//U2 7.4504E-03 354 -5.8813E-02 696
//U3 5.9493E-02 84 -5.8751E-01 61080
//E11 1.3777E-01 130 -1.3653E-01 77625
//E22 4.9199E-02 61 -5.4370E-02 102
//E33 6.8634E-02 51036 -6.1176E-02 30070
//E12 7.1556E-02 27808 -6.8093E-02 27863
//E23 5.3666E-02 56 -5.4347E-02 82
//E31 7.2396E-02 36168 -9.6621E-02 130
//S11 3.8626E+04 130 -3.6387E+04 28580
//S22 1.6628E+04 130 -1.5743E+04 28580
//S33 1.6502E+04 30033 -1.5643E+04 28580
//S12 5.7795E+03 27808 -5.4998E+03 27863
//S23 4.3345E+03 56 -4.3896E+03 82
//S31 5.8474E+03 36168 -7.8040E+03 130
//SMS 2.8195E+04 77625 1.2755E+00 75112

```

## 1.4 Static Analysis (Elasticity, Parallel)

The analysis of Section 4.1 was conducted in four parallel using the data of tutorial /02\_elastic\_hinge\_parallel.

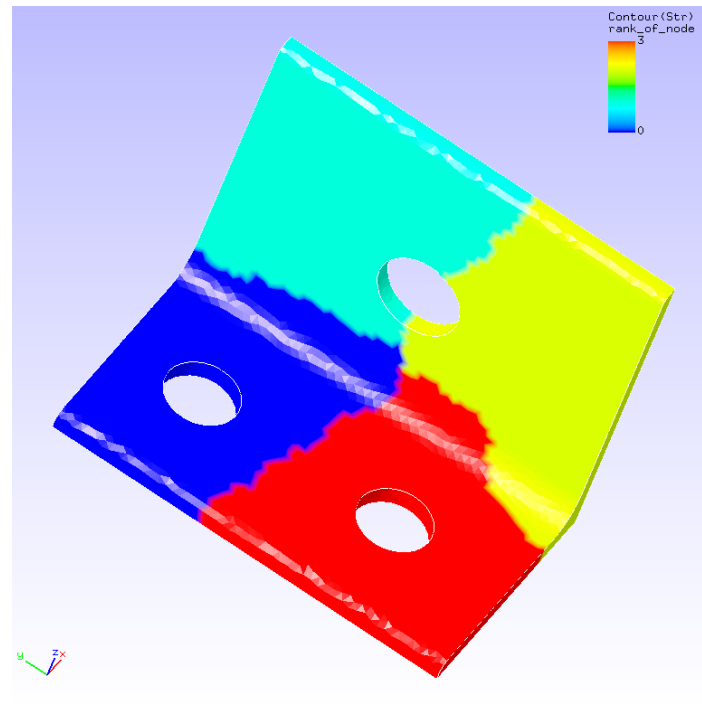


Figure 1: Analysis area of each node

Fig. 4.2.1 : Analysis area of each node

## 1.5 Static Analysis (Hyperelasticity, Part 1)

This analysis uses the data of tutorial /03\_hyperelastic\_cylinder.

### 1.5.1 Analysis target

The target of this analysis is a 1/8 model of a round bar whose shape and mesh data are shown in Figs. 4.3.1 and 4.3.2, respectively. The mesh is a hexahedral primary element with 432 elements and 629 nodes.

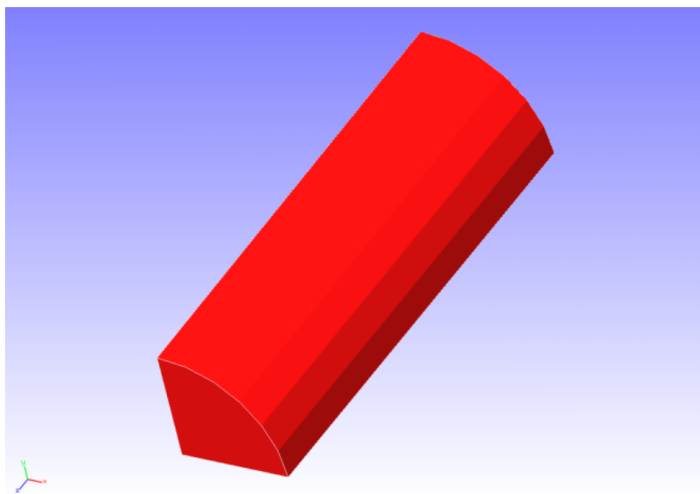


Fig. 4.3.1 : Shape of the round bar (1/8 model)

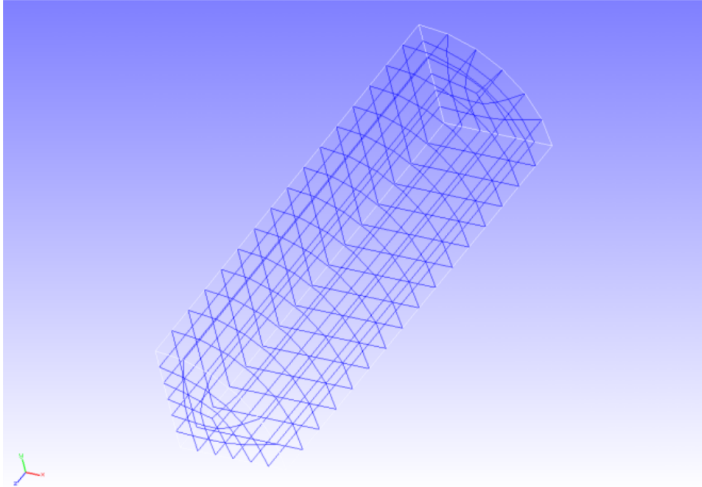


Fig. 4.3.2: Shape of the round bar (1/8 model)

### 1.5.2 Analysis content

In this stress analysis, an axial tensile displacement is given to a round bar. The Mooney–Rivlin model was used in the material constitutive equation of hyperelasticity. The analysis control data are presented below.

```
# Control File for FISTR
## Analysis Control
!VERSION
 3
!SOLUTION, TYPE=NLSTATIC
!WRITE,RESULT
!WRITE,VISUAL
## Solver Control
### Boundary Condition
!BOUNDARY, GRPID=1
  LOADS, 3, 3, -7.0
  FIX, 3, 3, 0.0
  XSYMM, 1, 1, 0.0
  YSYMM, 2, 2, 0.0
### STEP
!STEP, SUBSTEPS=5, CONVERG=1.0e-5
  BOUNDARY, 1
### Material
!MATERIAL, NAME=MAT1
!HYPERELASTIC, TYPE=MOONEY-RIVLIN
  0.1486, 0.4849, 0.0789
### Solver Setting
!SOLVER,METHOD=CG,PRECOND=1,ITERLOG=YES,TIMELOG=YES
  10000, 2
  1.0e-8, 1.0, 0.0
```

### 1.5.3 Analysis results

The analysis results of the fifth sub-step are shown in Fig. 4.3.3 as a deformation diagram with a Mises stress contour created with REVOCAP\_PrePost. Furthermore, a part of the log files of the analysis results is shown below as numerical data of the analysis.

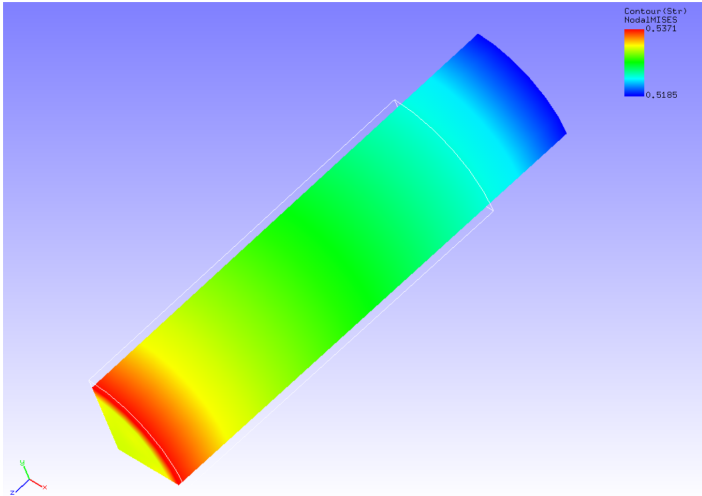


Fig. 4.3.3: Analysis results of deformation and Mises stress

```
##### Result step=      5
##### Local Summary @Node   :Max/IdMax/Min/IdMin#####
//U1    0.0000E+00      1 -6.7545E-01      7
//U2    0.0000E+00      1 -6.7545E-01     13
//U3    0.0000E+00      1 -7.0000E+00     38
//E11   -9.6951E-02    38 -1.0235E-01      7
//E22   -9.6951E-02    50 -1.0235E-01     13
//E33    3.0654E-01    13  2.8765E-01     50
//E12    6.9286E-04    53 -7.0533E-04     10
//E23    5.2256E-08    39 -3.2649E-03    86
//E31    5.2256E-08    49 -3.2649E-03    93
//S11    6.0251E-03    38 -6.6494E-03      7
//S22    6.0251E-03    50 -6.6495E-03     13
//S33    5.3529E-01    35  5.2006E-01    72
//S12    1.5458E-03    53 -1.6315E-03     10
//S23    1.5325E-07    38 -2.1554E-03    86
//S31    1.5325E-07    50 -2.1554E-03    93
//SMS   5.3730E-01     10  5.1836E-01    53
```

## 1.6 Static Analysis (Hyperelasticity, Part 2)

This analysis uses the data of tutorial /04\_hyperelastic\_spring.

### 1.6.1 Analysis target

The target of this analysis is a spring whose shape and mesh data are shown in Figs. 4.4.1 and 4.4.2, respectively. The mesh is a tetrahedral secondary element with 46454 elements and 78771 nodes.

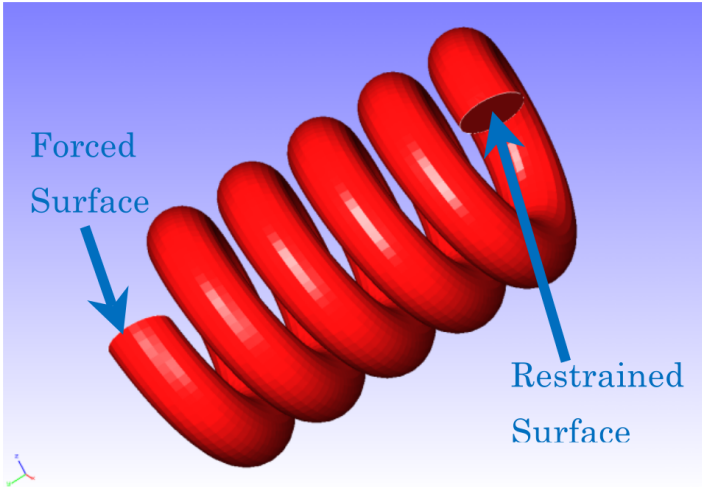


Fig. 4.4.1: Shape of the spring

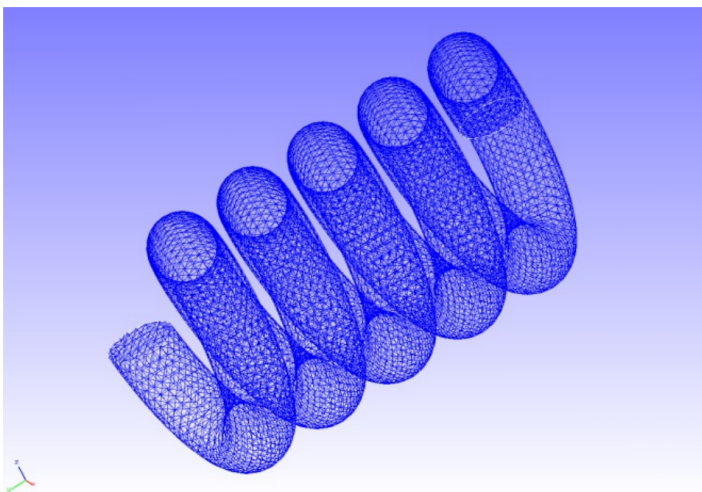


Fig. 4.4.2: Mesh data of the spring

### 1.6.2 Analysis content

In this stress analysis, the displacement of the constrained surface shown in Fig. 4.4.1 is restrained, and the displacement is given to the forced surface. The Arruda–Boyce model was used in the material constitutive equation of hyperelasticity. The analysis control data are presented below.

```
# Control File for FISTR
## Analysis Control
!VERSION
 3
!SOLUTION, TYPE=NLSTATIC
!WRITE,RESULT
!WRITE,VISUAL
## Solver Control
### Boundary Condition
!BOUNDARY, GRPID=1
  LOADS, 2, 2, -5.0
  FIX, 1, 3, 0.0
### STEP
!STEP, SUBSTEPS=1, CONVERG=1.0e-5
  BOUNDARY, 1
### Material
!MATERIAL, NAME=MAT1
!HYPERELASTIC, TYPE=ARRUDA_BOYCE
```

```

0.71 , 1.7029 , 0.1408
### Solver Setting
!SOLVER,METHOD=CG,PRECOND=1,ITERLOG=YES,TIMELOG=YES
10000 , 2
1.0e-8, 1.0 , 0.0

```

### 1.6.3 Analysis results

A deformation diagram with a displacement contour created with REVOCAP\_PrePost is shown in Fig. 4.4.3. Furthermore, a part of the log files of the analysis results is shown below as numerical data of the analysis.

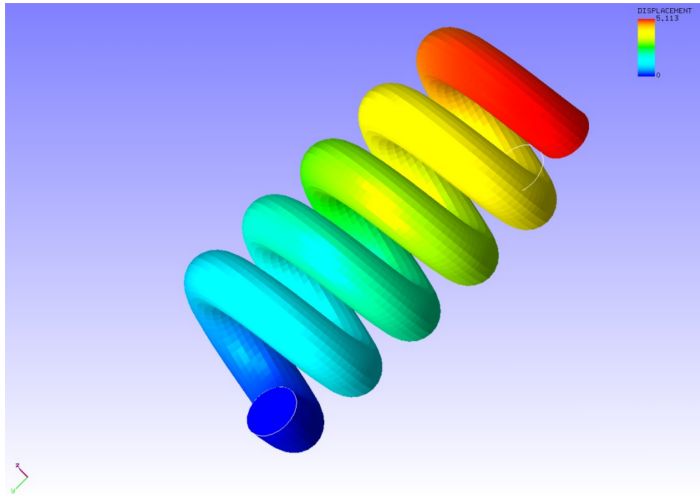


Fig. 4.4.3: Analysis results of deformation and displacement

```

##### Result step= 1
##### Local Summary :Max/IdMax/Min/IdMin#####
//U1 2.8588E-01    42179 -2.6512E-01    22274
//U2 2.2657E-02    6381 -5.0291E+00    22825
//U3 7.4573E-02    7058 -9.5095E-01    48324
//E11 4.8291E-03    2851 -4.2788E-03    3429
//E22 2.4161E-03    55960 -1.4539E-03   44761
//E33 5.3256E-03    25260 -4.6858E-03   27938
//E12 1.3574E-02    56003 -1.3081E-02   45120
//E23 2.8679E-02    48353 -1.8970E-02   48322
//E13 1.0897E-02    47938 -9.1054E-03   27344
//S11 5.1605E-02    2814 -5.0895E-03   10408
//S22 5.0635E-02    55965 -3.6174E-03   45307
//S33 4.9662E-02    39836 -5.1017E-03   4949
//S12 1.2059E-02    56003 -1.1865E-02   45120
//S23 2.6123E-02    48353 -1.7281E-02   56868
//S13 1.0133E-02    47938 -8.2330E-03   27344
//SMS 4.9365E-02    48353 3.2148E-04   64553

```

## 1.7 Static Analysis (Elastoplastic, Part 1)

This analysis uses the data of tutorial /05\_plastic\_cylinder.

### 1.7.1 Analysis target

The target of this analysis is the same 1/8 model of a round bar used in Section 4.3, Static Analysis (Hyperelasticity, Part 1).

### 1.7.2 Analysis content

The necking phenomenon of round bars caused by plastic deformation is analyzed. The Mises model was used as the yield function. The analysis control data are presented below.

```
# Control File for FISTR
## Analysis Control
!VERSION
 3
!SOLUTION, TYPE=NLSTATIC
!WRITE,RESULT,FREQUENCY=10
!WRITE,VISUAL,FREQUENCY=10
## Solver Control
### Boundary Condition
!BOUNDARY, GRPID=1
  LOADS, 3, 3, -7.0
  FIX, 3, 3, 0.0
  XSYMM, 1, 1, 0.0
  YSYMM, 2, 2, 0.0
### STEP
!STEP, SUBSTEPS=40, CONVERG=4.6e-3
  BOUNDARY, 1
### Material
!MATERIAL, NAME=MAT1
!ELASTIC
  206900.0, 0.29
!PLASTIC, YIELD=MISES, HARDEN=MULTILINEAR
  450.0, 0.0
  608.0, 0.05
  679.0, 0.1
  732.0, 0.2
  752.0, 0.3
  766.0, 0.4
  780.0, 0.5
### Output
!OUTPUT_VIS
  NSTRAIN, ON
!OUTPUT_RES
  ISTRESS, ON
### Solver Setting
!SOLVER,METHOD=CG,PRECOND=1,ITERLOG=NO,TIMELOG=YES
  2000, 2
  1.0e-8, 1.0, 0.0
```

### 1.7.3 Analysis results

The analysis results of the 35th sub-step are shown in Fig. 4.5.1 as a deformation diagram with a Mises stress contour created with REVOCAP\_PrePost. Furthermore, a part of the log files of the analysis results is shown below as numerical data of the analysis.

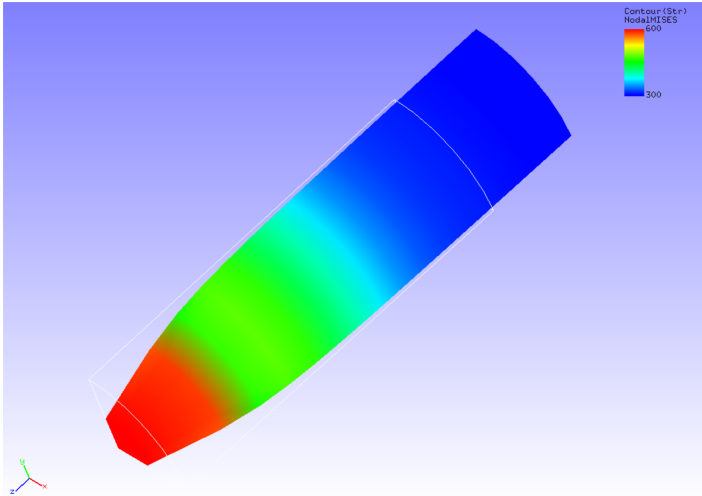


Fig. 4.5.1: Analysis results of deformation and Mises stress

```
##### Result step= 40
##### Local Summary @Node :Max/IdMax/Min/IdMin#####
//U1 0.0000E+00 1 -7.2695E-01 7
//U2 0.0000E+00 1 -7.2695E-01 13
//U3 0.0000E+00 1 -7.0000E+00 38
//E11 -1.0810E-01 38 -1.2378E-01 7
//E22 -1.0810E-01 50 -1.2378E-01 13
//E33 2.4788E-01 13 2.1876E-01 38
//E12 9.9178E-04 53 -1.1026E-03 10
//E23 8.1094E-08 38 -3.4137E-03 86
//E31 8.1094E-08 50 -3.4137E-03 93
//S11 1.0846E+01 1 -1.2094E+01 44
//S22 1.0846E+01 1 -1.2094E+01 44
//S33 7.5130E+02 1 7.2331E+02 44
//S12 1.3859E+00 148 -2.0846E+00 136
//S23 1.7004E+00 100 -5.6058E+00 80
//S31 1.7004E+00 79 -5.6058E+00 99
//SMS 7.4086E+02 13 7.3505E+02 38
```

## 1.8 Static Analysis (Elastoplastic, Part 2)

This analysis uses the data of tutorial /06\_plastic\_can.

### 1.8.1 Analysis target

The target of this analysis is a 1/2 model of a container whose shape and mesh data are shown in Figs. 4.6.1 and 4.6.2, respectively. The mesh is a tetrahedral secondary element with 7236 elements and 14119 nodes.

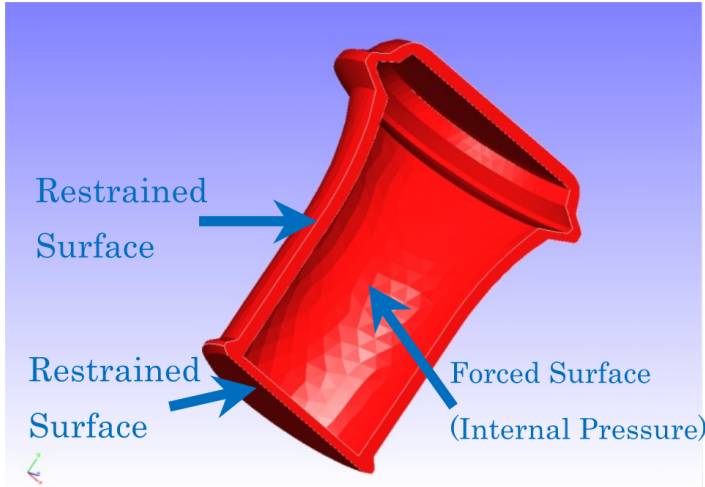


Fig. 4.6.1: Shape of the container

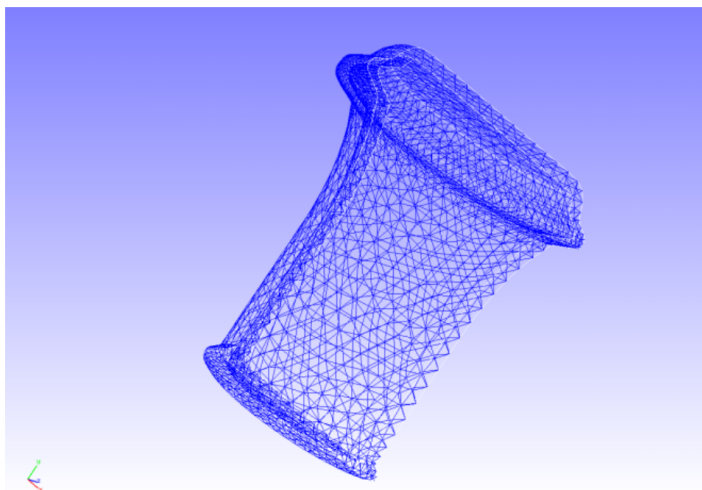


Fig. 4.6.2: Mesh data of the container

### 1.8.2 Analysis content

In this stress analysis, the displacement of the constrained surface shown in Fig. 4.6.1 is restrained, and a concentrated load is applied to the internal part of the container (the forced surface). The Drucker–Prager model is used as the yield function. The analysis control data are presented below.

```
# Control File for FISTR
## Analysis Control
!VERSION
 3
!SOLUTION, TYPE=NLSTATIC
## Solver Control
### Boundary Condition
!BOUNDARY, GRPID=1
  BND0, 3, 3, 0.000000
!BOUNDARY, GRPID=1
  BND1, 1, 1, 0.000000
  BND1, 2, 2, 0.000000
  BND1, 3, 3, 0.000000
!DLOAD,GRPID=1
  DL0, S, 1.0
!DLOAD,GRPID=1
  DL1, S, 1.0
!DLOAD,GRPID=1
```

```

DL2, S, 0.5
### STEP
!STEP, SUBSTEPS=10, CONVERG=1.0e-5
  BOUNDARY, 1
  LOAD, 1
### Material
!MATERIAL, NAME=M1
!ELASTIC
  24000.0, 0.2
!PLASTIC, YIELD = DRUCKER-PRAGER
  500.0, 20.0, 0.0
### Solver Setting
!SOLVER,METHOD=CG,PRECOND=1,ITERLOG=NO,TIMELOG=YES
  20000, 2
  1.0e-8, 1.0, 0.0

```

### 1.8.3 Analysis results

The analysis results of the 10th sub-step are shown in Fig. 4.6.3 as a deformation diagram with a Mises stress contour created with REVOCAP\_PrePost. The deformation magnification was set to 30. Furthermore, a part of the log files of the analysis results is shown below as numerical data of the analysis.

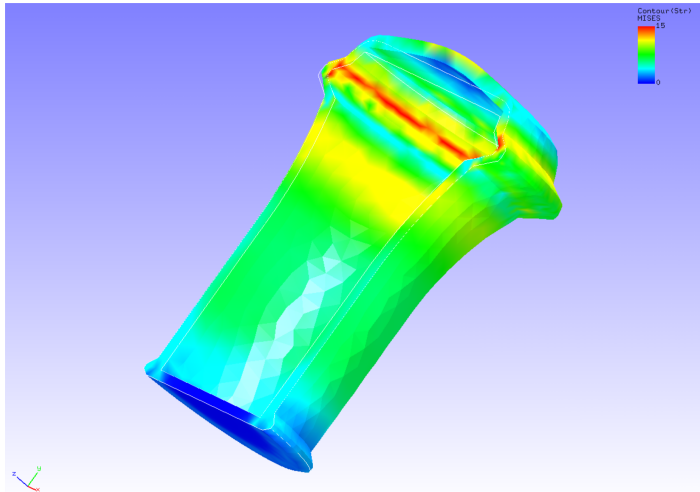


Fig. 4.6.3: Analysis results of deformation and Mises stress

```

##### Result step= 10
##### Local Summary @Node :Max/IdMax/Min/IdMin#####
//U1    1.6169E+00      1600 -1.6123E+00      11901
//U2    1.9278E+01      6877 -4.5292E-01      7096
//U3    1.6086E+00      7016 -1.5103E+00      6934
//E11   9.9223E-04     11242 -6.5878E-04     1404
//E22   1.5016E-03     13972 -5.4206E-04     2367
//E33   9.8440E-04     6833 -6.4767E-04     7000
//E12   1.6817E-03     2698 -1.7171E-03     11906
//E23   1.7077E-03     6749 -1.4466E-03     13509
//E31   1.2095E-03     12475 -1.1185E-03    11342
//S11   2.7784E+01      1086 -1.9437E+01    2363
//S22   3.7880E+01     13972 -1.4554E+01    2367
//S33   2.7338E+01      1086 -1.9739E+01    13082
//S12   1.6819E+01     2698 -1.7172E+01    11906
//S23   1.7079E+01     6749 -1.4466E+01    13509
//S31   1.2089E+01     12475 -1.1180E+01    11342
//SMS   3.7455E+01      2834  2.7593E-04     7333

```

## 1.9 Static Analysis (Elastoplastic, Part 2)

This analysis uses the data of tutorial /06\_plastic\_can.

### 1.9.1 Analysis target

The target of this analysis is a 1/2 model of a container whose shape and mesh data are shown in Figs. 4.6.1 and 4.6.2, respectively. The mesh is a tetrahedral secondary element with 7236 elements and 14119 nodes.

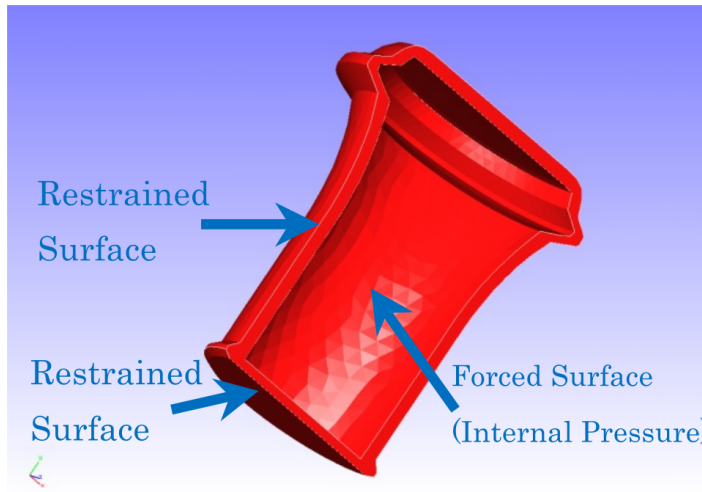


Fig. 4.6.1: Shape of the container

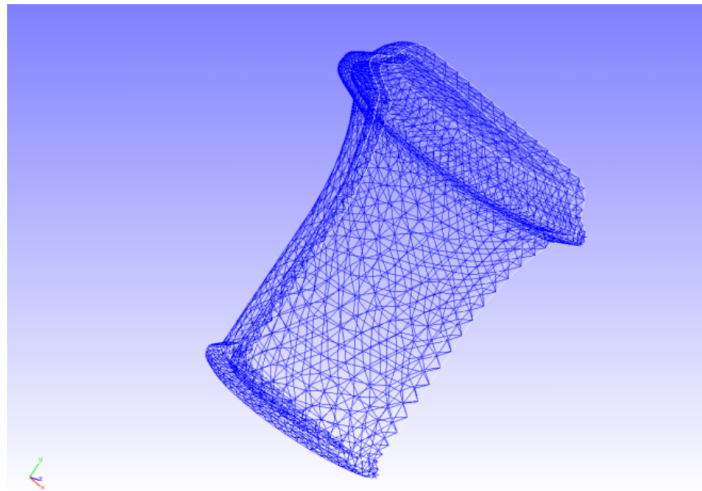


Fig. 4.6.2: Mesh data of the container

### 1.9.2 Analysis content

In this stress analysis, the displacement of the constrained surface shown in Fig. 4.6.1 is restrained, and a concentrated load is applied to the internal part of the container (the forced surface). The Drucker–Prager model is used as the yield function. The analysis control data are presented below.

```
# Control File for FISTR
## Analysis Control
!VERSION
 3
!SOLUTION, TYPE=NLSTATIC
## Solver Control
### Boundary Condition
!BOUNDARY, GRPID=1
  BND0, 3, 3, 0.000000
!BOUNDARY, GRPID=1
```

```

BND1, 1, 1, 0.000000
BND1, 2, 2, 0.000000
BND1, 3, 3, 0.000000
!DLOAD, GRPID=1
    DL0, S, 1.0
!DLOAD, GRPID=1
    DL1, S, 1.0
!DLOAD, GRPID=1
    DL2, S, 0.5
### STEP
!STEP, SUBSTEPS=10, CONVERG=1.0e-5
    BOUNDARY, 1
    LOAD, 1
### Material
!MATERIAL, NAME=M1
!ELASTIC
    24000.0, 0.2
!PLASTIC, YIELD = DRUCKER-PRAGER
    500.0, 20.0, 0.0
### Solver Setting
!SOLVER,METHOD=CG,PRECOND=1,ITERLOG=NO,TIMELOG=YES
    20000, 2
    1.0e-8, 1.0, 0.0

```

### 1.9.3 Analysis results

The analysis results of the 10th sub-step are shown in Fig. 4.6.3 as a deformation diagram with a Mises stress contour created with REVOCAP\_PrePost. The deformation magnification was set to 30. Furthermore, a part of the log files of the analysis results is shown below as numerical data of the analysis.

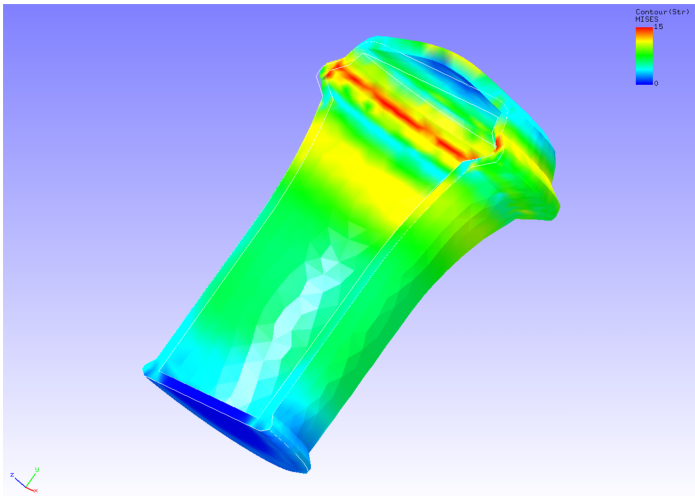


Fig. 4.6.3: Analysis results of deformation and Mises stress

```

##### Result step= 10
##### Local Summary @Node :Max/IdMax/Min/IdMin#####
//U1 1.6169E+00 1600 -1.6123E+00 11901
//U2 1.9278E+01 6877 -4.5292E-01 7096
//U3 1.6086E+00 7016 -1.5103E+00 6934
//E11 9.9223E-04 11242 -6.5878E-04 1404
//E22 1.5016E-03 13972 -5.4206E-04 2367
//E33 9.8440E-04 6833 -6.4767E-04 7000
//E12 1.6817E-03 2698 -1.7171E-03 11906
//E23 1.7077E-03 6749 -1.4466E-03 13509
//E31 1.2095E-03 12475 -1.1185E-03 11342

```

```

//S11  2.7784E+01    1086 -1.9437E+01    2363
//S22  3.7880E+01    13972 -1.4554E+01   2367
//S33  2.7338E+01    1086 -1.9739E+01  13082
//S12  1.6819E+01    2698 -1.7172E+01  11906
//S23  1.7079E+01    6749 -1.4466E+01  13509
//S31  1.2089E+01   12475 -1.1180E+01  11342
//SMS  3.7455E+01    2834  2.7593E-04   7333

```

## 1.10 Static Analysis (Viscoelasticity)

This analysis uses the data of tutorial /07\_viscoelastic\_cylinder.

### 1.10.1 Analysis target

The target of this analysis is the same 1/8 model of a round bar used in Section 4.3, Static Analysis (Hyperelasticity, Part 1).

### 1.10.2 Analysis content

In this stress relaxation analysis, an axial tensile displacement is given to a round bar. The analysis control data are presented below.

```

# Control File for FISTR
## Analysis Control
!VERSION
 3
!SOLUTION, TYPE=NLSTATIC
!WRITE,VISUAL
!WRITE,RESULT
## Solver Control
### Boundary Condition
!BOUNDARY, GRPID=1
  LOADS, 3, 3, -7.0
  FIX, 3, 3, 0.0
  XSYMM, 1, 1, 0.0
  YSYMM, 2, 2, 0.0
### STEP
!STEP, TYPE=VISCO, CONVERG=1.0e-5
  0.2, 2.0
  BOUNDARY, 1
### Material
!MATERIAL, NAME=MAT1
!ELASTIC
  206900.0, 0.29
!VISCOELASTIC
  0.5, 1.0
### Solver Setting
!SOLVER,METHOD=CG,PRECOND=1,ITERLOG=YES,TIMELOG=YES
  10000, 2
  1.0e-8, 1.0, 0.0

```

### 1.10.3 Analysis results

A deformation diagram with a Mises stress contour created with REVOCAP\_PrePost is shown in Fig. 4.7.1. This is the analysis results after 2 s (10th step.) Furthermore, a part of the log files of the analysis results is shown below as numerical data of the analysis.

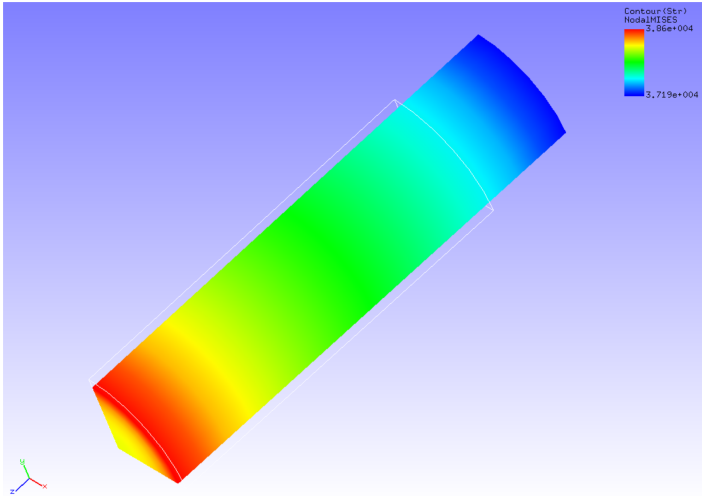


Fig. 4.7.1: Analysis results of deformation and Mises stress

```
##### Result step=
10
##### Local Summary :Max/IdMax/Min/IdMin#####
//U1 0.0000E+00      1 -7.4531E-01    91
//U2 0.0000E+00      1 -7.4531E-01    88
//U3 0.0000E+00      1 -7.0000E+00    38
//E11 -1.0763E-01    38 -1.1244E-01    7
//E22 -1.0763E-01    50 -1.1244E-01   13
//E33 3.0270E-01     13 2.9129E-01   50
//E12 9.8113E-04     53 -9.9997E-04   10
//E23 1.1878E-04     72 -3.2869E-03  84
//E13 1.1878E-04     64 -3.2869E-03  95
//S11 1.4135E+02     13 -1.3699E+02  50
//S22 1.4135E+02      7 -1.3699E+02  38
//S33 3.8691E+04     13 3.7107E+04  50
//S12 4.6701E+01     53 -4.7594E+01  10
//S23 5.2254E+00     72 -1.5313E+02  84
//S13 5.2254E+00     64 -1.5313E+02  95
//SMS 3.8602E+04     13 3.7194E+04  50
```

## 1.11 Static Analysis (Creep)

This analysis uses the data of tutorial /08\_creep\_cylinder.

### 1.11.1 Analysis target

The target of this analysis is the same 1/8 model of a round bar used in Section 4.3, Static Analysis (Hyperelasticity, Part 1).

### 1.11.2 Analysis content

In this creep behavior analysis, an axial tensile displacement is given to a round bar. The analysis control data are presented below.

```
# Control File for FISTR
## Analysis Control
!VERSION
 3
!SOLUTION, TYPE=NLSTATIC
!WRITE,RESULT
!WRITE,VISUAL
## Solver Control
```

```

### Boundary Condition
!BOUNDARY, GRPID=1
  LOADS, 3, 3, -7.0
  FIX, 3, 3, 0.0
  XSYMM, 1, 1, 0.0
  YSYMM, 2, 2, 0.0
### STEP
!STEP, SUBSTEPS=5, CONVERG=1.0e-5
  BOUNDARY, 1
### Material
!MATERIAL, NAME=MAT1
!ELASTIC
  206900.0, 0.29
!CREEP, TYPE=NORTON
  1.e-10, 5.0, 0.0
### Solver Setting
!SOLVER, METHOD=CG, PRECOND=1, ITERLOG=YES, TIMELOG=YES
  10000, 2
  1.0e-8, 1.0, 0.0

```

### 1.11.3 Analysis results

The analysis results of the fifth sub-step are shown in Fig. 4.8.1 as a deformation diagram with a Mises stress contour created with REVOCAP\_PrePost. Furthermore, a part of the log files of the analysis results is shown below as numerical data of the analysis.

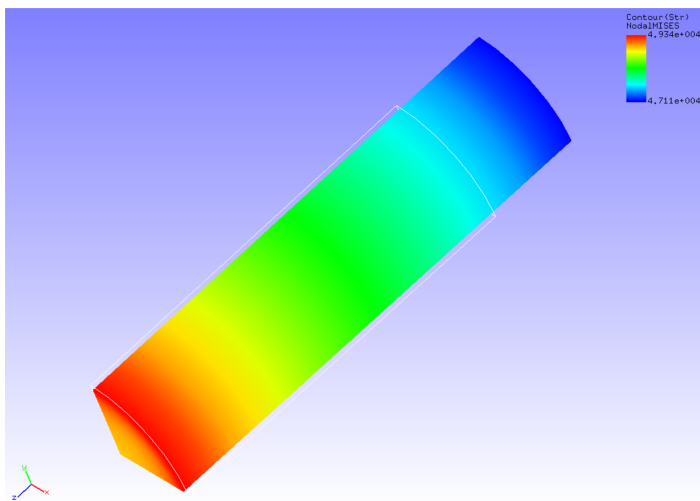


Fig. 4.8.1: Analysis results of deformation and Mises stress

```

##### Result step= 5
##### Local Summary :Max/IdMax/Min/IdMin#####
//U1  0.0000E+00          1  -4.1832E-01    91
//U2  0.0000E+00          1  -4.1832E-01    88
//U3  0.0000E+00          1  -7.0000E+00    38
//E11 -6.5815E-02         38  -6.9387E-02    7
//E22 -6.5815E-02         50  -6.9387E-02   13
//E33  2.3854E-01         13  2.2765E-01   38
//E12  5.4317E-04         53  -5.5746E-04   10
//E23  8.9875E-05         72  -2.2085E-03   84
//E13  8.9875E-05         64  -2.2085E-03   95
//S11  1.1317E+02         14  -1.1102E+02   49
//S22  1.1317E+02         6   -1.1102E+02   39
//S33  4.9374E+04         13  4.7081E+04   38
//S12  4.3566E+01         53  -4.4697E+01   10

```

```

//S23 7.6408E+00      72 -1.6768E+02      84
//S13 7.6408E+00      64 -1.6768E+02      95
//SMS 4.9340E+04      13 4.7114E+04      38

```

## 1.12 Contact Analysis (Part 1)

This analysis uses the data of tutorial /09\_contact\_hertz.

### 1.12.1 Analysis target

This analysis is a Hertz contact problem with a target whose shape and mesh data of the analysis are shown in Figs. 4.9.1 and 4.9.2, respectively. The mesh is a hexahedral primary element with 168 elements and 408 nodes.

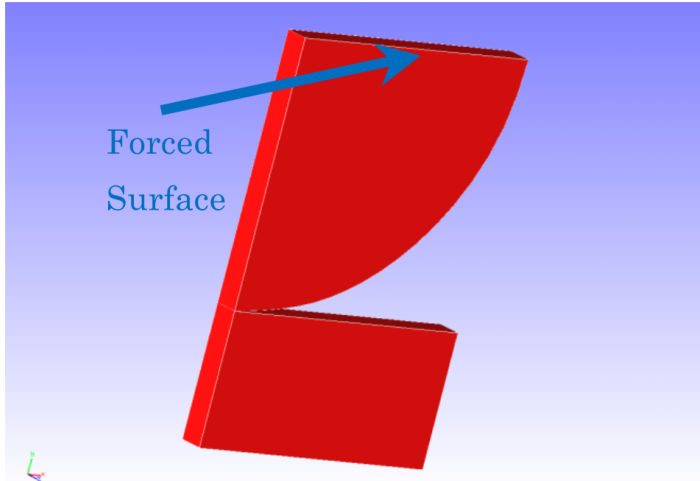


Fig. 4.9.1: Shape of the analysis target

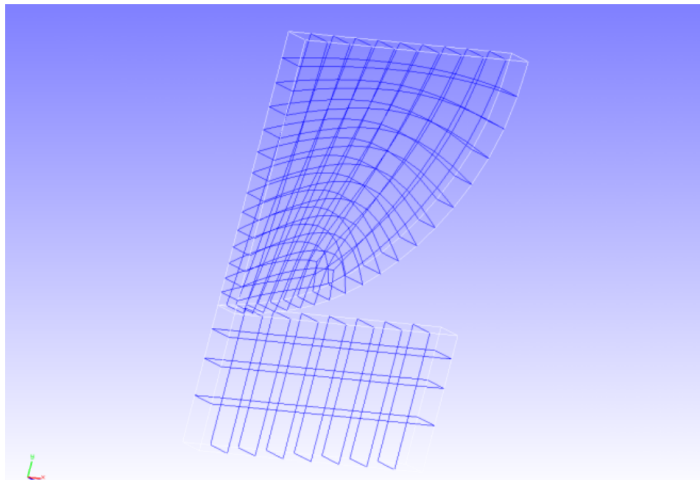


Fig. 4.9.2: Mesh data of the analysis target

### 1.12.2 Analysis content

This is a contact analysis performed with the expanded method of Lagrange multipliers. A forced displacement in the compression direction is applied to the surface of a 1/4 model of a disk. The analysis control data are presented below.

```

# Control File for FISTR
## Analysis Control
!VERSION
 3
!SOLUTION, TYPE=NSTATIC

```

```

!WRITE,RESULT
!WRITE,VISUAL
## Solver Control
### Boundary Condition
!BOUNDARY, GRPID=1
    ALL, 3, 3, 0.0
    BOTTOM, 2, 2, 0.0
    CENTER, 1, 1, 0.0
    UPPER, 2, 2, -0.306
!CONTACT_ALGO, TYPE=LAGRANGE
!CONTACT, GRPID=1
    CP1, 0.0
### STEP
!STEP, SUBSTEPS=5, CONVERG=1.0e-5
    BOUNDARY, 1
    CONTACT, 1

```

### 1.12.3 Analysis results

The analysis results of the fifth sub-step are shown in Fig. 4.9.3 as a deformation diagram with a y-direction displacement contour created with REVOCAP\_PrePost. Furthermore, a part of the log files of the analysis results is shown below as numerical data of the analysis.

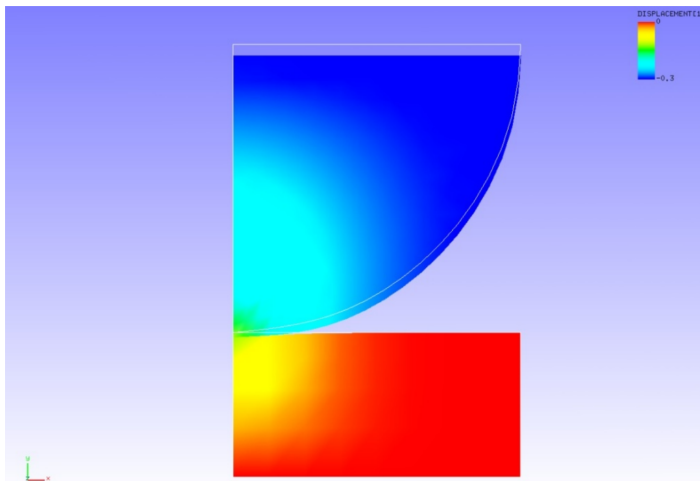


Fig. 4.9.3: Analysis results of deformation and y-direction displacement

## 1.13 Contact Analysis (Part 2)

This analysis uses the data of tutorial /10\_contact\_2tubes.

### 1.13.1 Analysis target

This analysis is a pushing problem of a cylinder with a target whose shape and mesh data are shown in Figs. 4.10.1 and 4.10.2, respectively. The mesh is a hexahedral primary element with 2888 elements and 4000 nodes.

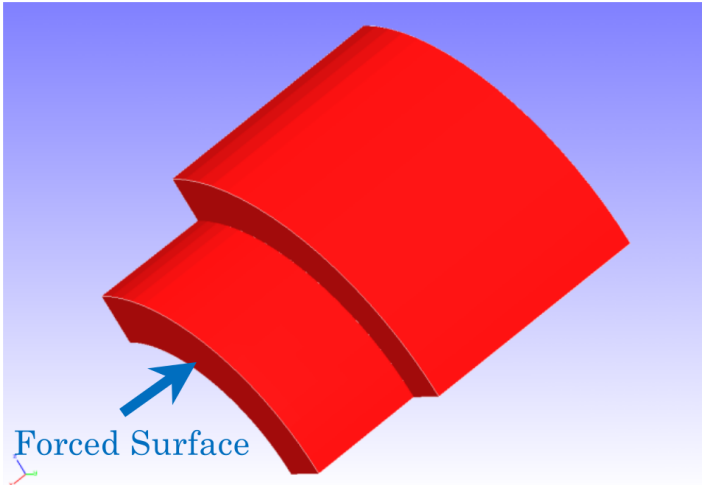


Fig. 4.10.1: Shape of the analysis target

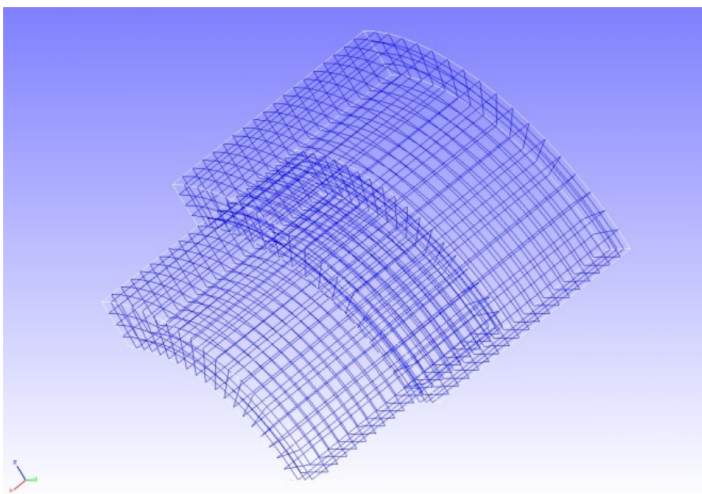


Fig. 4.10.2: Mesh data of the analysis target

### 1.13.2 Analysis content

This is a contact analysis performed with the method of Lagrange multipliers. A forced displacement in the pushing direction is applied to the forced surface shown in Fig. 4.10.1. The analysis control data are presented below.

```
# Control File for FISTR
## Analysis Control
!VERSION
 3
!SOLUTION, TYPE=NLSTATIC
!WRITE,RESULT
!WRITE,VISUAL
## Solver Control
### Boundary Condition
!BOUNDARY, GRPID=1
  X0, 1, 3, 0.0
  Y0, 2, 2, 0.0
  Z0, 3, 3, 0.0
!BOUNDARY, GRPID=2
  X1, 1, 1, 0.0
!BOUNDARY, GRPID=3
  X1, 1, 1, -1.0
!CONTACT_ALGO, TYPE=SLAGRANGE
```

```

!CONTACT, GRPID=1, INTERACTION=FSLID, NPENALTY=1.0e+2
CP1, 0.0, 1.0e+5
### STEP
!STEP, SUBSTEPS=4, CONVERG=1.0e-5
BOUNDARY, 1
BOUNDARY, 3
CONTACT, 1
### Material
!MATERIAL, NAME=M1
!ELASTIC
2.1e+5, 0.3
### Solver Setting
!SOLVER,METHOD=MUMPS

```

### 1.13.3 Analysis results

The analysis results of the fourth sub-step are shown in Fig. 4.10.3 as a deformation diagram with a Mises stress contour created with REVOCAP\_PrePost. Furthermore, a part of the log files of the analysis results is shown below as numerical data of the analysis.

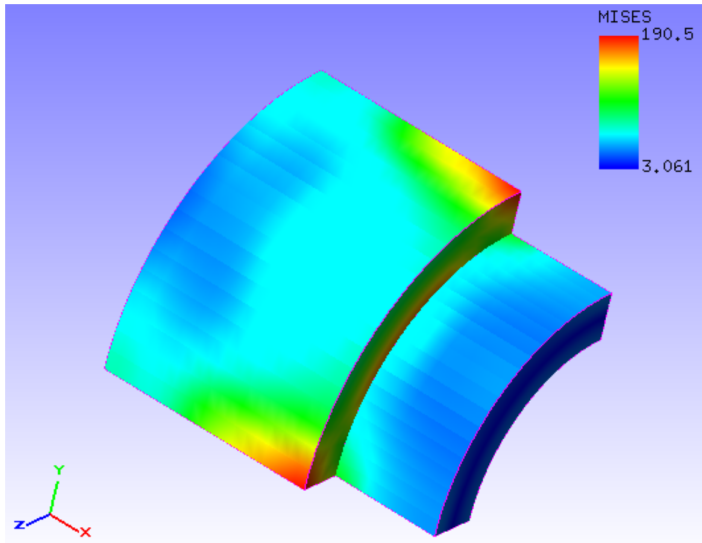


Fig. 4.10.3: Analysis results of deformation and Mises stress

```

##### Result step= 4
##### Local Summary @Node :Max/IdMax/Min/IdMin#####
//U1 8.6939E-04      32 -1.0021E+00    2006
//U2 8.7641E-03      104 -7.0520E-03   2006
//U3 8.7641E-03      4   -7.0519E-03   1901
//E11 7.5294E-04     1901 -4.1253E-04  105
//E22 9.8421E-04     2   -9.2894E-04  2058
//E33 9.8423E-04     102 -9.2886E-04 3843
//E12 5.3499E-04     133 -2.8306E-04 278
//E23 1.2480E-03     1901 -1.4177E-03 4
//E31 5.3509E-04     33  -2.8312E-04 1678
//S11 7.7145E+01     103 -8.9999E+01 101
//S22 2.0117E+02     2   -2.2935E+02 1905
//S33 2.0117E+02     102 -2.2937E+02 2010
//S12 4.3211E+01     133 -2.2863E+01 278
//S23 1.0080E+02     1901 -1.1451E+02 4
//S31 4.3219E+01     33  -2.2867E+01 1678
//SMS 2.9963E+02     1901 3.1611E+00 2454

```

## 1.14 Contact Analysis (Part 3)

This analysis uses the data of tutorial /11\_contact\_2beam.

### 1.14.1 Analysis target

This analysis is a contact problem of two beams. The outline of the analysis model is shown in Fig. 4.11.1. The mesh is a hexahedral primary element with 80 elements and 252 nodes.

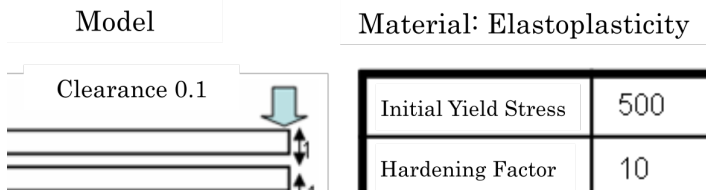


Fig. 4.11.1 Outline of Analysis Model

### 1.14.2 Analysis contents

This is a contact analysis performed with the method of Lagrange multipliers. A forced displacement is applied to the upper side of the edge of the beam. The analysis control data are presented below.

```
!!
!! Control File for FISTR
!!
!VERSION
3
!SOLUTION, TYPE=NLSTATIC
!WRITE,RESULT
!WRITE,VISUAL
!BOUNDARY, GRPID=1
ng1, 1, 3, 0.0
ng2, 1, 3, 0.0
ng3, 3, 3, -3.0
!CONTACT_ALGO, TYPE=SLAGRANGE
!CONTACT, GRPID=1, INTERACTION=FSLID
CP1, 0.0, 1.0e+5
!STEP, SUBSTEPS=100, CONVERG=1.0e-4
BOUNDARY, 1
CONTACT, 1
!MATERIAL, NAME=M1
!ELASTIC
2.1e+5, 0.3
!PLASTIC, YIELD=MISES
500.0, 10.0
!SOLVER,METHOD=MUMPS
```

### 1.14.3 Analysis results

The analysis results of the 100th sub-step are shown in Fig. 4.11.2 as a deformation diagram with a Mises stress contour created with REVOCAP\_PrePost. Furthermore, a part of the log files of the analysis results is illustrated below as numerical data of the analysis.

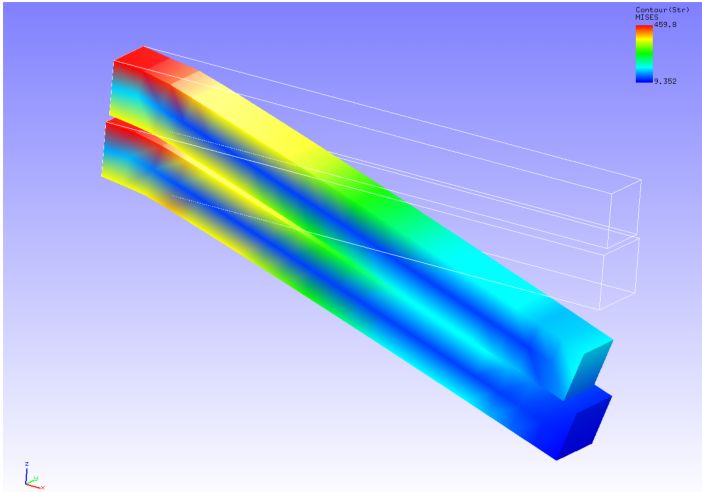


Fig. 4.11.2: Analysis results of deformation and Mises stress

```
##### Result step= 100
##### Local Summary @Node :Max/IdMax/Min/IdMin#####
//U1    1.4100E-01      196 -6.1103E-01      6
//U2    4.5708E-02      11 -4.5708E-02     195
//U3    0.0000E+00       1 -3.0000E+00      8
//E11   1.6026E-01      195 -1.3021E-01     49
//E22   5.9692E-02      49 -7.5443E-02     195
//E33   7.3913E-02      152 -8.7368E-02    30
//E12   8.6161E-02      7 -8.6161E-02     192
//E23   9.8977E-02      11 -9.8977E-02    195
//E31   6.0651E-02      90 -1.2885E-01    192
//S11   5.7685E+02      30 -6.3641E+02    152
//S22   1.2740E+02      129 -1.2723E+02   194
//S33   1.4934E+02      129 -1.4146E+02   1
//S12   1.4662E+02      70 -1.4662E+02   235
//S23   1.7892E+02      109 -1.7892E+02   172
//S31   1.6198E+02      153 -2.4815E+02   194
//SMS   6.2475E+02      152  8.3120E+00    2
```

## 1.15 Linear Dynamic Analysis

This analysis uses the data of tutorial /12\_dynamic\_beam.

### 1.15.1 Analysis target

The target of this analysis is a cantilever whose shape and mesh data are shown in Figs. 4.12.1 and 4.12.2, respectively. The mesh is a tetrahedral secondary element with 240 elements and 525 nodes.

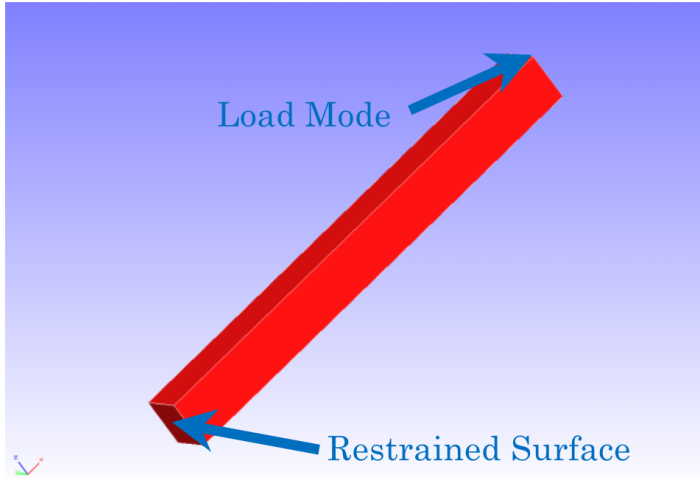


Fig. 4.12.1: Shape of the cantilever

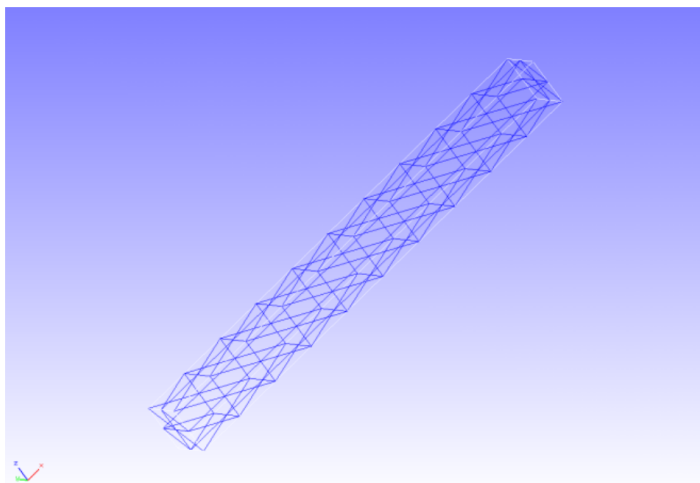


Fig. 4.12.2: Mesh data of the cantilever

### 1.15.2 Analysis contents

A linear dynamic analysis is performed after restraining the displacement of the constrained surface shown in Fig. 4.12.1 and applying a concentrated load to the load nodes. The analysis control data are presented below.

```
# Control File for FISTR
## Analysis Control
!VERSION
      3
!WRITE,LOG,FREQUENCY=5000
!WRITE,RESULT,FREQUENCY=5000
!SOLUTION, TYPE=DYNAMIC
!DYNAMIC, TYPE=LINEAR
      11 , 1
      0.0, 1.0, 500000, 1.0000e-8
      0.5, 0.25
      1, 1, 0.0, 0.0
      100000, 3121, 500
      1, 1, 1, 1, 1, 1
## Solver Control
### Boundary Condition
!BOUNDARY, AMP=AMP1
    FIX, 1, 3, 0.0
!CLOAD, AMP=AMP1
```

```

CL1, 3, -1.0
### Solver Setting
!SOLVER,METHOD=CG,PRECOND=1,ITERLOG=NO,TIMELOG=NO
10000, 2
1.0e-06, 1.0, 0.0

```

### 1.15.3 Analysis results

The time-series display of the displacement of the monitoring nodes, specified with the analysis control data (load nodes, nodal number 3121) and created with Microsoft Excel, is shown in Fig. 4.12.3. Furthermore, a part of the displacement output files of the monitoring nodes (dyna\_disp\_p1.out) is shown in Fig. 4.12.3 as numerical data of the analysis.

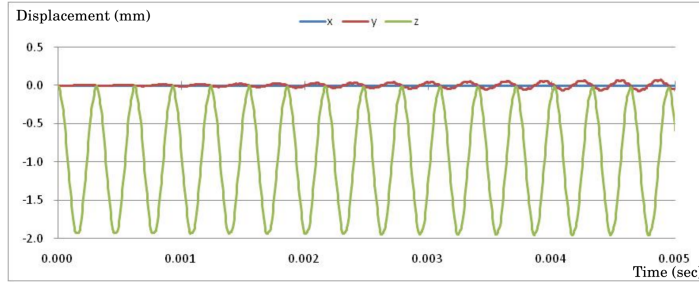


Fig. 4.12.3: Time-series displacement of monitoring nodes

0	0.0000E+000	3121	0.0000E+000	0.0000E+000	0.0000E+000
500	5.0000E-006	3121	5.5959E-005	-2.0679E-006	-1.5563E-002
1000	1.0000E-005	3121	5.3913E-005	2.0947E-005	-4.3950E-002
1500	1.5000E-005	3121	7.6105E-005	5.8799E-005	-8.0795E-002
2000	2.0000E-005	3121	6.8543E-006	4.0956E-005	-1.2329E-001
2500	2.5000E-005	3121	5.4725E-005	7.0881E-005	-1.7742E-001
3000	3.0000E-005	3121	6.8226E-005	1.7597E-004	-2.2801E-001
3500	3.5000E-005	3121	4.2923E-005	1.1791E-004	-2.7290E-001
4000	4.0000E-005	3121	-1.2087E-005	1.2552E-004	-3.2393E-001
4500	4.5000E-005	3121	3.4969E-005	-3.4512E-005	-3.8844E-001
5000	5.0000E-005	3121	6.1592E-005	1.2820E-004	-4.6425E-001
5500	5.5000E-005	3121	1.3188E-005	1.9002E-005	-5.4590E-001
6000	6.0000E-005	3121	3.1393E-005	-7.4604E-005	-6.4556E-001
6500	6.5000E-005	3121	9.8931E-005	-1.9078E-004	-7.5561E-001
7000	7.0000E-005	3121	4.2308E-005	1.1593E-004	-8.6826E-001
7500	7.5000E-005	3121	-2.7019E-005	3.0277E-004	-9.6826E-001

## 1.16 Non-Linear Dynamic Analysis

This analysis uses the data of tutorial /13\_dynamic\_beam\_nonlinear.

### 1.16.1 Analysis target

The target of this analysis is the same cantilever used in Section 4.12, Linear Dynamic Analysis.

### 1.16.2 Analysis content

A non-linear dynamic analysis is performed after restraining the displacement of the constrained surface shown in Fig. 4.12.1 and applying a concentrated load to the load nodes. The analysis control data are presented below.

node. The analysis control data is shown in the following.

```

# Control File for FISTR
## Analysis Control
!VERSION
 3
!WRITE,RESULT,FREQUENCY=100

```

```

!SOLUTION, TYPE=DYNAMIC
!DYNAMIC, TYPE=NONLINEAR
  1 , 1
  0.0,  0.1,  100000,  1.0000e-8
  0.5,  0.25
  1,  1,  0.0,  0.0
  1000, 3121,  100
  1,  1,  1,  1,  1,  1
## Solver Control
#### Boundary Condition
!BOUNDARY, GRPID=1, AMP=AMP1
  FIX, 1, 3, 0.0
!CLOAD, GRPID=1, AMP=AMP1
  CL1, 3, -1.0
#### STEP
!STEP, CONVERG=1.0e-3
  BOUNDARY, 1
  LOAD, 1
#### Material
!DENSITY
  1.0e-8
!HYPERELASTIC, TYPE=NEOHOOKE
  1000.0, 0.00005
#### Solver Setting
!SOLVER,METHOD=CG,PRECOND=1,ITERLOG=NO,TIMELOG=NO
  10000, 2
  1.0e-06, 1.0, 0.0

```

### 1.16.3 Analysis results

The time-series display of the displacement of the monitoring nodes, specified with analysis control data (load nodes, nodal number 3121) and created with Microsoft Excel, is shown in Fig. 4.13.1. Furthermore, a part of the displacement output files of the monitoring nodes (dyna\_disp\_p1.out) is shown below as numerical data of the analysis.

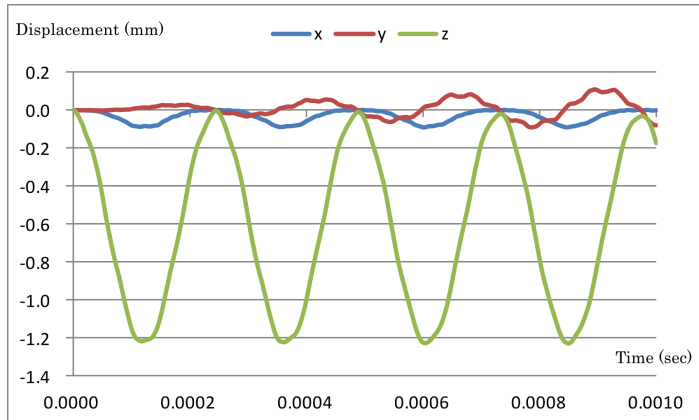


Fig. 4.13.1: Time-series displacement of monitoring nodes

0	0.0000E+000	3121	0.0000E+000	0.0000E+000	0.0000E+000
100	1.0000E-006	3121	7.6535E-005	-7.4007E-005	-6.0637E-004
200	2.0000E-006	3121	3.3644E-005	-7.8807E-006	-8.2096E-004
300	3.0000E-006	3121	8.7159E-005	-5.5454E-005	-1.2450E-003
400	4.0000E-006	3121	6.2478E-005	-2.8447E-005	-1.9154E-003
500	5.0000E-006	3121	2.9599E-005	-4.1870E-005	-2.6827E-003
600	6.0000E-006	3121	9.3686E-005	-2.0169E-005	-3.4036E-003
700	7.0000E-006	3121	4.8174E-005	-2.4760E-005	-4.1900E-003
800	8.0000E-006	3121	4.1022E-005	-3.2953E-005	-5.2161E-003

900	9.0000E-006	3121	8.1994E-005	4.0719E-006	-6.1061E-003
1000	1.0000E-005	3121	2.7155E-005	-2.5723E-005	-7.1002E-003
1100	1.1000E-005	3121	6.8486E-005	-1.8213E-005	-8.3100E-003
1200	1.2000E-005	3121	4.9497E-005	-9.4011E-006	-9.3339E-003
1300	1.3000E-005	3121	3.4481E-005	-1.6904E-006	-1.0512E-002
1400	1.4000E-005	3121	6.7383E-005	-1.3895E-005	-1.1826E-002
1500	1.5000E-005	3121	8.2829E-006	3.2817E-006	-1.3019E-002

## 1.17 Non-Linear Contact Dynamic Analysis

This analysis uses the data of tutorial /14\_dynamic\_plate\_contact.

### 1.17.1 Analysis target

The target of this analysis is the falling impact of a square material on the floor surface. The shape and mesh data of the material are shown in Figs. 4.14.1 and 4.14.2, respectively. The mesh is a hexahedral primary element with 8232 elements and 10712 nodes.

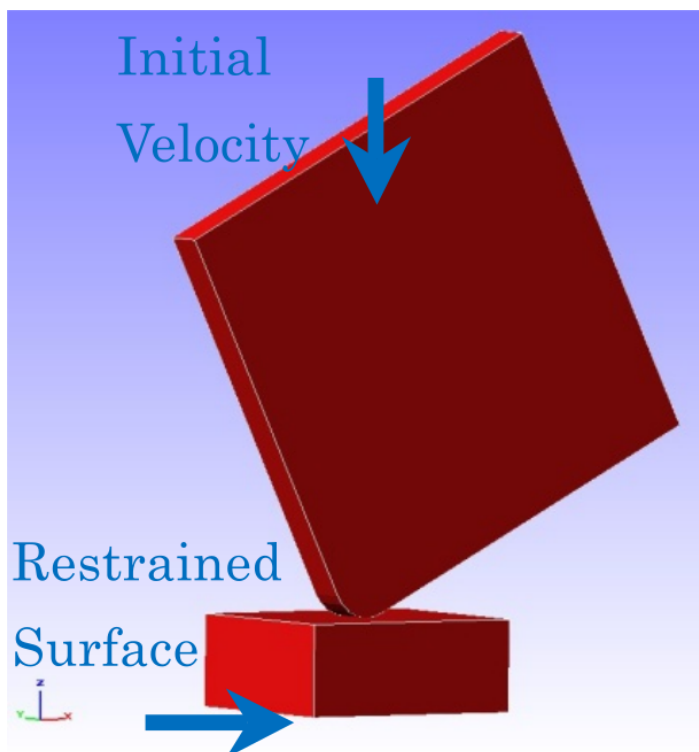


Fig. 4.14.1: Shape of the floor surface and square material

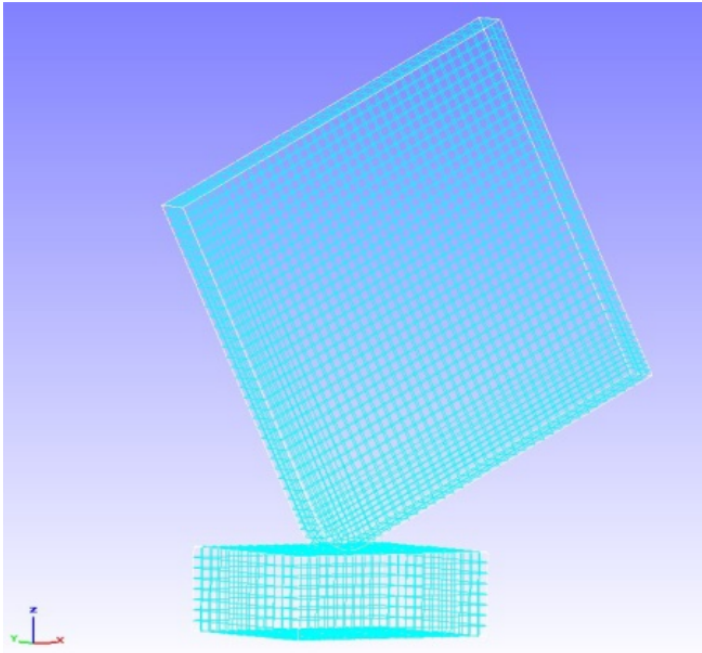


Fig. 4.14.2: Mesh data of the floor surface and square material

### 1.17.2 Analysis content

A contact dynamic analysis is performed with the analysis target (square material) configured with an initial speed of 4427 mm/s. The analysis control data are presented below.

```
!! Control File for FISTR
!VERSION
      3
!WRITE,LOG,FREQUENCY=20
!WRITE,RESULT,FREQUENCY=20
!SOLUTION, TYPE=DYNAMIC
!DYNAMIC, TYPE=NONLINEAR
      1 , 1
      0.0, 1.0, 200, 1.0000e-8
      0.65, 0.330625
      1, 1, 0.0, 0.0
      20, 2621, 1
      1, 1, 1, 1, 1, 1
!BOUNDARY, GRPID = 1
      bottom, 1, 3, 0.0
!VELOCITY, TYPE = INITIAL
      plate, 3, 3, -4427.0
!CONTACT_ALGO, TYPE=SLAGRANGE
!CONTACT, GRPID=1, INTERACTION=FSLID
      CP1, 0.0, 1.0e+5
!STEP, CONVERG=1.0e-8, ITMAX=100
      BOUNDARY, 1
      CONTACT, 1
!MATERIAL, NAME = M1
!ELASTIC
      2.00000e+5, 0.3
!PLASTIC
      1.0e+8, 0.0
!MATERIAL, NAME = M2
!ELASTIC
      1.16992e+5, 0.3
```

```

!PLASTIC
 70.0 , 0.0
!SOLVER,METHOD=MUMPS

```

### 1.17.3 Analysis Results

A contour diagram of a Mises stress of the falling impact is shown in Fig. 4.14.3. Furthermore, a part of the energy output files of the monitoring nodes (dyna\_energy.txt) is shown below as numerical data of the analysis.

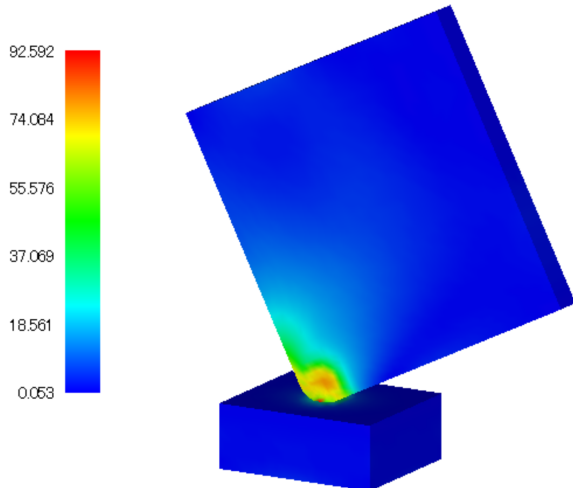


Fig. 4.14.3: Mises stress of the falling impact

## 1.18 Eigenvalue Analysis

This analysis uses the data of tutorial /15\_eigen\_spring.

### 1.18.1 Analysis target

The target of this analysis is the same spring used in Section 4.4, Static Analysis (Hyperelasticity, Part 2).

### 1.18.2 Analysis content

The displacement of the constrained surface shown in Fig. 4.4.1 is restrained, and the eigenvalue analysis is performed up to the fifth order. The analysis control data are presented below.

```

# Control File for FISTR
## Analysis Control
!VERSION
 3
!SOLUTION, TYPE=EIGEN
!EIGEN
 5, 1.0E-8, 60
!WRITE,RESULT
!WRITE,VISUAL
## Solver Control
### Boundary Condition
!BOUNDARY
  XFIX, 1, 1, 0.0
  YFIX, 2, 2, 0.0
  ZFIX, 3, 3, 0.0
### Material
# define in mesh file
### Solver Setting
!SOLVER,METHOD=DIRECT

```

### 1.18.3 Analysis results

The third vibration mode (compression and decompression in y-direction of the spring,) created with REVO-CAP\_PrePost using the analysis result data file spring.res.0.3, is shown in Fig. 4.15.1. The deformation magnification was set to 1000. Furthermore, a list of eigenfrequency output to the analysis result log file is shown below as numerical data of the analysis.

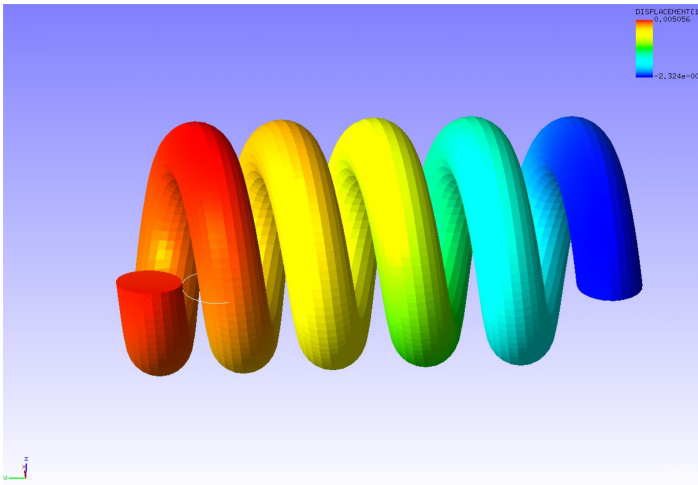


Fig. 4.15.1: Third vibration mode of a spring

```
*****
*RESULT OF EIGEN VALUE ANALYSIS*
*****
```

NUMBER OF ITERATIONS = 7  
TOTAL MASS = 3.4184E-06

EFFECTIVE MASS			ANGLE	FREQUENCY	PARTICIPATION FACTOR		
NO.	EIGENVALUE	FREQUENCY	(HZ)	X	Y	Z	
X	Y	Z					
1	7.8309E+06 1.3005E-06	2.7984E+03 9.7019E-09	4.4537E+02 6.11117E-07	1.0289E+00	-8.8864E-02	-7.0531E-01	
2	7.8718E+06 6.1297E-07	2.8057E+03 1.4597E-08	4.4654E+02 1.2891E-06	6.9690E-01	1.0754E-01	1.0106E+00	
3	3.2601E+07 3.5327E-11	5.7097E+03 2.5942E-06	9.0873E+02 1.0869E-08	4.5547E-03	1.2343E+00	-7.9889E-02	
4	3.8393E+07 7.8507E-10	6.1962E+03 1.2161E-07	9.8616E+02 1.5963E-11	2.8996E-02	-3.6087E-01	-4.1346E-03	
5	1.2966E+08 3.3022E-07	1.1387E+04 4.5327E-09	1.8122E+03 4.0426E-07	5.3557E-01	6.2747E-02	5.9258E-01	

## 1.19 Heat Conduction Analysis

This analysis uses the data of tutorial /16\_heat\_block.

### 1.19.1 Analysis target

The target of this analysis is a perforated block whose shape and mesh data are shown in Figs. 4.16.1 and 4.16.2, respectively. The mesh is a hexahedral primary element with 32160 elements and 37386 nodes.

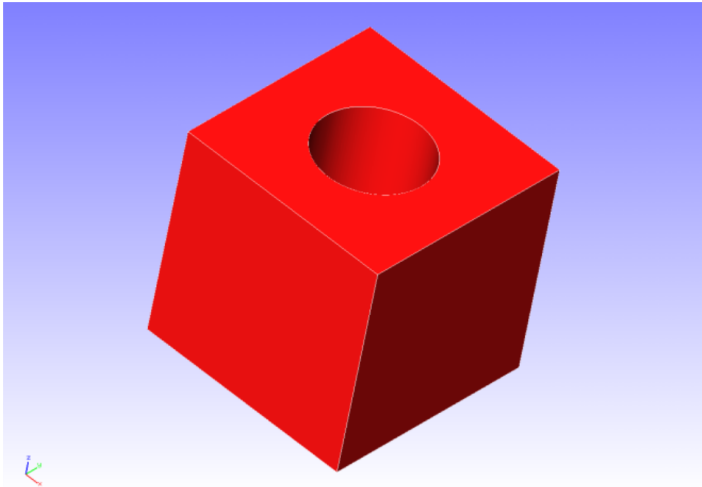


Fig. 4.16.1: Shape of the perforated block

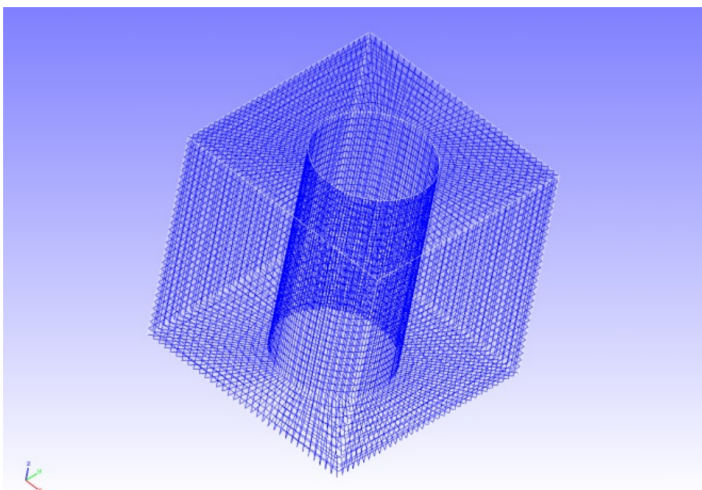


Fig. 4.16.2: Mesh data of the perforated block

### 1.19.2 Analysis content

This is a steady-state heat conduction analysis wherein a heat source is provided to the cylindric internal surface of the analysis target. The analysis control data are presented below.

```
# Control File for FISTR
## Analysis Control
!VERSION
 3
!SOLUTION, TYPE=HEAT
!HEAT
 0.0
!WRITE,RESULT
!WRITE,VISUAL
## Solver Control
### Boundary Condition
!FIXTEMP
FTMPC, 100.0
FTMPS1, 20.0
FTMPS2, 20.0
FTMPS3, 20.0
FTMPS4, 20.0
### Material
# define in mesh file
```

```

### Solver Setting
!SOLVER,METHOD=CG,PRECOND=1,ITERLOG=YES,TIMELOG=YES
100, 1
1.0e-8, 1.0, 0.0

```

### 1.19.3 Analysis results

This analysis uses the data of tutorial /17\_freq\_beam. The first step of the analysis is to change the overall control data for eigenvalue analysis, hecmw\_ctrl\_eigen.dat, to hecmw\_ctrl.dat and perform eigenvalue analysis. Further, change the overall control data for frequency response analysis, hecmw\_ctrl\_freq.dat, to hecmw\_ctrl.dat, and the eigenvalue analysis result log file, 0.log, to ‘eigen\_0.log’ (which is specified within the analysis control data for frequency response analysis.) Finally, frequency response analysis is performed.

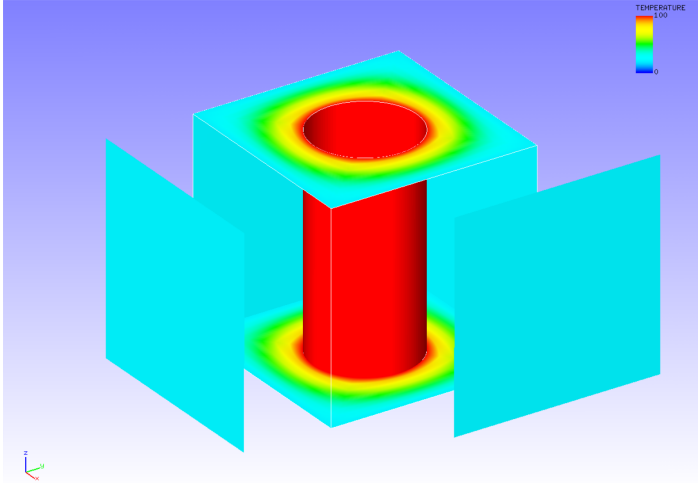


Fig. 4.16.3: Analysis results of temperature

```

ISTEP =      1
Time   =     0.000
Maximum Temperature :    100.000
Maximum Node No.    :        9
Minimum Temperature :    20.000
Minimum Node No.    :       85

```

## 1.20 Frequency Response Analysis

This analysis uses the data of tutorial /17\_freq\_beam. The first step of the analysis is to change the overall control data for eigenvalue analysis, hecmw\_ctrl\_eigen.dat, to hecmw\_ctrl.dat and perform eigenvalue analysis. Further, change the overall control data for frequency response analysis, hecmw\_ctrl\_freq.dat, to hecmw\_ctrl.dat, and the eigenvalue analysis result log file, 0.log, to eigen\_0.log (which is specified within the analysis control data for frequency response analysis.) Finally, frequency response analysis is performed.

### 1.20.1 Analysis target

The target of this analysis is a cantilever whose shape and mesh data are shown in Figs. 4.17.1 and 4.17.2, respectively. The mesh is a tetrahedral primary element with 126 element and 55 nodes.

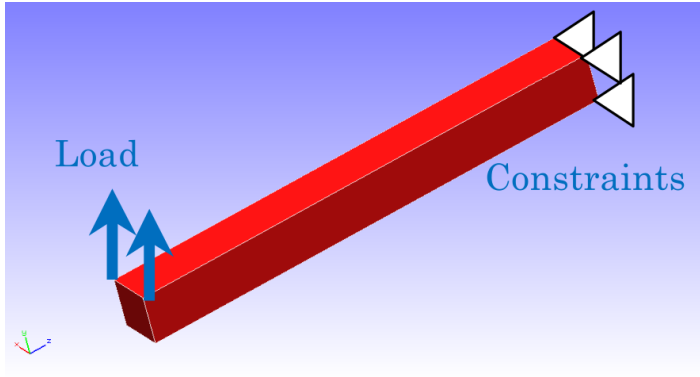


Fig. 4.17.1 : Shape of the cantilever

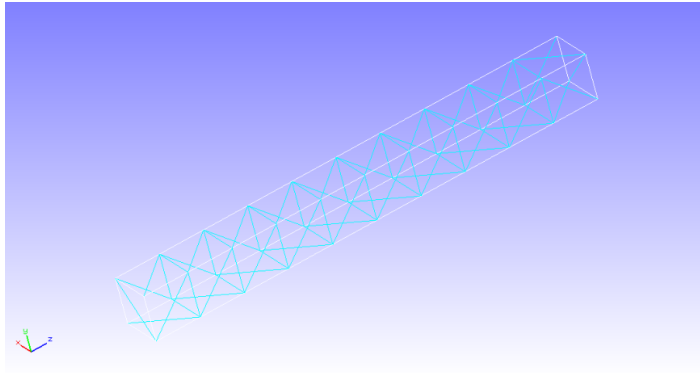


Fig. 4.17.2 : Mesh data of the cantilever

### 1.20.2 Analysis content

This is a frequency response analysis in which the edge of the cantilever was fully restrained, and concentrated load was added to two nodes on the opposite edge. After performing eigenvalue analysis up to the tenth order with the same boundary conditions, the frequency response analysis was conducted with the eigenvalues and eigenvectors up to the fifth order. The analysis control data for frequency response analysis is shown below.

```
# Control File for FISTR
!VERSION
 3
!WRITE,RESULT
!WRITE,VISUAL
!SOLUTION, TYPE=DYNAMIC
!DYNAMIC
 11 , 2
 14000, 16000, 20, 15000.0
 0.0, 6.6e-5
 1, 1, 0.0, 7.2E-7
 10, 2, 1
 1, 1, 1, 1, 1, 1
!EIGENREAD
 eigen_0.log
 1, 5
!BOUNDARY
 _PickedSet4, 1, 3, 0.0
!FLOAD, LOAD CASE=2
 _PickedSet5, 2, 1.
!FLOAD, LOAD CASE=2
 _PickedSet6, 2, 1.
!SOLVER, METHOD=CG, PRECOND=1, ITERLOG=NO, TIMELOG=YES
 10000, 2
```

1.0e-8, 1.0, 0.0

### 1.20.3 Analysis results

The relationship between frequency and displacement amplitude of the monitoring nodes, specified with analysis control data (nodal number 1) and created with Microsoft Excel, is shown in Fig. 4.17.3. Furthermore, a part of the log files of the analysis results is shown below as numerical data of the analysis.

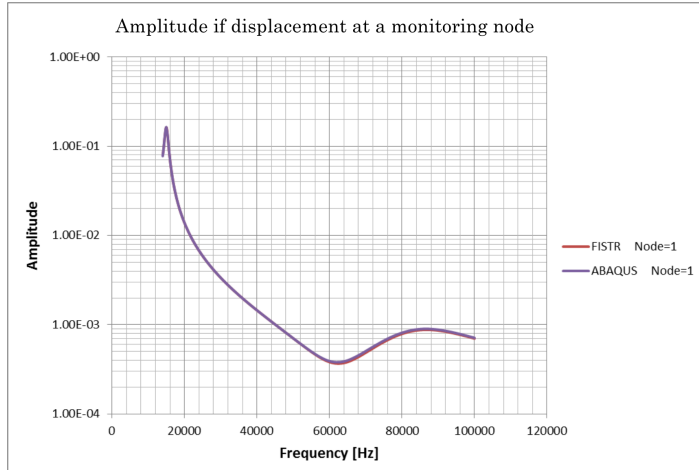


Fig.4.17.3 Relationship between frequency and displacement amplitude of the monitoring nodes

```

Rayleigh alpha: 0.000000000000000
Rayleigh beta: 7.199999999999999E-007
read from=eigen_0.log
start mode= 1
end mode= 5
start frequency: 14000.00000000000
end frequency: 16000.00000000000
number of the sampling points 20
monitor nodeid= 1
 14100.000000000000 [Hz] : 8.3957630463152688E-002
 14100.000000000000 [Hz] : 1 .res
 14200.000000000000 [Hz] : 9.1237051959262350E-002
 14200.000000000000 [Hz] : 2 .res
 14300.000000000000 [Hz] : 9.9610213760033539E-002
 14300.000000000000 [Hz] : 3 .res
 14400.000000000000 [Hz] : 0.10918495323840580
 14400.000000000000 [Hz] : 4 .res
 14500.000000000000 [Hz] : 0.11996212788265602
 14500.000000000000 [Hz] : 5 .res
 14600.000000000000 [Hz] : 0.13169277524043285
 14600.000000000000 [Hz] : 6 .res
 14700.000000000000 [Hz] : 0.14365135321213662
 14700.000000000000 [Hz] : 7 .res
 14800.000000000000 [Hz] : 0.15439888482329628
 14800.000000000000 [Hz] : 8 .res
 14900.000000000000 [Hz] : 0.16182392983620905
 14900.000000000000 [Hz] : 9 .res

```

## 1.21 Verification by Simple-Shaped Model

### 1.21.1 Elastic static analysis

This verification was performed with a mesh-divided cantilever, as shown in Fig. 9.1.1. The analysis was performed with seven load conditions, exA-exG, as illustrated in Fig. 9.1.2. Please note that exG has the same load conditions as those of exA using the direct method solver.

The verification result of each load condition is presented in Tables 9.1.1–9.1.7.

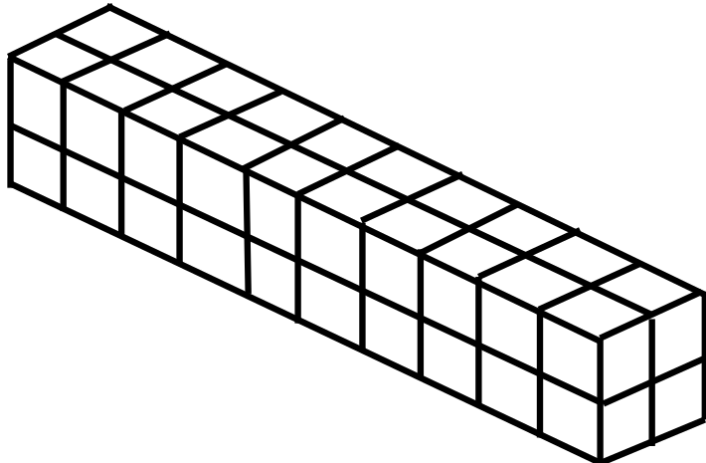
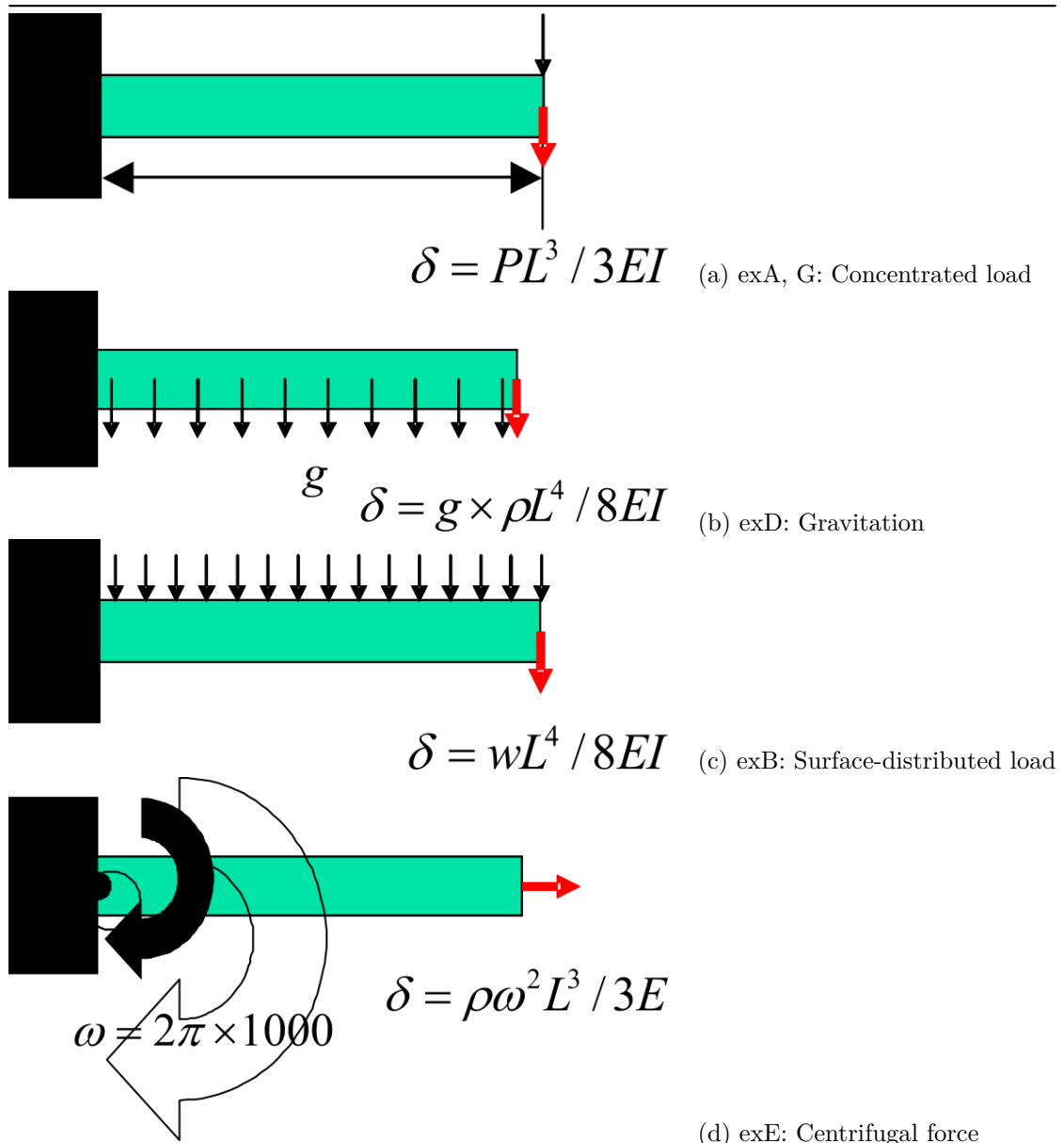
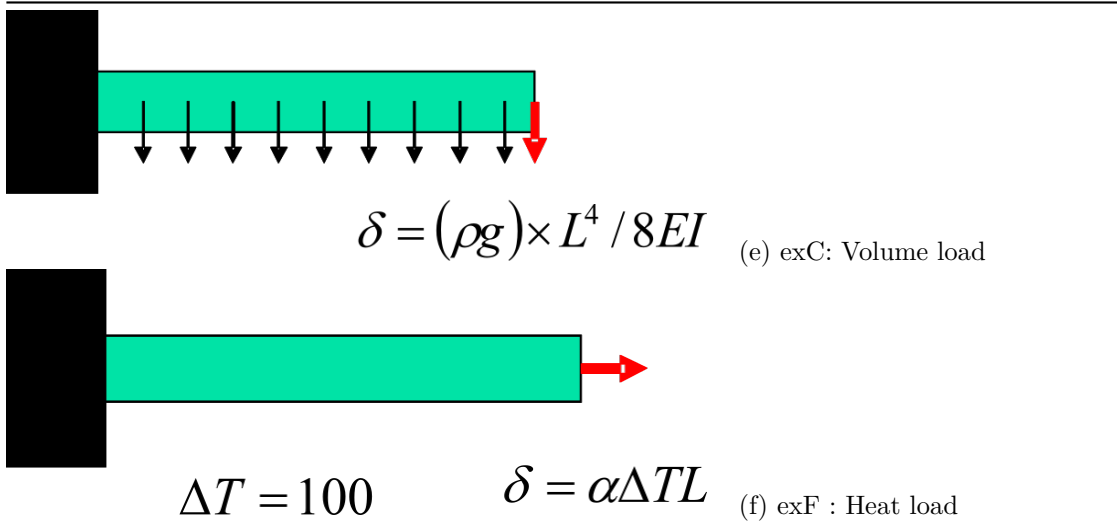


Fig. 9.1.1: Example of Mesh Partitioned Cantilever Beam (Hexahedral Element)





Item	Value
Young's Modulus	$E = 4000.0 \text{ kgf/mm}^2$
Length	$L = 10.0 \text{ mm}$
Poisson's Ratio	$\nu = 0.3$
Sectional area	$A = 1.0 \text{ mm}^2$
Mass density	$\rho = 8.0102 \times 10^{-10} \text{ kg s}^2/\text{mm}^4$
Second moment of area	$I = 1.0/12.0 \text{ mm}^4$
Gravitational acceleration	$g = 9800.0 \text{ mm/s}^2$
Linear coefficient of thermal expansion	$\alpha = 1.0 \times 10^{-5}$

Fig. 9.1.2: Verification conditions of the cantilever model

Table 9.1.1: exA: Verification results of the concentrated load problem

Case Name	Number of elements	NAS-TRAN	Predi-cated Value : $\delta_{max} = -1.000$	ABAQUS	Fron-tISTR	Remarks
A231	40	-0.338	-0.371	-0.371		33 nodes / plane stress status problem
A232	40		-0.942	-1.002	-1.002	105 nodes / plane stress status problem
A241	20		-0.720	-0.711	-0.711	33 nodes / plane stress status problem
A242	20		-0.910	-1.002	-1.002	85 nodes / plane stress status problem
A341	240		-0.384	-0.384	-0.386	99 nodes
A342	240		-0.990	-0.990	-0.999	525 nodes
A351	80		-0.353	-0.355	-0.351	99 nodes
A352	80		-0.993	-0.993	-0.992	381 nodes
A361	40		-0.954	-0.985	-0.984	99 nodes

Case Name	Number of elements			Predicated Value : $\delta_{max} =$ -1.000	Remarks
A362	40	-0.994	-0.993	-0.993	220 nodes
A731	40	-	-	-0.991	33 nodes / direct method
A741	20	-	-	-0.996	33 nodes / direct method

Table 9.1.2: exB: Verification results of the surface-distributed load problem

Case name	Number of elements	NASTRAN	ABAQUS	Predicated value : $\delta_{max} =$ -3.750	FrontISTR	Remarks
B231	40	-1.281	-1.403	-	-1.403	33 nodes / plane stress status problem
B232	40	-3.579	-3.763	-	-3.763	105 nodes / plane stress status problem
B241	20	-3.198	-2.680	-	-2.680	33 nodes / plane stress status problem
B242	20	-3.426	-3.765	-	-3.765	85 nodes / plane stress status problem
B341	240	-1.088	-1.449	-	-1.454	99 nodes
B342	240	-3.704	-3.704	-	-3.748	525 nodes
B351	80	-3.547	-1.338	-	-1.325	99 nodes
B352	80	-0.3717	-3.716	-	-3.713	381 nodes
B361	40	-3.557	-3.691	-	-3.688	99 nodes
B362	40	-3.726	-3.717	-	-3.717	220 nodes
B731	40	-	-	-	-3.722	33 nodes / direct method
B741	20	-	-	-	-3.743	33 nodes / direct method

Table 9.1.3: exC: Verification results of the volume load problem

Case Name	Number of elements	NASTRAN	ABAQUS	Predicated Value : $\delta_{max} =$ $-2.944^{-5}$	FrontISTR	Remarks
C231	40	-	-1.101e-5	-	-1.101e-5	33 nodes / plane stress problem
C232	40	-	-2.951e-5	-	-2.951e-5	105 nodes / plane stress problem
C241	20	-	-2.102e-5	-	-2.102e-5	33 nodes / plane stress problem

Case Name	Number of elements		Predicated Value : $\delta_{max} = -2.944^{-5}$		Remarks
C242	20	-	-2.953e-5	-2.953e-5	85 nodes / plane stress problem
C341	240	-	-1.136e-5	-1.140e-5	99 nodes
C342	240	-	-2.905e-5	-2.937e-5	525 nodes
C351	80	-	-1.050e-5	-1.039e-5	99 nodes
C352	80	-	-2.914e-5	-2.911e-5	381 nodes
C361	40	-	-2.895e-5	-2.893e-5	99 nodes
C362	40	-	-2.915e-5	-2.915e-5	220 nodes
C731	40	-	-	-2.922e-5	33 nodes / direct method
C741	20	-	-	-2.938e-5	33 nodes / direct method

Table 9.1.4: exD: Verification results of the gravitation problem

Case name	Number of elements	NASTRAN	ABAQUS	Predicated Value : $\delta_{max} = -2.944^{-5}$	Remarks
D231	40	-1.101e-5	-1.101e-5	-1.101e-5	33 nodes / plane stress status problem
D232	40	-2.805e-5	-2.951e-5	-2.951e-5	105 nodes / plane stress status problem
D241	20	-2.508e-5	-2.102e-5	-2.102e-5	33 nodes / plane stress status problem
D242	20	-2.684e-5	-2.953e-5	-2.953e-5	85 nodes / plane stress status problem
D341	240	-1.172e-5	-1.136e-5	-1.140e-5	99 nodes
D342	240	-2.906e-5	-2.905e-5	-2.937e-5	525 nodes
D351	80	-1.046e-5	-1.050e-5	-1.039e-5	99 nodes
D352	80	-2.917e-5	-2.914e-5	-2.911e-5	381 nodes
D361	40	-2.800e-5	-2.895e-5	-2.893e-5	99 nodes
D362	40	-2.919e-5	-2.915e-5	-2.915e-5	220 nodes
D731	40	-	-	-2.922e-5	33 nodes / direct method
D741	20	-	-	-2.938e-5	33 nodes / direct method

Table 9.1.5: exE: Verification results of the centrifugal force problem

Case name	Number of elements	NASTRAN	ABAQUS	Predicated value : $\delta_{max} = 2.635^{-3}$	Remarks
E231	40	2.410e-3	2.616e-3	2.650e-3	33 nodes / plane stress status problem

Case name	Number of elements		Predicated value : $\delta_{max} = 2.635^{-3}$		Remarks
E232	40	2.447e-3	2.627e-3	2.628e-3	105 nodes / plane stress status problem
E241	20	2.386e-3	2.622e-3	2.624e-3	33 nodes / plane stress status problem
E242	20	2.387e-3	2.627e-3	2.629e-3	85 nodes / plane stress status problem
E341	240	2.708e-3	2.579e-3	2.625e-3	99 nodes
E342	240	2.639e-3	2.614e-3	2.638e-3	525 nodes
E351	80	2.642e-3	2.598e-3	2.625e-3	99 nodes
E352	80	2.664e-3	2.617e-3	2.616e-3	381 nodes
E361	40	2.611e-3	2.603e-3	2.603e-3	99 nodes
E362	40	2.623e-3	2.616e-3	2.616e-3	220 nodes
E731	40	-	-	2.619e-3	33 nodes / direct method
E741	20	-	-	2.622e-3	33 nodes / direct method

Table 9.1.6: exF: Verification results of the thermal stress load problem

Case name	Number of elements	NASTRAN	Predicated Value : $\delta_{max} = 1.000^{-2}$	ABAQUS	FrontISTR	Remarks
F231	40	-	1.016e-2	1.007e-2	1.007e-2	33 nodes / plane stress status problem
F232	40	-	1.007e-2	1.007e-2	1.007e-2	105 nodes / plane stress status problem
F241	20	-	1.010e-2	1.010e-2	1.010e-2	33 nodes / plane stress status problem
F242	20	-	1.006e-2	1.006e-2	1.006e-2	85 nodes / plane stress status problem
F341	240	-	1.047e-2	1.083e-2	1.083e-2	99 nodes
F342	240	-	1.018e-2	1.022e-2	1.022e-2	525 nodes
F351	80	-	1.031e-2	1.062e-2	1.062e-2	99 nodes
F352	80	-	1.015e-2	1.017e-2	1.017e-2	381 nodes
F361	40	-	1.026e-2	1.026e-2	1.026e-2	99 nodes
F362	40	-	1.016e-2	1.016e-2	1.016e-2	220 nodes

Table 9.1.7: exG: Verification results of the direct method (concentrated load problem)

Case name	Number of elements	Predicated value : $\delta_{max} = -1.000$			Remarks
		NASTRAN	ABAQUS	FrontISTR	
G231	40	-0.338	-0.371	-0.371	33 nodes / plane stress status problem
G232	40	-0.942	-1.002	-1.002	105 nodes / plane stress status problem
G241	20	-0.720	-0.711	-0.711	33 nodes / plane stress status problem
G242	20	-0.910	-1.002	-1.002	85 nodes / plane stress status problem
G341	240	-0.384	-0.384	-0.386	99 nodes
G342	240	-0.990	-0.990	-0.999	52 nodes
G351	80	-0.353	-0.355	-0.351	99 nodes
G352	80	-0.993	-0.993	-0.992	381 nodes
G361	40	-0.954	-0.985	-0.984	99 nodes
G362	40	-0.994	-0.993	-0.993	220 nodes
G731	40	-	-	-0.991	33 nodes / direct method
G741	20	-	-	-0.996	33 nodes / dierct method

## 1.21.2 Non-linear static analysis

### 1.21.2.1 (2-1) exnl1: Geometrical non-linear analysis

The verification model of exI is the same as those of exA–G. A schematic diagram of the verification model is shown in Fig. 9.1.3. A geometric non-linear analysis was performed on this model. The verification results are presented in Table 9.1.8.

The non-linear calculation is a ten-step process with an increment value of 0.1 P and a final load of 1.0 P.



Fig. 9.1.3: Verification model

Table 9.1.8: exI: Verification results (maximum deflection amount log)

Case Name	0.1	0.2	0.3	0.4	0.5	0.6	0.7	0.8	0.9	1.0	Linear Solution
I231	-	-	-	-	-	-	-	-	-	-	-
I232	-	-	-	-	-	-	-	-	-	-	-
I241	-	-	-	-	-	-	-	-	-	-	-
I242	-	-	-	-	-	-	-	-	-	-	-
I341	0.039	0.077	0.116	0.154	0.193	0.232	0.270	0.309	0.348	0.386	0.386
I342	0.099	0.200	0.300	0.400	0.499	0.599	0.698	0.797	0.896	0.995	0.999
I351	0.035	0.070	0.105	0.141	0.176	0.211	0.246	0.281	0.316	0.351	0.351
I352	0.099	0.198	0.298	0.397	0.496	0.595	0.693	0.792	0.890	0.987	0.992
I361	0.070	0.139	0.209	0.278	0.348	0.417	0.487	0.556	0.625	0.694	0.984
I362	0.099	0.197	0.298	0.397	0.496	0.595	0.694	0.793	0.891	0.988	0.993

### 1.21.2.2 (2-2) exnl2: Elastoplasticity deformation analysis

Based on the test conducted at National Agency for Finite Element Methods and Standards (NAFEMS; U.K.): Test NL1, this verification problem was verified by elastoplastic deformation analysis that incorporated geometric non-linearity and multiple hardening rules. The elastoplastic deformation analysis model is shown in Fig. 9.1.4.

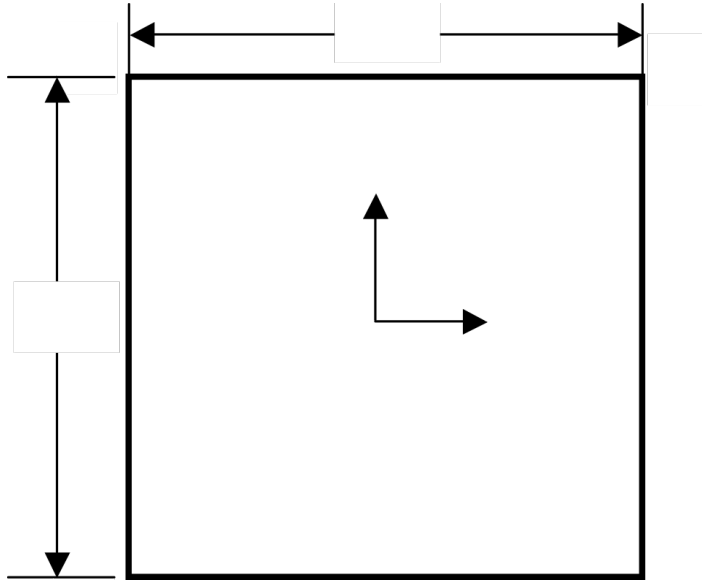


Fig. 9.1.4: Elastoplasticity deformation analysis Model

(1) Verification conditions:

Item	Value
Material	Mises elastoplastic material
Young's Modulus	$E = 250GPa$
Poisson's Ratio	$\nu = 0.25$
Initial yield stress	$5MPa$
Initial yield strain	$0.25 \times 10^{-4}$
Isotropic hardening factor	$H_i = 0$ or $62.5GPa$

(2) Boundary conditions

Item	Boundary conditions	Value
step 1	Forced displacement in nodes 2 and 3	$u_x = 0.2500031251 * 10^{-4}$
step 2	Forced displacement in nodes 2 and 3	$u_x = 0.25000937518 * 10^{-4}$
step 3	Forced displacement in nodes 3 and 4	$u_y = 0.2500031251 * 10^{-4}$
step 4	Forced displacement in nodes 3 and 4	$u_y = 0.25000937518 * 10^{-4}$
step 5	Forced displacement in nodes 2 and 3	$u_x = -0.25000937518 * 10^{-4}$
step 6	Forced displacement in nodes 2 and 3	$u_x = -0.2500031251 * 10^{-4}$
step 7	Forced displacement in nodes 3 and 4	$u_y = -0.25000937518 * 10^{-4}$
step 8	Forced displacement in nodes 3 and 4	$u_y = -0.2500031251 * 10^{-4}$

All the nodes that are not mentioned here are fully constrained. The theoretical solution for this problem is presented as follows:

Strain ( $\times 10^{-4}$ ) $[\varepsilon_x, \varepsilon_y, \varepsilon_z]$	Equivalent Stress (MPa) $[H_i = 0 H_k = 0; H_i = 62.5 H_k = 0]$
0.25, 0, 0	5.0; 5.0
0.50, 0, 0	5.0; 5.862
0.50, 0.25, 0	5.0; 5.482
0.50, 0.50, 0	5.0; 6.362

Strain ( $\times 10^{-4}$ ) [ $\varepsilon_x, \varepsilon_y, \varepsilon_z$ ]	Equivalent Stress (MPa) [ $H_i = 0 H_k = 0; H_i = 62.5 H_k = 0$ ]
0.25, 0.50, 0	5.0; 6.640
0, 0.50, 0	5.0; 7.322
0, 0.25, 0	3.917; 4.230
0, 0, 0	5.0; 5.673

The results of the calculations are as follows:

Strain ( $\times 10^{-4}$ ) [ $\varepsilon_x, \varepsilon_y, \varepsilon_z$ ]	Equivalent Stress (MPa) [ $H_i = 0 H_k = 0; H_i = 62.5 H_k = 0$ ]
0.25, 0, 0	5.0 (0.0%); 5.0 (0.0%)
0.50, 0, 0	5.0 (0.0%); 5.862 (0.0%)
0.50, 0.25, 0	5.0 (0.0%); 5.482 (0.0%)
0.50, 0.50, 0	5.0 (0.0%); 6.362 (-0.05%)
0.25, 0.50, 0	5.0 (0.0%); 6.640 (-0.21%)
0, 0.50, 0	5.0 (0.0%); 7.322 (-0.34%)
0, 0.25, 0	3.824 (-2.4%); 4.230 (-2.70%)
0, 0, 0	5.0 (0.0%); 5.673 (5.673 (-2.50%))

### 1.21.3 Contact analysis (1)

Based on the contact patch test problem (CGS-4) from NAFEMS (U.K.), this verification problem tests the finite sliding contact problem function with friction. The contact analysis model is shown in Fig. 9.1.5

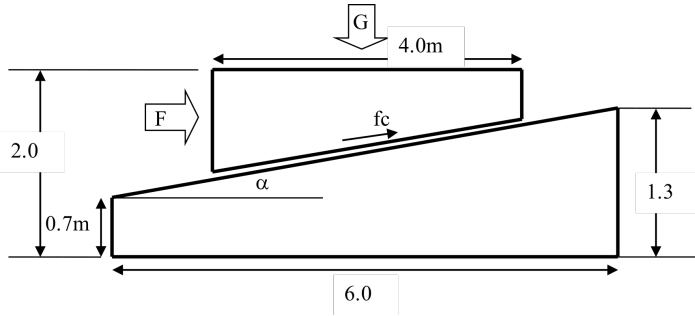


Fig. 9.1.5: Contact analysis model

The equilibrium condition of this problem is as follows:

$$F \cos \alpha - G \sin \alpha = \pm f_c$$

In the adhesive friction stage, the frictional force is as follows:

$$f_c = E_t \Delta u$$

In the sliding friction stage, the frictional force is as follows:

$$f_c = \mu(G \cos \alpha + F \sin \alpha)$$

The comparison between the calculation results and the analysis solution is as follows.

$\mu$	$F/G$ Analysis Solution	$F/G$ Calculation Results
0.0	0.1	0.1
0.1	0.202	0.202
0.2	0.306	0.306
0.3	0.412	0.412

#### 1.21.4 Contact analysis (2): Hertz contact problem

In this verification, the Hertz contact problem between a cylinder of infinite length and an infinite plane was analyzed. The cylinder's radius was  $R=8$  mm, and the deformable body's Young's modulus  $E$  and Poisson's ratio  $\mu$  were 1100 MPa and 0.0, respectively. Moreover, assuming that the contact area was much smaller than the cylinder's radius, and also considering the symmetry of the problem, the analysis was performed with a quarter model of the cylinder.

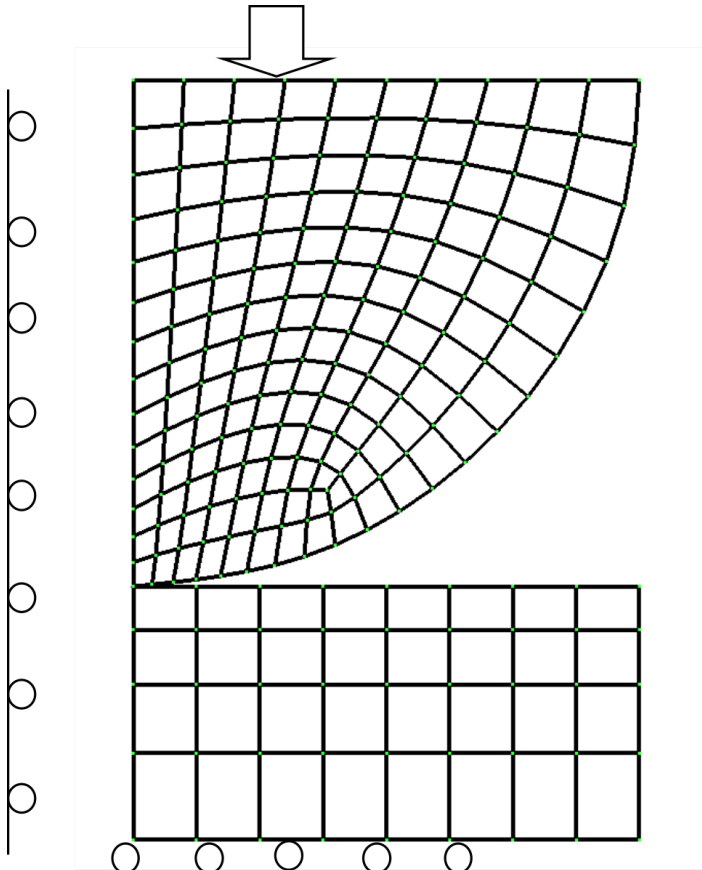


Fig. 9.1.6: Hertz contact problem analysis model

##### 1.21.4.1 (1) Verification results of contact radius

The theoretical formula to calculate the contact radius is as follows:

$$a = \sqrt{\frac{4FR}{\pi E^*}}$$

where

$$E^* = \frac{E}{2(1 - \mu^2)}$$

With the actual calculation, when the pressure is  $F = 100$ , the contact radius is  $a = 1.36$ .

Fig. 9.1.7 shows the equivalent nodal force of the contact point. The contact radius is obtained by extrapolating this nodal force distribution.

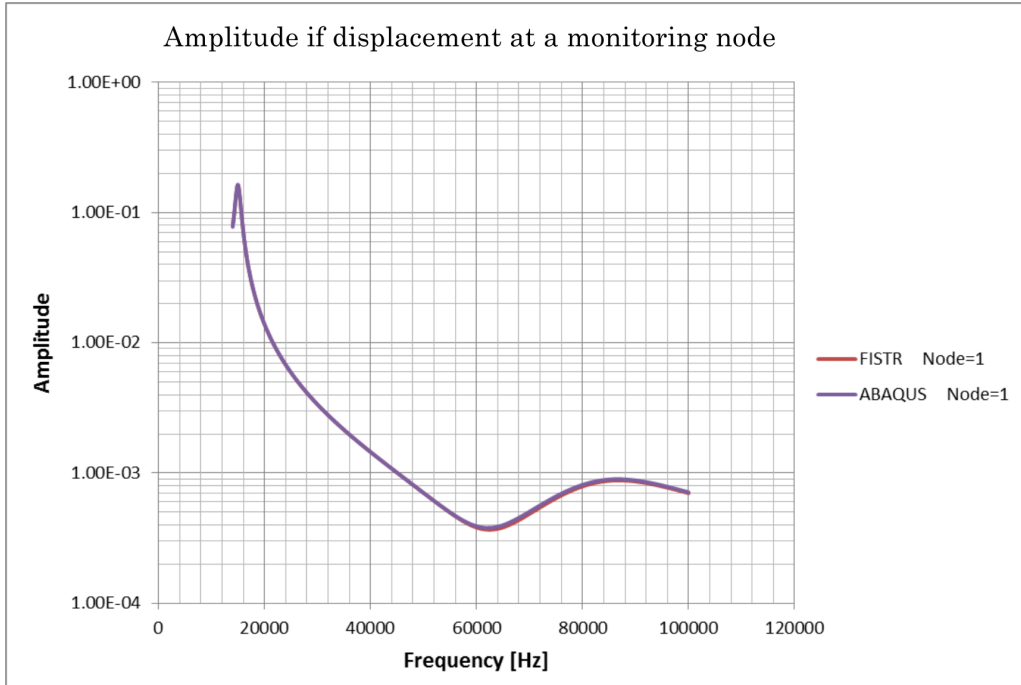


Fig. 9.1.7: Equivalent nodal force distribution of the contact point

#### 1.21.4.2 (2) Verification results of maximum shear stress

With the theoretical solution, when the contact position is  $z = 0.78a$ , the maximum shear stress is as follows:

$$\tau_{max} = 0.30 \sqrt{\frac{FE^*}{\pi R}}$$

With the actual calculation conditions, it becomes

$$\tau_{max} = 14.2$$

The actual result obtained was

$$\tau_{max} = 15.6$$

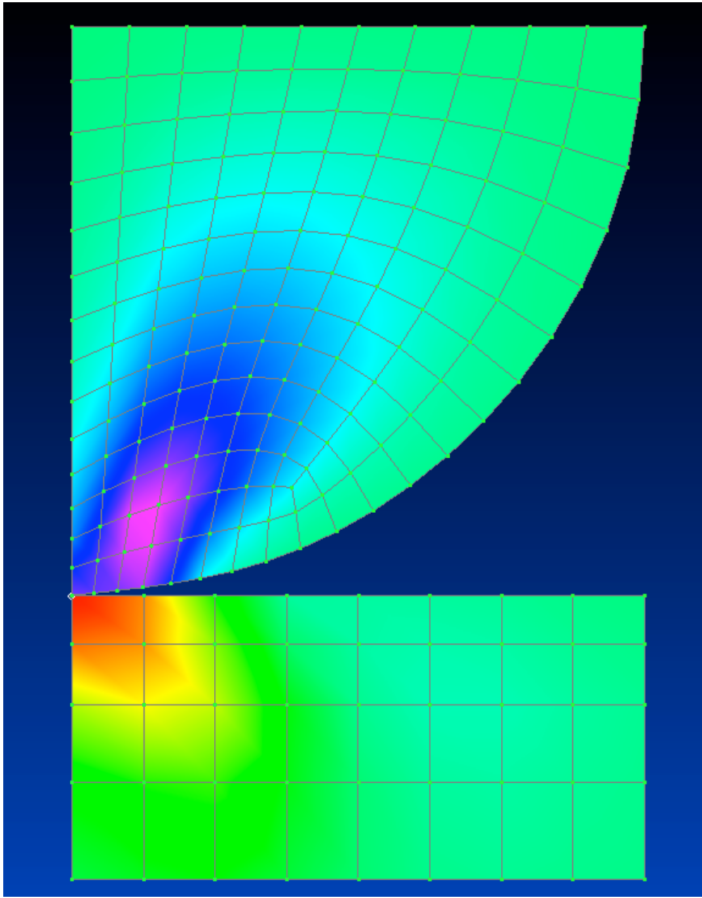


Fig. 9.1.8: Shear stress distribution (maximum value = 15.6)

### 1.21.5 (3) Eigenvalue analysis

The verification models of exJ and exK are the same as those of exA–G. A schematic diagram of the verification model is shown in Fig. 9.1.9. An eigenvalue analysis was performed for this model to determine the primary, secondary, and tertiary eigenvalues. The iteration and direct method solvers were used for exJ and exK, respectively. Furthermore, the verification results are presented in Tables 9.1.9–9.1.12.



Fig. 9.1.9: Verification Model

The vibration eigenvalue of the cantilever is determined by the following equations:

Primary :

$$n_1 = \frac{1.875^2}{2\pi l^2} \sqrt{\frac{gEI}{\omega}}$$

Secondary :

$$n_2 = \frac{4.694^2}{2\pi l^2} \sqrt{\frac{gEI}{\omega}}$$

Tertiary :

$$n_3 = \frac{7.855^2}{2\pi l^2} \sqrt{\frac{gEI}{\omega}}$$

The property values of the verification model are:

Item	Value
$I$	10.0mm
$E$	4000.0kgf/mm <sup>2</sup>
$l$	1.0/12.0mm <sup>4</sup>
$\omega$	7.85 * 10 <sup>-6</sup> kgf/mm <sup>3</sup>
$g$	9800.0mm/sec <sup>2</sup>

Therefore, the primary to tertiary eigenvalue are as follows:

Mode number	Value
$n_1$	3.609e3
$n_2$	2.262e4
$n_3$	6.335e4

Table 9.1.9: exJ: Iteration method verification results with the primary eigenvalue

Case Name	Number of elements	Predicated value : n1=3.609e3	Remarks		
NASTRAN	FrontISTR				
J231	40	5.861e3	5.861e3	33 nodes / plane stress status problem	
J232	40	3.596e3	3.593e3	105 nodes / plane stress status problem	
J241	20	3.586e3	4.245e3	33 nodes / plane stress status problem	
J242	20	3.590e3	3.587e3	85 nodes / plane stress status problem	
J341	240	5.442e3	5.429e3	99 nodes	
J342	240	3.621e3	3.595e3	525 nodes	
J351	80	3.695e3	4.298e3	99 nodes	
J352	80	3.610e3	3.609e3	381 nodes	
J361	40	3.679e3	3.619e3	99 nodes	
J362	40	3.611e3	3.606e3	220 nodes	

Table 9.1.10: Iteration method verification results of exJ with the secondary eigenvalue

Case name	Number of elements	Predicated value : n2=2.262e4	Remarks		
NASTRAN	FrontISTR				
J231	40	3.350e4	3.351e4	33 nodes / plane stress status problem	
J232	40	2.163e4	2.156e4	105 nodes / plane stress status problem	
J241	20	2.149e4	2.516e4	33 nodes / plane stress status problem	
J242	20	2.149e4	2.143e4	85 nodes / plane stress status problem	
J341	240	3.145e4	3.138e4	99 nodes	
J342	240	2.171e4	2.155e4	525 nodes	
J351	80	2.208e4	2.546e4	99 nodes	
J352	80	2.156e4	2.149e4	381 nodes	
J361	40	2.202e4	2.168e4	99 nodes	
J362	40	2.154e4	2.144e4	220 nodes	

Note: In the three-dimensional (3D) models, the primary and secondary values have equal roots.  
Therefore, the secondary value in the table represents the tertiary calculation value.

Table 9.1.11: Direct method verification results of exK with the primary eigenvalue

Case name	Number of elements	Predicated Value : n1=3.609e3		Remarks
		NASTRAN	FrontISTR	
J231	40	5.861e3	5.861e3	33 nodes / plane stress status problem
J232	40	3.596e3	3.593e3	105 nodes / plane stress status problem
J241	20	3.586e3	4.245e3	33 nodes / plane stress status problem
J242	20	3.590e3	3.587e3	85 nodes / plane stress status problem
J341	240	5.442e3	5.429e3	99 nodes
J342	240	3.621e3	3.595e3	525 nodes
J351	80	3.695e3	4.298e3	99 nodes
J352	80	3.610e3	3.609e3	381 nodes
J361	40	3.679e3	3.619e3	99 nodes
J362	40	3.611e3	3.606e3	220 nodes
J731	40	-	3.606e3	220 nodes
J741	20	-	3.594e3	220 nodes

Table 9.1.12: Direct method verification results of exK with the secondary eigenvalue

Case name	Number of elements	Predicated value : n2=2.262e4		Remarks
		NASTRAN	FrontISTR	
J231	40	3.350e4	3.351e4	33 nodes / plane stress status problem
J232	40	2.163e4	2.156e4	105 nodes / plane stress status problem
J241	20	2.149e4	2.516e4	33 nodes / plane stress status problem
J242	20	2.149e4	2.143e4	85 nodes / plane stress status problem
J341	240	3.145e4	3.138e4	99 nodes
J342	240	2.171e4	2.155e4	525 nodes
J351	80	2.208e4	2.546e4	99 nodes
J352	80	2.156e4	2.149e4	381 nodes
J361	40	2.202e4	2.168e4	99 nodes
J362	40	2.154e4	2.144e4	220 nodes
J731	40	-	2.156e4	220 nodes
J741	20	-	2.153e4	220 nodes

Note: In the 3D models, the primary and secondary values have equal roots. Therefore, the secondary value in the table represents the tertiary calculation value.

### 1.21.6 (4) Heat conduction analysis

The common conditions for the steady-state heat conduction analysis are shown in Fig. 9.1.10. The individual conditions for the verification cases exM-exT are shown in Fig. 9.1.11. The mesh division used here is equivalent to that of exA.

The verification results (temperature distribution table) of each case are presented in Tables 9.1.13–9.1.20.

$$\begin{aligned} \text{Length between AB} &= L = 10.0m \\ \text{Cross-sectional area} &= A = 1.0mm^2 \end{aligned}$$

Temperature dependency of thermal conductivity

Thermal conductivity $\lambda(W/mK)$	Temperature ( $^{\circ}C$ )
50.0	0.0
35.0	500.0
20.0	1000.0

Fig. 9.1.10: Verification conditions of steady-heat conduction analysis

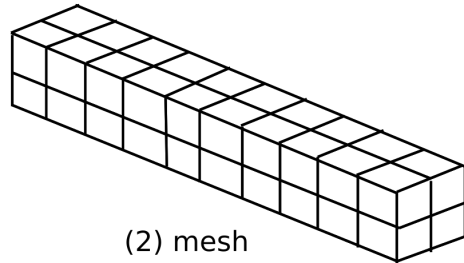
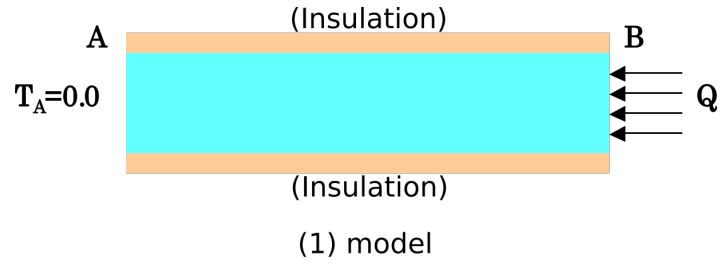
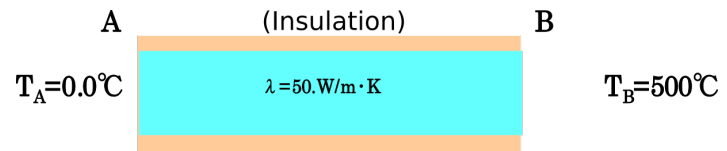
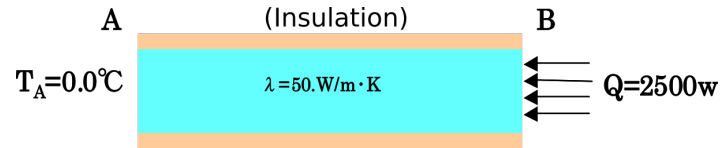


Figure 2: Heat conduction analysis

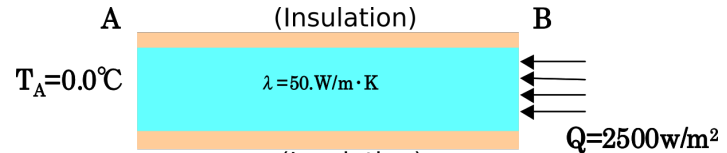
exM: Linear material



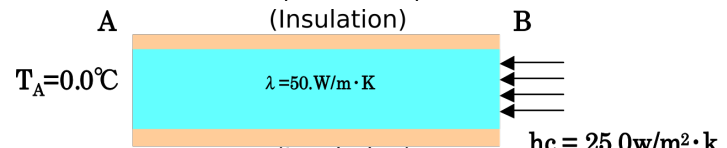
exN: Specified temperature problem



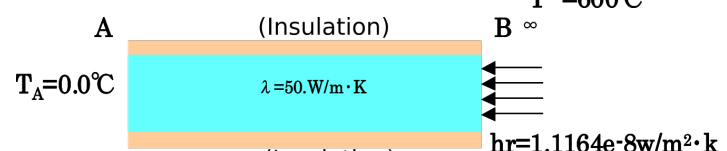
exO: Concentrated heat flux problem



exP: Distributed heat flux problem



exQ: Convective heat transfer problem



exR: Radiant heat transfer problem

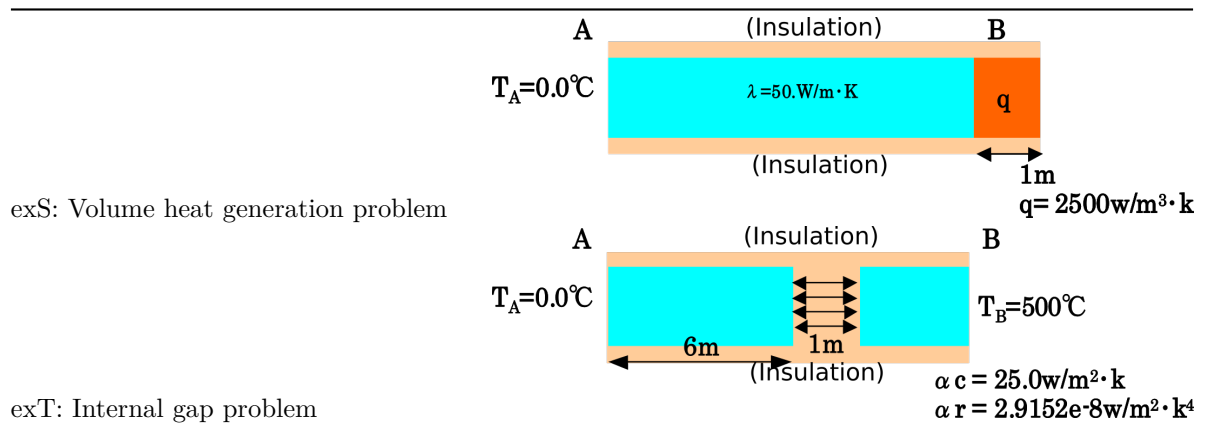


Fig. 9.1.11: Analysis conditions for each verification case

Table 9.1.13: Verification results of exM (steady-state calculation of linear material)

Case name	Element type	Number of elements/nodes	Distance from edge A (m)	Edge A	2.0	4.0	6.0	8.0	Edge B
M361A	361	40 33	0.0		100.0	200.0	300.0	400.0	500.0
M361B	361	40 105	0.0		100.0	200.0	300.0	400.0	500.0
M361C	361	20 33	0.0		100.0	200.0	300.0	400.0	500.0
M361D	361	20 85	0.0		100.0	200.0	300.0	400.0	500.0
M361E	361	240 99	0.0		100.0	200.0	300.0	400.0	500.0
M361F	361	24 525	0.0		100.0	200.0	300.0	400.0	500.0
M361G	361	80 99	0.0		100.0	200.0	300.0	400.0	500.0

Table 9.1.14: Verification results of exN (specified temperature problem)

Case name	Element type	Number of elements/nodes	Distance from edge A (m)	Edge A	2.0	4.0	6.0	8.0	Edge B
ABAQUS	361	40 99	0.0		87.3	179.7	278.2	384.3	500.0
N231	231	40 33	0.0		87.2	179.5	278.0	384.1	500.0
N232	232	40 105	0.0		86.0	178.3	276.8	382.9	500.0
N241	241	20 33	0.0		87.3	179.7	278.2	384.3	500.0
N242	242	20 85	0.0		87.3	179.7	278.2	384.3	500.0
N341	341	240 99	0.0		87.3	179.7	278.2	384.3	500.0
N342	342	24 525	0.0		87.9	179.9	278.0	383.6	500.0
N351	351	80 99	0.0		87.3	179.7	278.2	384.3	500.0
N352	352	80 381	0.0		87.3	179.7	278.2	384.3	500.0
N361	361	40 99	0.0		87.3	179.7	278.2	384.3	500.0
N362	362	40 330	0.0		87.3	179.7	278.2	384.3	500.0
N731	731	40 33	0.0		87.3	179.7	278.2	384.3	500.0
N741	741	20 33	0.0		87.3	179.7	278.2	384.3	500.0

Table 9.1.15: Verification results of exO (concentrated heat flux problem)

Case name	Element type	Number of elements/nodes	Distance from edge A (m)	Edge A	2.0	4.0	6.0	8.0	Edge B
ABAQUS	361	40 99	0.0		103.2	213.7	333.3	464.8	612.0
O231	231	40 33	0.0		103.2	213.7	333.3	464.8	612.0
O232	232	40 105	0.0		103.2	213.7	333.3	464.8	612.0
O241	241	20 33	0.0		103.2	213.7	333.3	464.8	612.0

Case name	Element type	Number of elements/nodes	Distance from edge A (m)	103.2	213.7	333.4	465.2	618.0
O242	242	20 85	0.0	-	-	-	-	-
O341	341	240 99	-	-	-	-	-	-
O342	342	24 525	0.0	104.4	214.9	334.7	466.3	614.0
O351	351	80 99	-	-	-	-	-	-
O352	352	80 381	0.0	103.2	213.7	333.3	465.0	624.0
O361	361	40 99	0.0	103.2	213.7	333.3	464.8	612.0
O362	362	40 330	0.0	103.2	213.7	333.4	465.5	623.0
O731	731	40 33	0.0	103.2	213.7	333.3	464.8	612.0
O741	741	20 33	0.0	103.2	213.7	333.3	464.8	612.0

Table 9.1.16: Verification results of exP (distribution heat flux problem)

Case name	Element type	Number of elements/nodes	Distance from edge A (m)	Edge A	2.0	4.0	6.0	8.0	Edge
ABAQUS	361	40 99	0.0	-	103.2	213.7	333.3	464.8	612.0
P231	231	40 33	0.0	-	103.2	213.7	333.3	464.8	612.0
P232	232	40 105	0.0	-	103.2	213.7	333.3	464.8	612.0
P241	241	20 33	0.0	-	103.2	213.7	333.3	464.8	612.0
P242	242	20 85	0.0	-	103.2	213.7	333.3	464.8	612.0
P341	341	240 99	-	-	-	-	-	-	-
P342	342	24 525	0.0	-	103.2	213.7	333.3	464.8	612.0
P351	351	80 99	-	-	-	-	-	-	-
P352	352	80 381	0.0	-	103.2	213.7	333.3	464.8	612.0
P361	361	40 99	0.0	-	103.2	213.7	333.3	464.8	612.0
P362	362	40 330	0.0	-	103.2	213.7	333.4	465.5	612.0
P731	731	40 33	0.0	-	103.2	213.7	333.3	464.8	612.0
P741	741	20 33	0.0	-	103.2	213.7	333.3	464.8	612.0

Table 9.1.17: Verification results of exQ (convective heat transfer problem)

Case name	Element type	Number of elements/nodes	Distance from edge A (m)	Edge A	2.0	4.0	6.0	8.0	Edge
ABAQUS	361	40 99	0.0	-	89.2	183.8	284.8	393.9	513.2
Q231	231	40 33	0.0	-	89.2	183.8	284.8	393.9	513.2
Q232	232	40 105	0.0	-	89.2	183.8	284.8	393.9	513.2
Q241	241	20 33	0.0	-	89.2	183.8	284.8	393.9	513.2
Q242	242	20 85	0.0	-	89.2	183.8	284.8	393.9	513.2
Q341	341	240 99	-	-	-	-	-	-	-
Q342	342	24 525	0.0	-	89.2	183.8	284.8	393.9	513.2
Q351	351	80 99	-	-	-	-	-	-	-
Q352	352	80 381	0.0	-	89.2	183.8	284.8	393.9	513.2
Q361	361	40 99	0.0	-	89.2	183.8	284.8	393.9	513.2
Q362	362	40 330	0.0	-	89.2	183.8	284.8	393.9	513.2
Q731	731	40 33	0.0	-	89.2	183.8	284.8	393.9	513.2
Q741	741	20 33	0.0	-	89.2	183.8	284.8	393.9	513.2

Table 9.1.18: Verification results of exR (radiation heat transfer problem)

Case name	Element type	Number of elements/nodes	Distance from edge A (m)	Edge A	2.0	4.0	6.0	8.0	Edge
ABAQUS	361	40 99	0.0	-	89.5	184.4	285.8	395.3	515.2
R231	231	40 33	0.0	-	89.5	184.4	285.8	395.3	515.2

Case name	Element type	Number of elements/nodes	Distance from edge A (m)						
R232	232	40 105	0.0		89.5	184.4	285.8	395.3	515.2
R241	241	20 33	0.0		89.5	184.4	285.8	395.3	515.2
R242	242	20 85	0.0		89.5	184.4	285.8	395.3	515.2
R341	341	240 99	-		-	-	-	-	-
R342	342	24 525	0.0		89.5	184.4	285.8	395.3	515.2
R351	351	80 99	-		-	-	-	-	-
R352	352	80 381	0.0		89.5	184.4	285.8	395.3	515.2
R361	361	40 99	0.0		89.5	184.4	285.8	395.3	515.2
R362	362	40 330	0.0		89.5	184.4	285.8	395.3	515.2
R731	731	40 33	0.0		89.5	184.4	285.8	395.3	515.2
R741	741	20 33	0.0		89.5	184.4	285.8	395.3	515.2

Table 9.1.19: Verification results of exS (volume heat generation problem)

Case name	Element type	Number of elements/nodes	Distance from edge A (m)						
			Edge A	2.0	4.0	6.0	8,0	Edge	
ABAQUS	361	40 99	0.0	103.2	213.7	333.3	464.8	612.0	
S231	231	40 33	0.0	103.2	213.7	333.3	464.8	612.0	
S232	232	40 105	0.0	103.2	213.7	333.3	464.8	612.0	
S241	241	20 33	0.0	103.2	213.7	333.3	464.8	612.0	
S242	242	20 85	0.0	103.2	213.7	333.3	464.8	612.0	
S341	341	240 99	-	-	-	-	-	-	-
S342	342	24 525	0.0	103.2	213.7	333.3	464.8	612.0	
S351	351	80 99	-	-	-	-	-	-	-
S352	352	80 381	0.0	103.2	213.7	333.3	464.8	612.0	
S361	361	40 99	0.0	103.2	213.7	333.3	464.8	612.0	
S362	362	40 330	0.0	103.2	213.7	333.3	464.8	612.0	
S731	731	40 33	0.0	103.2	213.7	333.3	464.8	612.0	
S741	741	20 33	0.0	103.2	213.7	333.3	464.8	612.0	

Table 9.1.20: Verification results of exT (internal gap problem)

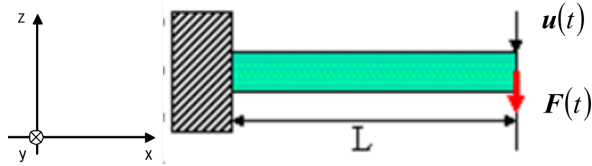
Case name	Element type	Number of elements/nodes	Distance from edge A (m)						
			Edge A	2.0	4.0	6.0	8,0	Edge	
ABAQUS	361	40 99	0.0	88.6	182.4	282.6	387.7	500.0	
S231	231	40 33	0.0	88.6	182.4	282.6	387.7	500.0	
S232	232	40 105	0.0	88.6	182.4	282.6	387.7	500.0	
S241	241	20 33	0.0	88.6	182.4	282.6	387.7	500.0	
S242	242	20 85	0.0	88.6	182.4	282.6	387.7	500.0	
S341	341	240 99	-	-	-	-	-	-	-
S342	342	24 525	0.0	88.6	182.4	282.6	387.7	500.0	
S351	351	80 99	-	-	-	-	-	-	-
S352	352	80 381	0.0	88.6	182.4	282.6	387.7	500.0	
S361	361	40 99	0.0	88.6	182.4	282.6	387.7	500.0	
S362	362	40 330	0.0	88.6	182.4	282.6	387.7	500.0	
S731	731	40 33	0.0	88.6	182.4	282.6	387.7	500.0	
S741	741	20 33	0.0	88.6	182.4	282.6	387.7	500.0	

### 1.21.7 (5) Linear dynamic analysis

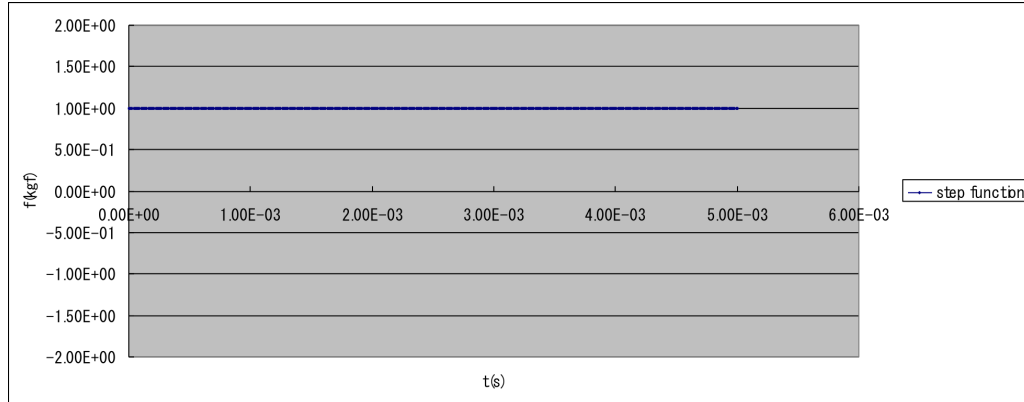
In exW, a linear dynamic analysis was performed on the same mesh-divided cantilever that was discussed earlier in the Elastic static analysis subsection, with the verification conditions shown in Fig. 9.1.12. The objective was to verify the impact of time increment on the results with the same mesh division. Both the implicit and explicit

methods of dynamic analysis and the element types 361 and 342 were used. The verification results are presented in Table 9.1.22 and shown in Figs. 9.1.13–9.1.15.

#### Analysis Model



#### Analysis Model



Time history of external force  $F$

The theoretical solution for vibration point displacement is as follows:

$$F(t) = F_0 I(t)$$

where

$$F_0 : \text{Constant vector}$$

$$I(t) = \begin{cases} 0, & t < 0 \\ 1, & 0 \leq t \end{cases}$$

$$u(t) = \frac{F_0 l^3}{EI} \sum_{i=1}^{\infty} i = 1 \frac{1 - \cos \omega_i t}{\lambda_i^4} \left\{ \cosh \lambda_i - \cos \lambda_i - \frac{\cosh \lambda_i + \cos \lambda_i}{\sin \lambda_i + \sinh \lambda_i} (\sinh \lambda_i - \sin \lambda_i) \right\}^2$$

Fig. 9.1.12: Verification conditions of linear dynamic analysis

Verification conditions:

Length	$L$	10.0 mm
Cross-sectional width	$a$	1.0 mm
Cross-sectional height	$b$	1.0 mm
Young's modulus	$E$	4000.0 kgf/mm <sup>2</sup>
Poisson's ratio	$\nu$	0.3
Density	$\rho$	1.0E-09 kgf s <sup>2</sup> /mm <sup>3</sup>
Gravitational acceleration	$g$	9800.0 mm/s <sup>2</sup>
External force	$F_0$	1.0 kgf

Element	Hexahedral linear element
Tetrahedral secondary element	

Solution	Implicit method
Parameter $\gamma$ of Newmark- $\beta$ method	1/2
Parameter $\beta$ of Newmark- $\beta$ method	1/4
Explicit method	
Damping	N/A

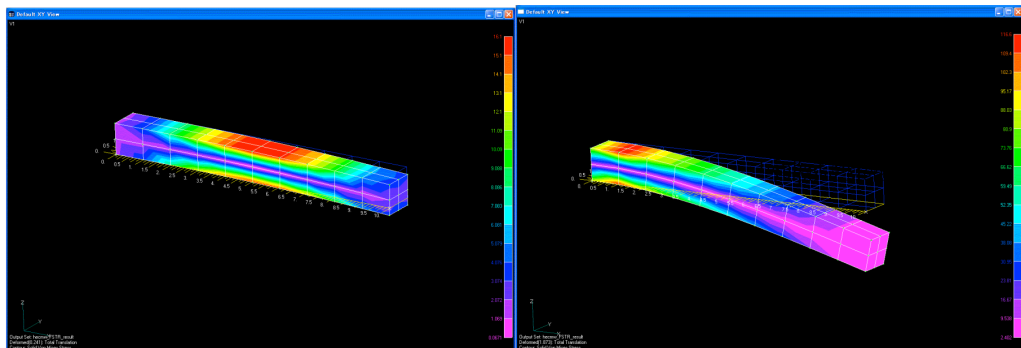
Table 9.1.21: Verification conditions of the linear dynamic analysis (continuation)

Case Name	Element Type	No. of Nodes	No. of Elements	Solution	Time Increment $\Delta t$ [sec]
W361_c0_in36in2_t1		99	40	Implicit method	1.0E-06
W361_c0_in36in2_t2		99	40	Implicit method	1.0E-05
W361_c0_in36in2_t3		99	40	Implicit method	1.0E-04
W361_c0_ex36in2_t1		99	40	Explicit method	1.0E-08
W361_c0_ex36in2_t2		99	40	Explicit method	1.0E-07
W361_c0_ex36in2_t3		99	40	Explicit method	1.0E-06
W342_c0_in34in2_t1		525	240	Implicit method	1.0E-06
W342_c0_in34in2_t2		525	240	Implicit method	1.0E-05
W342_c0_in34in2_t3		525	240	Implicit method	1.0E-04
W342_c0_ex34in2_t1		525	240	Explicit method	1.0E-08
W342_c0_ex34in2_t2		525	240	Explicit method	5.0E-08
W342_c0_ex34in2_t3		525	240	Explicit method	1.0E-07

Table 9.1.22: Verification results of linear dynamic analysis of exW (cantilever)

Case name	Element type	Number of nodes	Number of elements	Solu-tion	z-direction displacement: $u_z$ (mm) when time $t = 0.002(s)$	Fron-tISTR
W361_c036in_m2_t199		40		Theoretical solution repeated to sextic equation		
W361_c036in_m2_t299		40		Im-plicit method	1.9753	1.9302
W361_c036in_m2_t399		40		Im-plicit method	1.9753	1.8686
W361_c036k_m2_t199		40		Im-plicit method	1.9753	0.3794
W361_c036k_m2_t299		40		Ex-plicit method	1.9753	1.9302
W361_c036k_m2_t399		40		Ex-plicit method	1.9753	1.9247

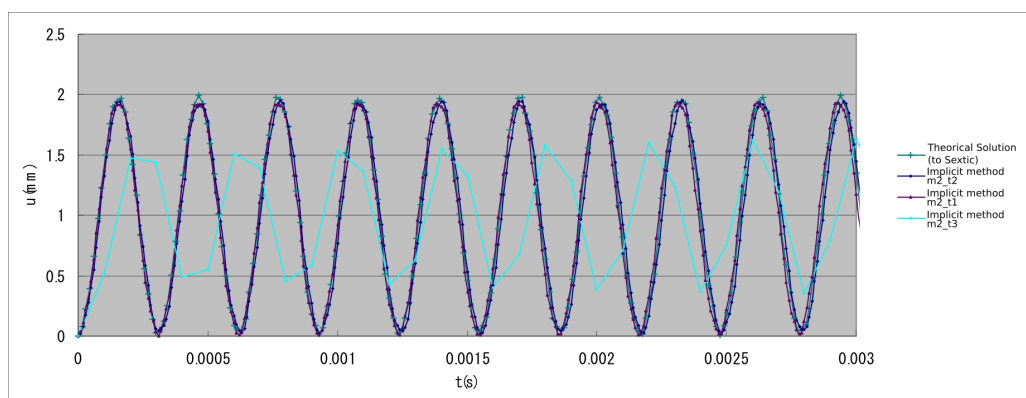
Case name	Element type	Number of nodes	Number of elements	Solu-tion	z-direction displacement: $u_z(mm)$ when time $t = 0.002(s)$	
W361_c036k_m2_t399			40	Ex-plicit method	1.9753	Diver-gence
W342_c034h_m2_t525			240	Im-plicit method	1.9753	1.9431
W342_c034h_m2_t2525			240	Im-plicit method	1.9753	1.8719
W342_c034h_m2_t325			240	Im-plicit method	1.9753	0.3873
W342_c034k_m2_t1525			240	Ex-plicit method	1.9753	1.9359
W342_c034k_m2_t2525			240	Ex-plicit method	1.9753	1.9358
W342_c034k_m2_t3525			240	Ex-plicit method	1.9753	Diver-gence



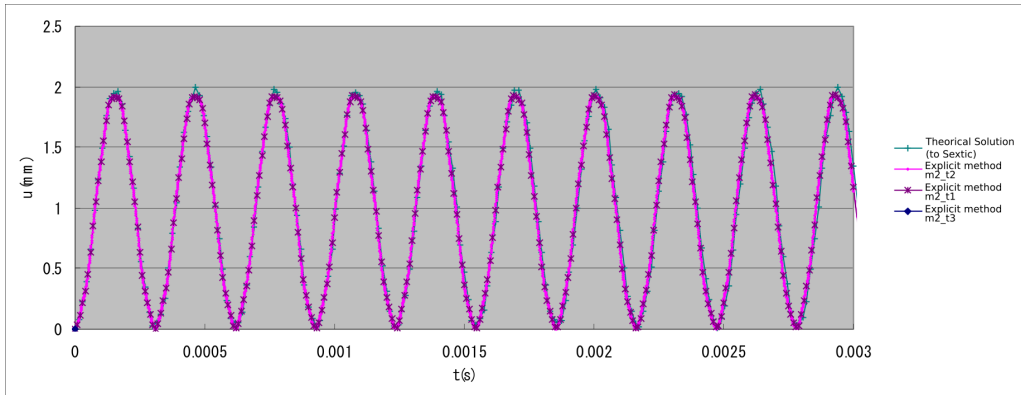
(a)  $t=2.0E-03(s)$

(b)  $t=4.0E-03(s)$

Fig. 9.1.13: Deformation diagram and equivalent stress distribution of the cantilever (W361\_c0\_im\_m2\_t2)

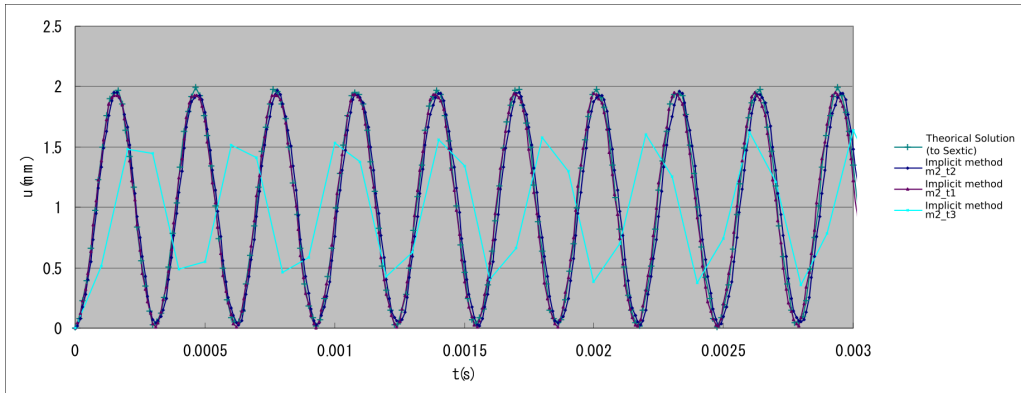


(a) Element Type 361 : Implicit method

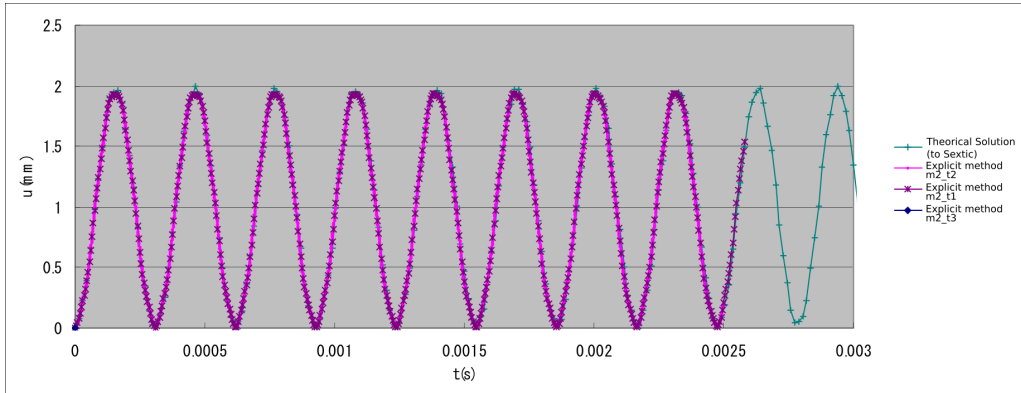


(b) Element Type 361 : Explicit method

Fig. 9.1.14: Time history of vibration point displacement  $u_z$



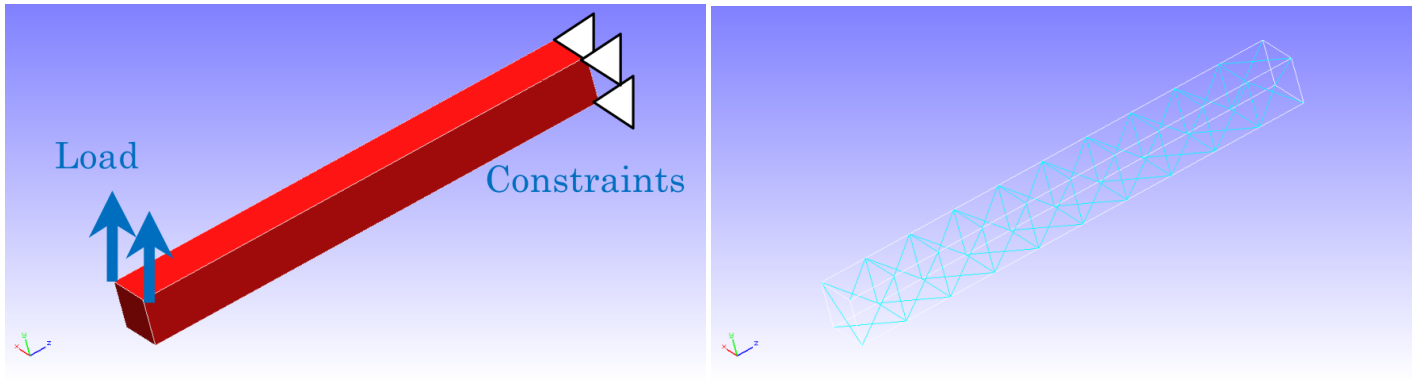
(a) Element Type 342 : Implicit method



(b) Element Type 342 : Explicit method

### 1.21.8 (6) Frequency response analysis

In this verification, a frequency response analysis was performed on a cantilever, and the results were compared with those obtained using the ABAQUS software. The analysis model and verification conditions are presented below:



Analysis conditions:

Young's modulus	$E$	$210000 \text{ N/mm}^2$
Poisson's ratio	$\nu$	0.3
Density	$\rho$	$7.89E - 09 \text{ t/mm}^3$
Gravitational acceleration	$g$	$9800.0 \text{ mm/s}^2$
Load	$F_0$	1.0 N
Parameter of Rayleigh damping	$R_m$	0.0
Parameter of Rayleigh damping	$R_k$	$7.2E - 07$

Fig. 9.1.15 : Analysis model (tetrahedral primary element (126 elements and 55 nodes))

The eigenvalues up to the fifth order and the frequency response of the vibration points obtained from eigenvalue analysis are as follows:

mode	FrontISTR	ABAQUS
1	14952	14952
2	15002	15003
3	84604	84539
4	84771	84697
5	127054	126852

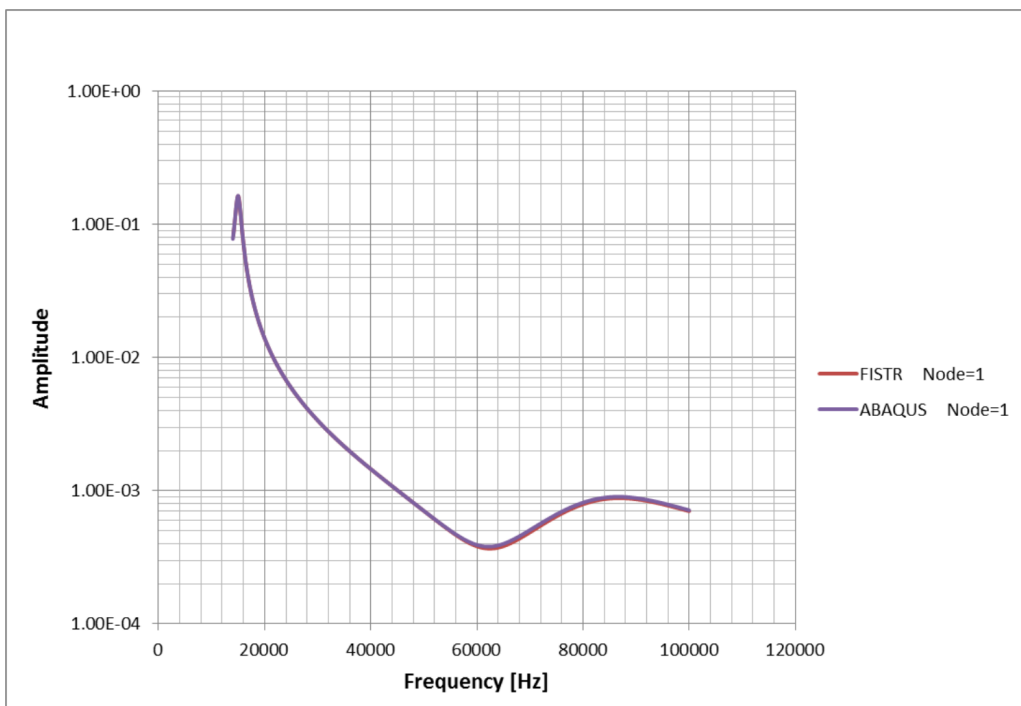


Fig. 9.1.16 : Frequency dependence of displacement strength of vibration points

## 1.22 Actual Model Examples for Elastic Static Analysis

### 1.22.1 Analysis Model

A list of actual model verification examples for elastic static analysis are presented in Table 9.2.1. The different shapes of the models are shown in Figs. 9.2.1–9.2.5 (some models are excluded). The examples of the element types 731 and 741 require a separate direct method solver.

Table 9.2.1: Actual model verification examples for elastic static analysis

Case name	Element type	Verification model	Number of nodes	Freedom frequency
EX01A	342	Connecting rod (100,000 nodes)	94,074	282,222
EX01B	342	Connecting rod (330,000 nodes)	331,142	993,426
EX02	361	Block with hole	37,386	112,158
EX03	342	Turbine blade	10,095	30,285
EX04	741	Cylindrical shell	10,100	60,600
EX05A	731	Wine glass (coarse)	7,240	43,440
EX05B	731	Wine glass (midium)	48,803	292,818
EX05C	731	Wine glass (fine)	100,602	603,612

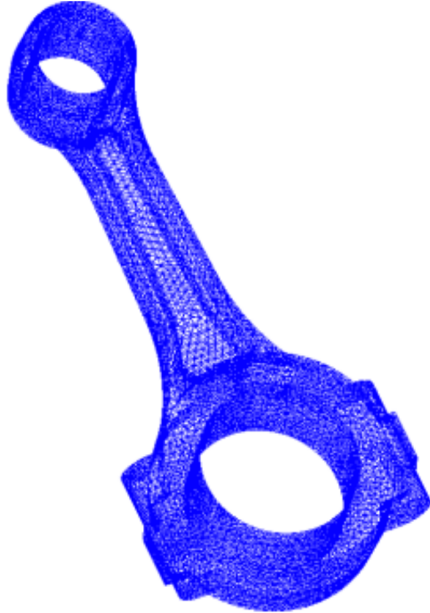


Fig. 9.2.1: Connecting Rod (EX01A)

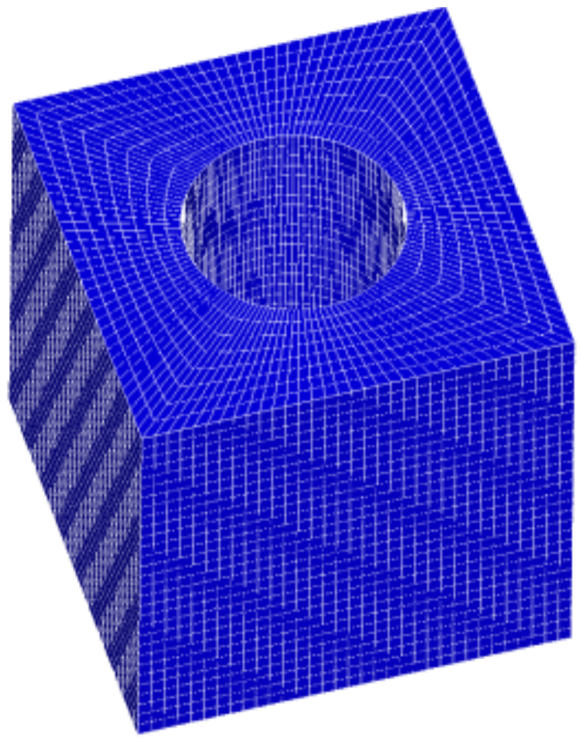


Fig. 9.2.2: Perforated block (EX02)

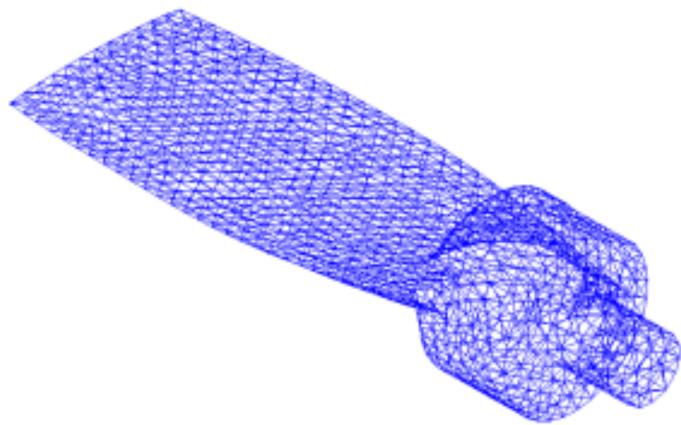


Fig. 9.2.3: Turbine blade (EX03, EX06)

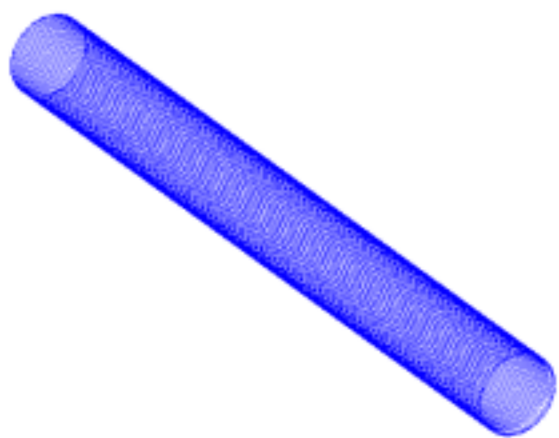


Fig. 9.2.4: Cylindrical shell (EX04, EX09)

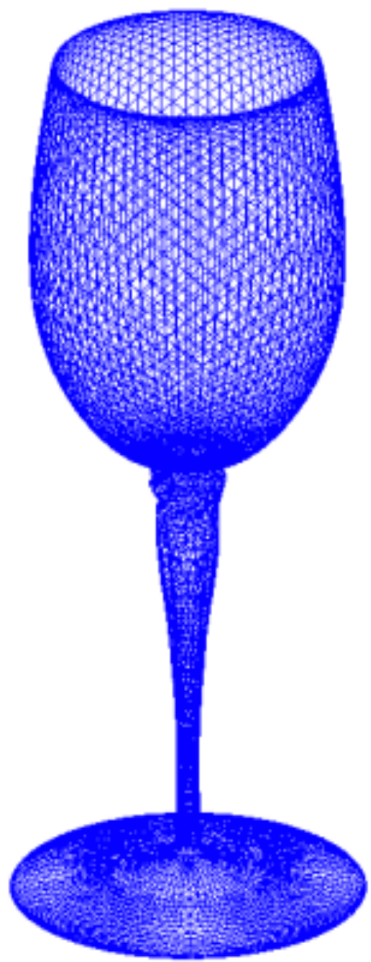


Fig. 9.2.5: Wine Glass (EX05, EX10A)

### 1.22.2 Analysis results

#### 1.22.2.1 Example of analysis results

Examples of the analysis results are shown in Figs. 9.2.6–9.2.9.

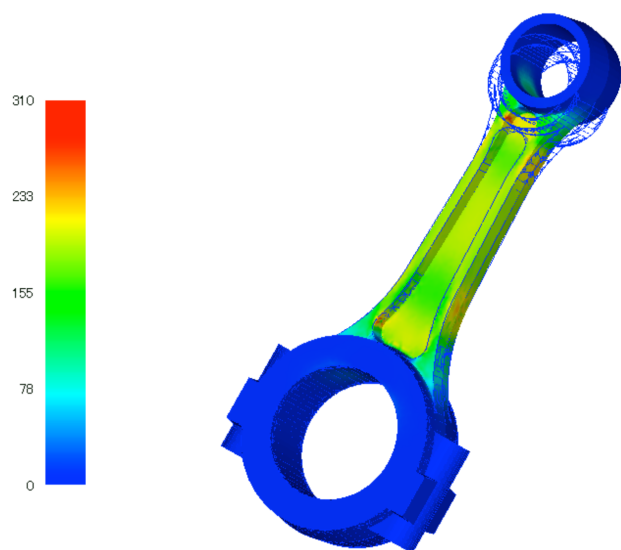


Fig. 9.2.6: EX01 analysis results (Mises stress and deformation diagram (10 times))

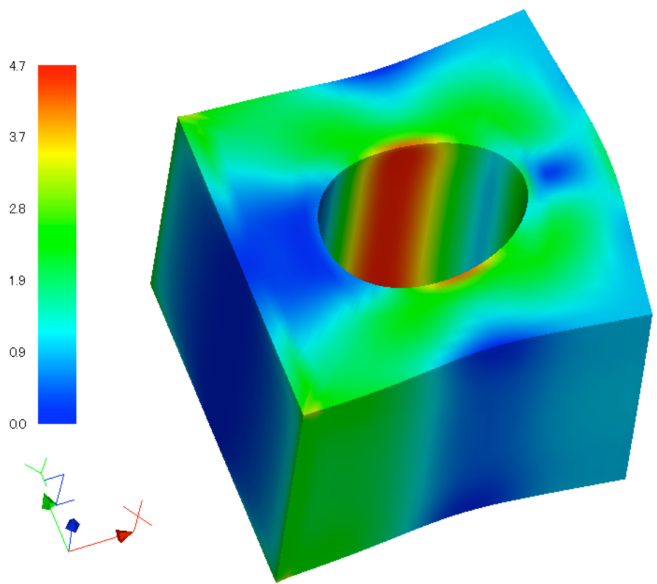


Fig. 9.2.7: EX02 analysis results (Mises stress and deformation diagram (100 times))

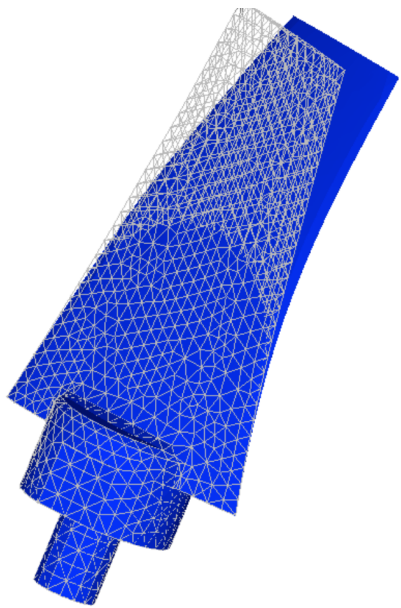
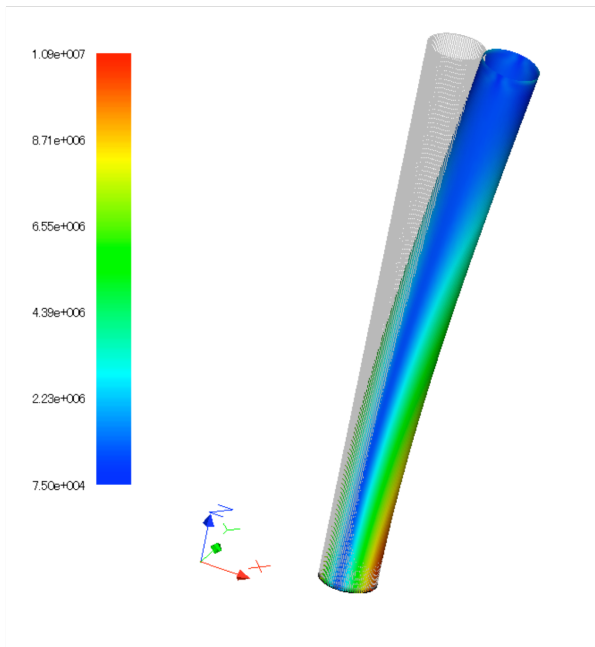


Fig. 9.2.8: EX03 analysis results (deformation diagram (10 times))



9.2.9: EX04 Analysis Results (Deformed Figure (100 times))

Fig. 9.2.9: EX04 analysis results (deformation diagram (100 times))

### 1.22.2.2 Verification Results of Analysis Performance with Example EX02

An analysis was performed with the commercial software ABAQUS using a model equivalent to the verification example model EX02 (perforated block). A comparison of the maximum and minimum values of the stress components with the results of FrontISTR is shown in Fig. 9.2.10. It can be seen that the stress components are very close to each other.

The effect of area division on stress distribution was also analyzed. The division was performed according to the RCB method, i.e., the model was halved in each of the X, Y, and Z axial directions, creating eight areas in total. Fig. 9.2.11 shows the division, while Fig. 9.2.12 shows the stress distribution of the analysis results with a single area and with the area divided into eight areas.

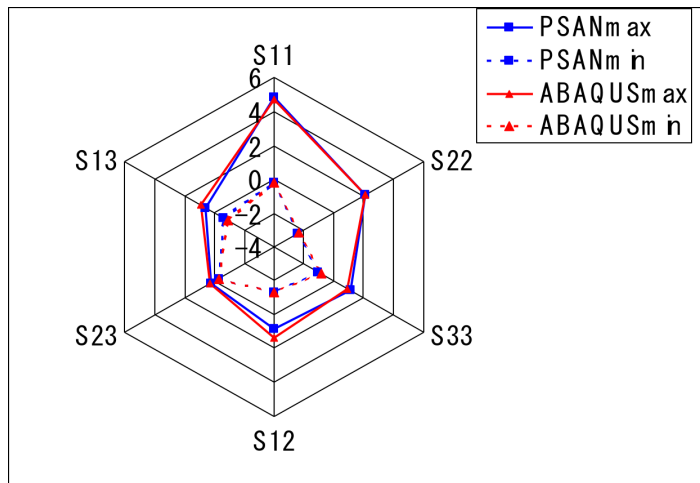


Fig. 9.2.10: Comparison of the stress components of EX02 with the commercial software

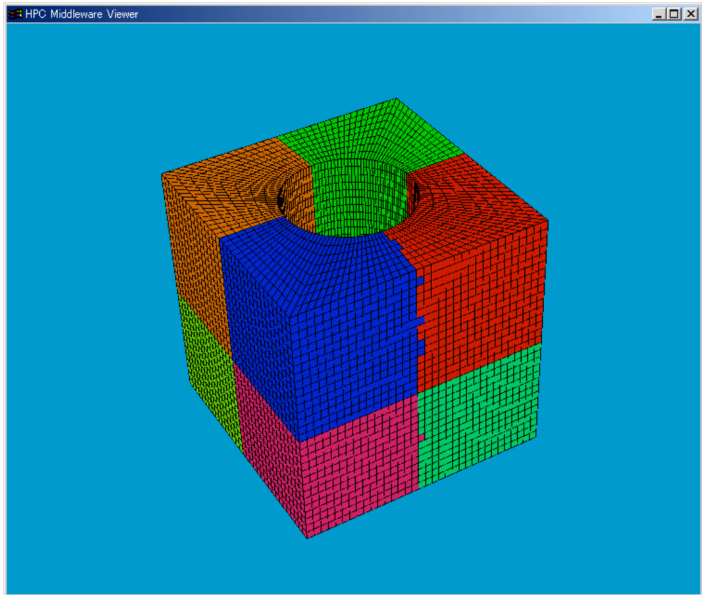


Fig. 9.2.11: Result of the division of EX02 in eight areas by the RCB method

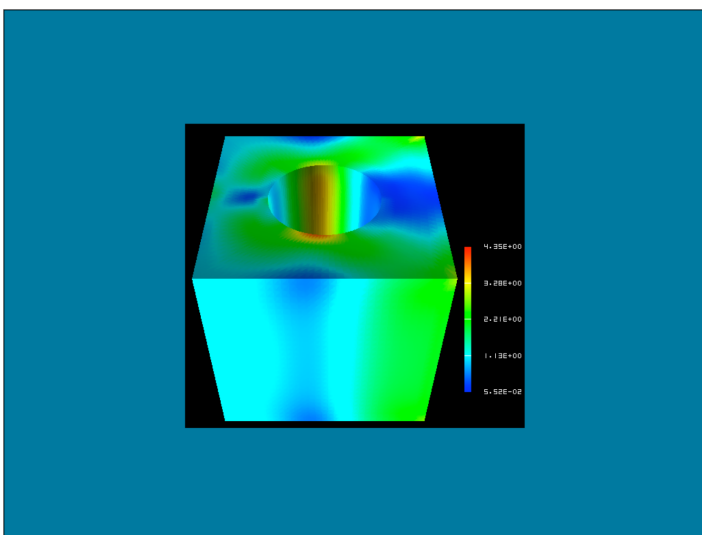


Fig. 9.2.12: No difference between the stress distribution of the analysis results with a single area and with the area divided into eight areas

Furthermore, a comparison of the execution time with the settings of the HEC-MW solver used is presented in Table 9.2.2. Fig. 9.2.13 shows the convergence history until the solution was found.

Table 9.2.2: Comparison of execution time with HEC-MW solvers

Solver	Execution Time(s)
CGI	38.79
CGscale	52.75
BCGS	60.79
CG8	6.65

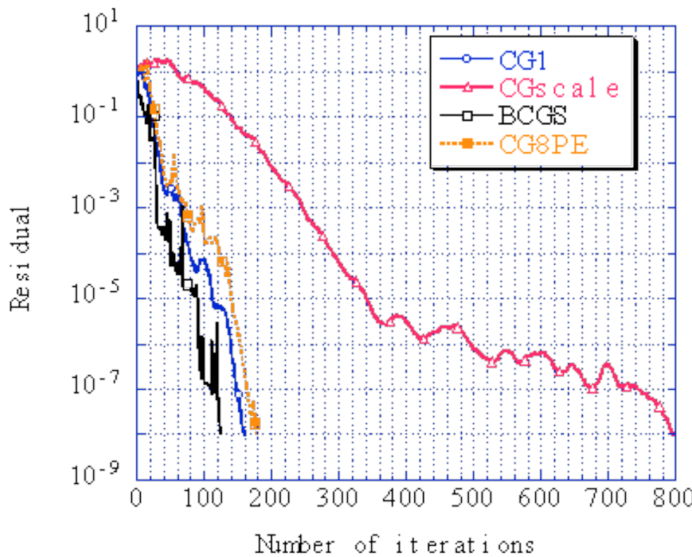


Fig. 9.2.13: Comparison of convergence history with the HEC-MW solver (convergence threshold:  $1.0 \times 10^{-8}$  )

### 1.22.2.3 Comparison of calculation time with verification example EX01A

The increase rate of the calculation speed because of area division was verified with the example EX01A (connecting rod.) The test was conducted with a Xeon 2.8 GHz 24 node cluster computer, and the results are shown in Fig. 9.2.14. This figure shows that the calculation speed increases proportionally to the number of areas.

The difference in the calculation time because of the computer environment was also analyzed. The results are presented in Table 9.2.3.

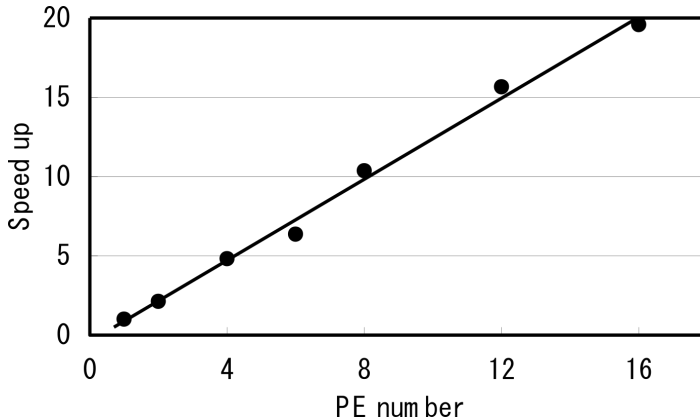


Fig. 9.2.14: Speed-increasing effect because of area division

Table 9.2.3: Comparison of calculation time with different computers (one CPU)

CPU	Frequency [GHz]	OS	CPU Time [sec]	solver time [sec]
Xeon	2.8	Linux	850	817
Pentium III	0.866	Win2000	2008	1980
Pentium M	0.760	WinXP	1096	1070
Pentium 4	2.0	WinXP	802	785
Pentium 4	2.8	WinXP	738	718
Celeron	0.700	Win2000	2252	2215
Pentium 4	2.4	WinXP	830	804

## 1.23 Actual Model Examples for Eigenvalue Analysis

### 1.23.1 Analysis model

A list of examples of the actual verification models for eigenvalue analysis is presented in Table 9.3.1. The model shapes of EX07 (turbine rotor) and EX08 (spring) are also shown in Figs. 9.3.1 and 9.3.2. The other model shapes are the same as those of the examples previously discussed in the elastic static analysis, which has the same verification content. The examples of the element types 731 and 741 require a separate direct method solver.

Table 9.3.1: Examples of actual model verification for eigenvalue analysis

Case Name	Element Type	Verification Model	No. of Nodes	No. of Degrees of Freedom
EX06	342	Turbine blade	10,095	30,285
EX07	361	Turbine rotor	127,440	382,320
EX08	342	Spring	78,771	236,313
EX09	741	Cylindrical shell	10,100	60,600
EX10A	731	Wine glass (coarse)	7,240	43,440
EX10B	731	Wine glass (medium)	48,803	292,818

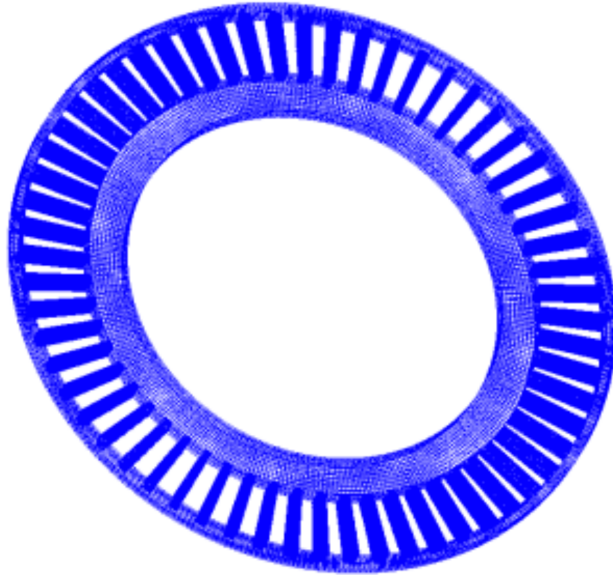


Fig. 9.3.1: Turbine rotor (EX07)

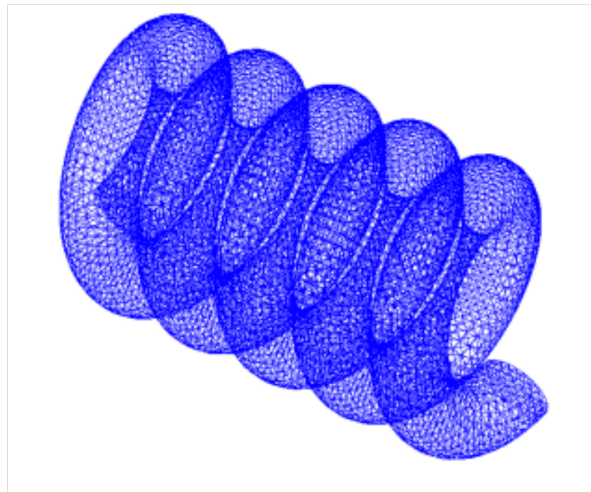


Figure 9.3.2: Spring (EX08)

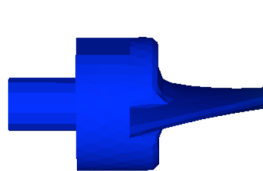
Fig. 9.3.2: Spring (EX08)

### 1.23.2 Analysis Results

The vibration mode and natural frequency are shown in the following.

#### 1.23.2.1 (1) EX06 Turbine blade

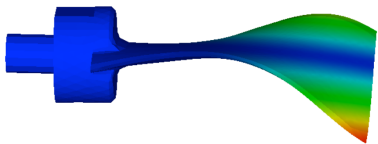
---



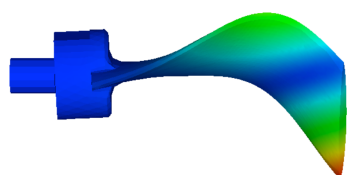
(a) Mode 1 (1170 kHz)



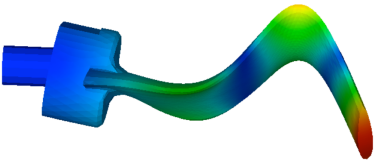
(b) Mode 2(3250kHz)



(c) Mode 3(4130kHz)



(d) Mode 4(4140kHz)



(e) Mode 5(8210kHz)

---

Fig. 9.3.3: EX06, turbine blade vibration mode

### 1.23.2.2 (2) EX07 Turbine rotor

---

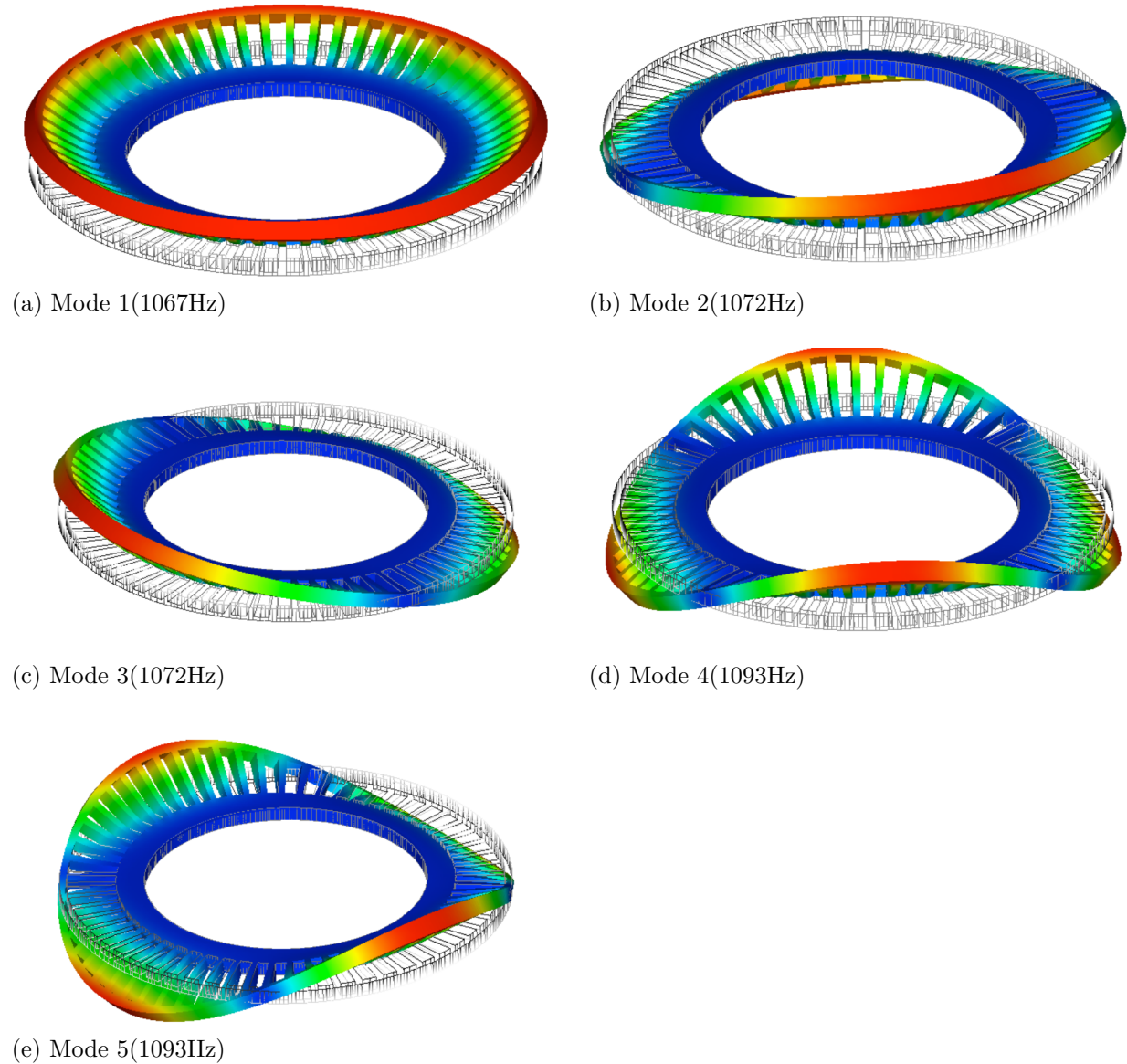
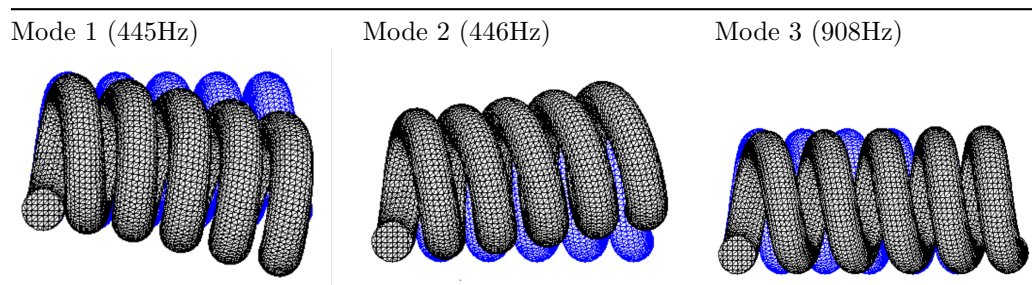


Fig. 9.3.4: EX07, Turbine rotor vibration mode

### 1.23.2.3 EX08 Spring



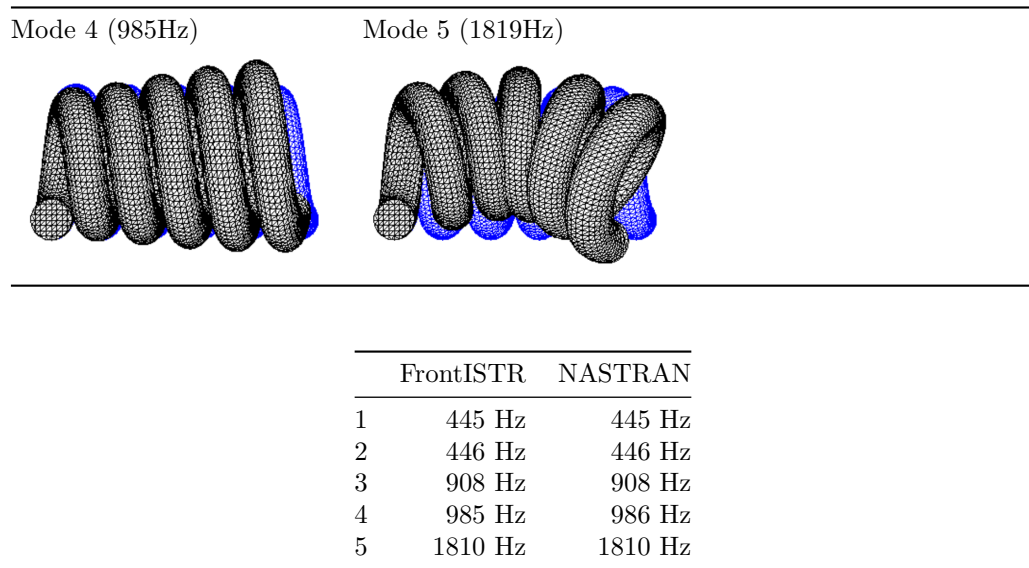


Fig. 9.3.5: EX08, spring vibration mode

#### 1.23.2.4 (4) EX09 Cylindrical shell

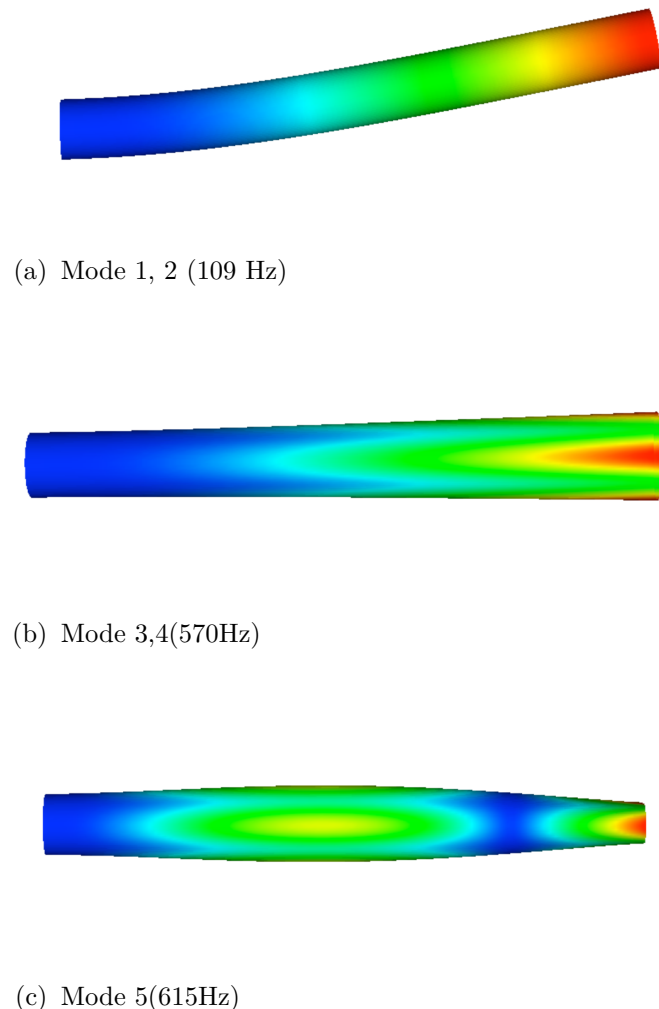


Fig. 9.3.6: EX09, cylindrical shell vibration mode

### 1.23.2.5 EX10A Wine glass

---

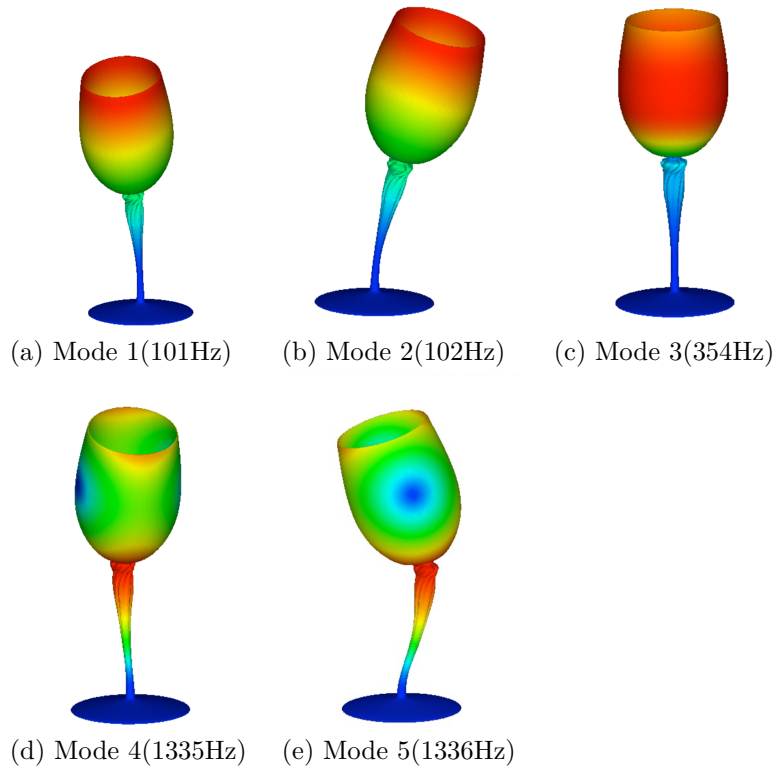


Fig. 9.3.7: EX10A Wine Glass Vibration Mode

## 1.24 Actual Model Examples for Heat Conduction Analysis

### 1.24.1 Analysis model

The heat conduction analysis was performed with a used nuclear fuel transport container as an actual model. For this analysis, three verification examples were set, each with a model of different mesh roughness, as presented in Table 9.4.1. The shapes of the models are shown in Figs. 9.4.1–9.4.4.

Table 9.4.1: Examples of actual verification models for heat conduction analysis

Case name	Element type	Verification model	Number of nodes	Freedom frequency
EX21A	361	Used unclear fuel transport container	88,938	79,920
EX21B	361		309,941	289,800
EX21C	361		1,205,765	1,159,200

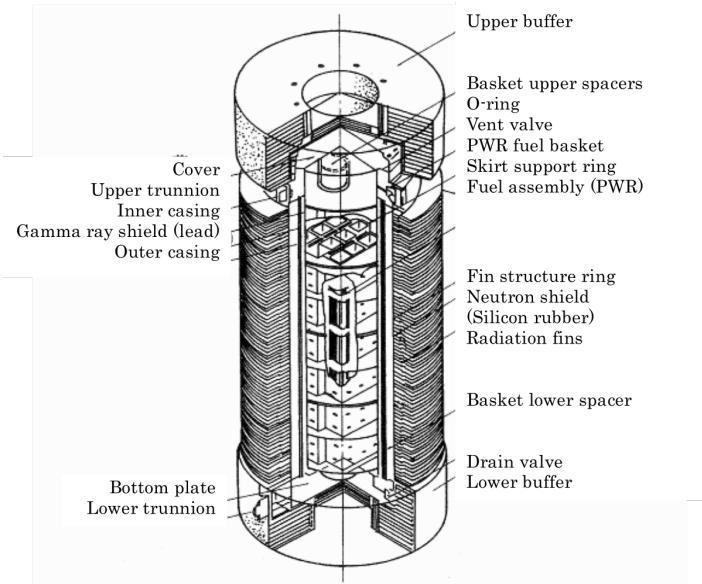


Fig. 9.4.1: Used nuclear fuel transport container

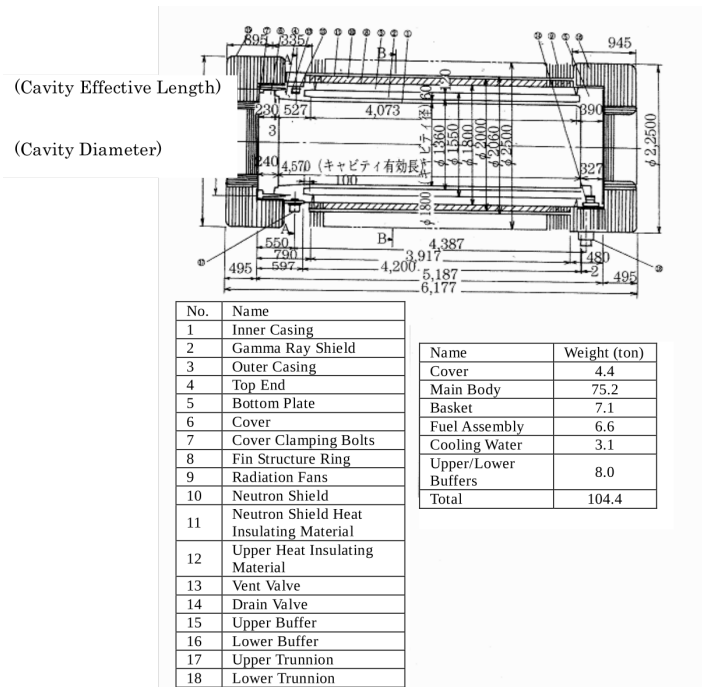


Fig. 9.4.2: Dimensions of the used nuclear fuel transport container

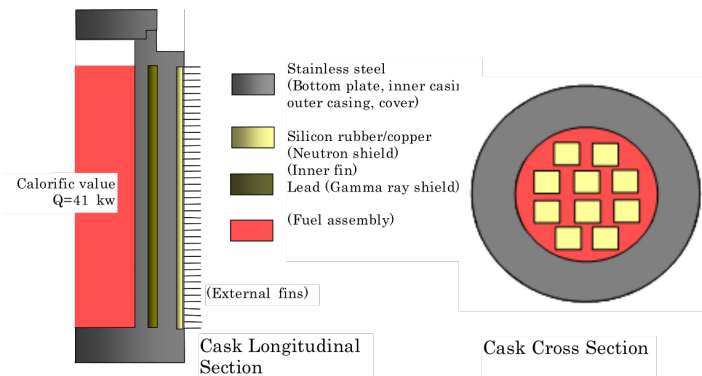


Fig. 9.4.3: Model's schematic diagram

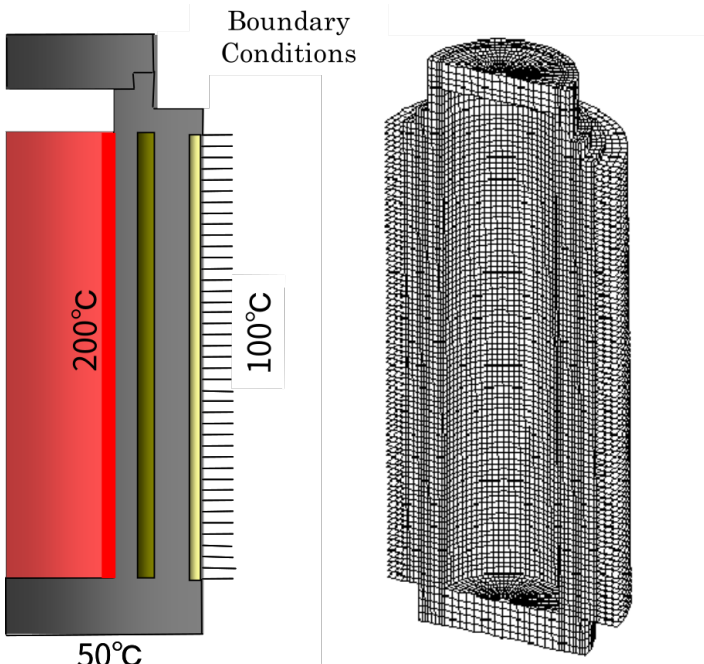


Fig. 9.4.4: Model's boundary conditions and mesh division diagram (EX21A)

#### 1.24.2 Analysis Results

Examples of analysis results are shown in Figs. 9.4.5–9.4.7.

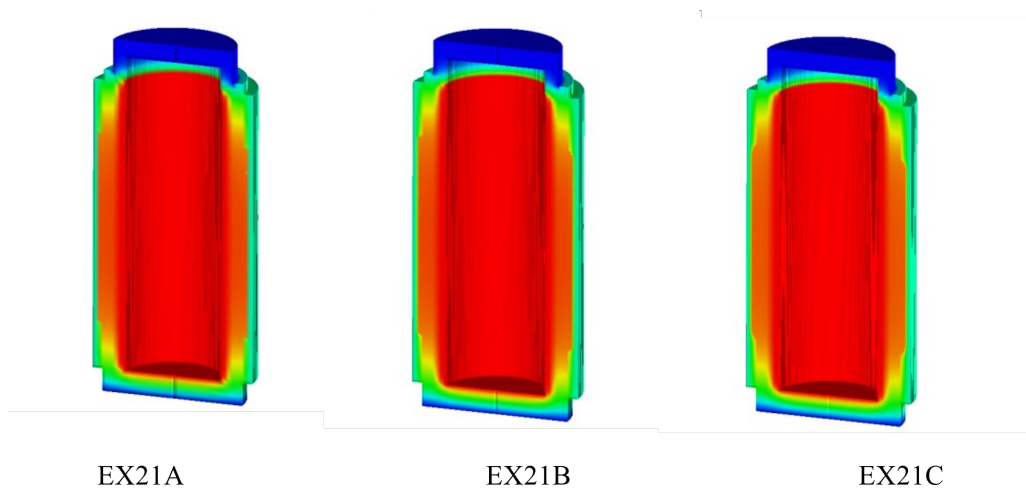


Fig. 9.4.5: Temperature distribution diagram

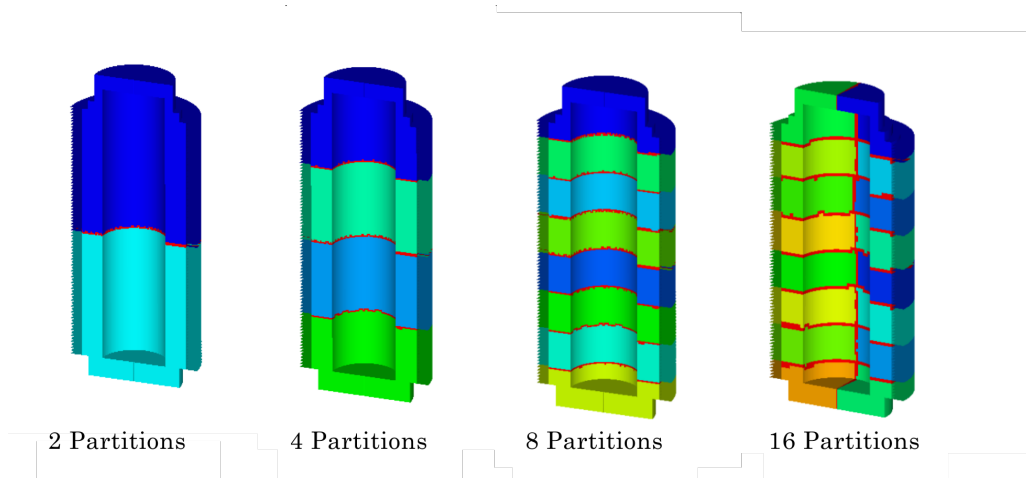


Fig. 9.4.6: Distributed model diagram

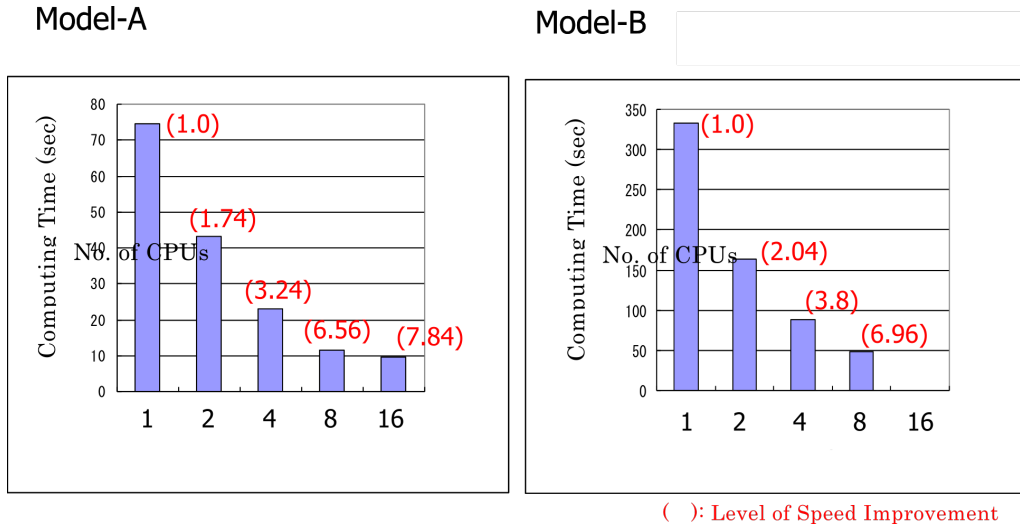


Fig. 9.4.7: Speed improvement degree because of dispersion treatment

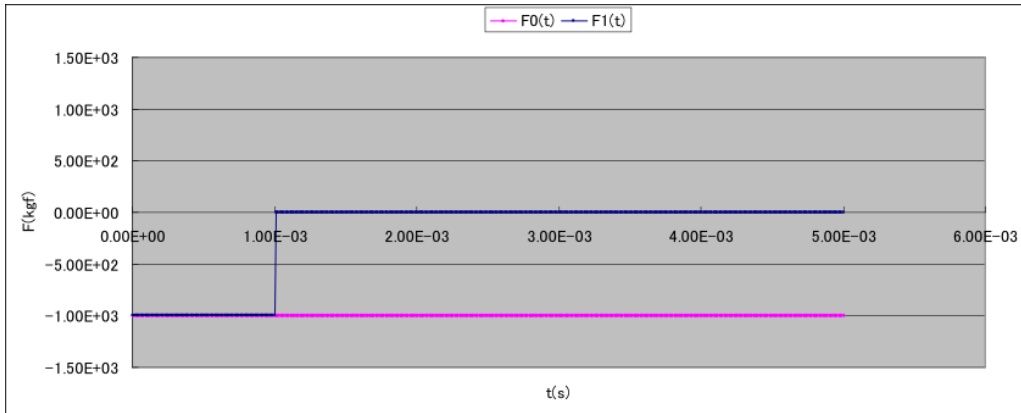
## 1.25 Actual Model Examples for Linear Dynamic Analysis

### 1.25.1 Analysis model

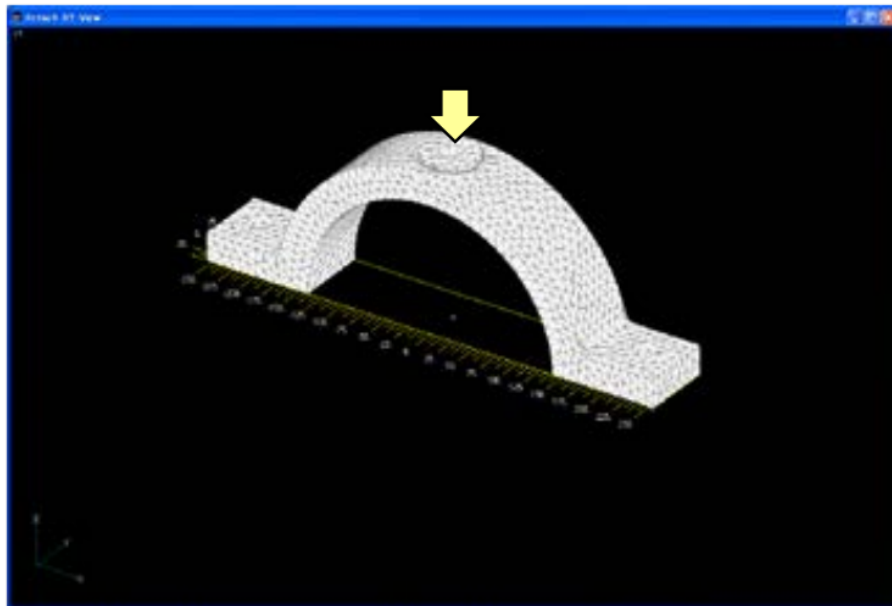
The linear dynamic analysis was performed with the machine parts shown in Fig. 9.5.1 as the actual models. For the analysis model, four cases were considered as verification examples with different load conditions and damping coefficients, as presented in Table 9.5.1.

Table 9.5.1: Verification Example of Actual Model for Linear Dynamic Analysis

Case Name	Element Type	Verification Model	Loading Conditions	Damping Conditions	No. of Nodes	No. of Degrees of Freedom
EX31A	342	Mesh model	Step load (F0)	No	15,214	45,642
EX31B	342		Step load (F0)	Yes	15,214	45,642
EX31C	342		Square wave pulse (F1)	No	15,214	45,642
EX31D	342		Square wave pulse (F1)	Yes	15,214	45,642



Loading Conditions

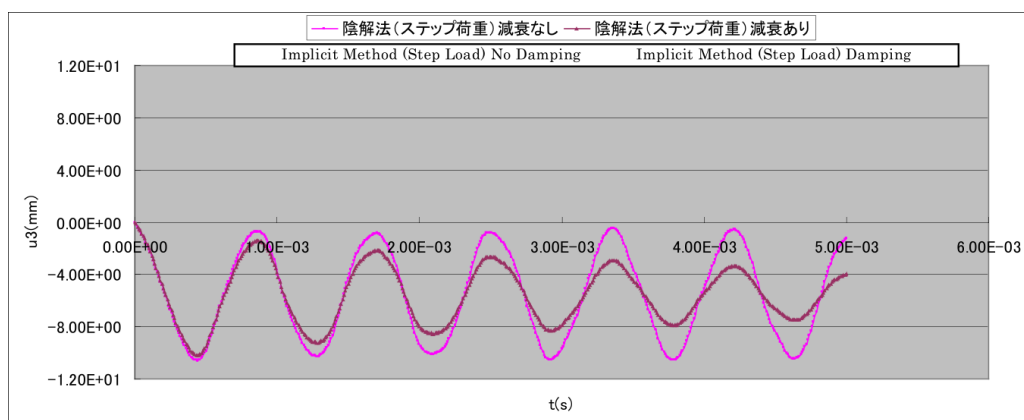


Mesh Figure

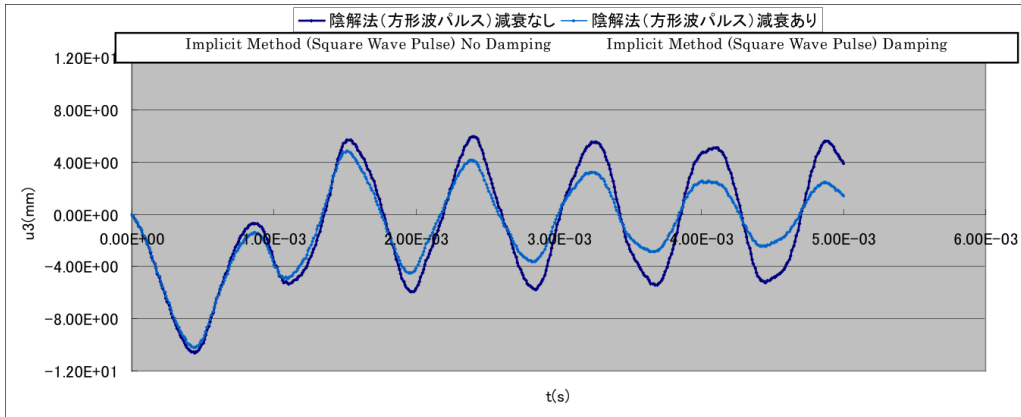
Fig. 9.5.1 : Mesh Model

### 1.25.2 Analysis results

Examples of the analysis results are shown in Fig. 9.5.2 ~ Fig. 9.5.3.

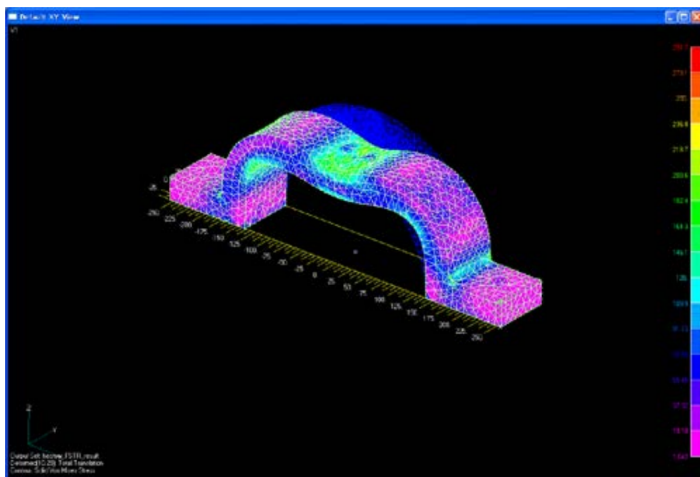


(a) In the case of Step Load

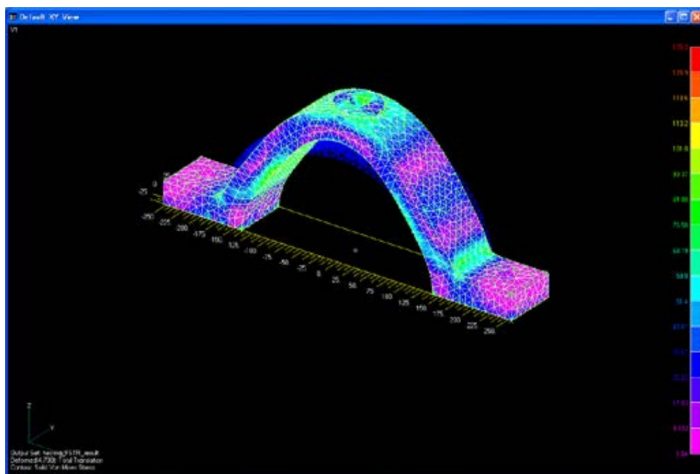


(b) In the case of Square Wave Pulse Load

Fig. 9.5.2: Time history of vibration point displacement  $u_z$



(a)  $t=5.0\text{E-}04(\text{s})$



(b)  $t=4.0\text{E-}03(\text{s})$

Fig. 9.5.3: Deformation diagram and equivalent stress distribution (deformation ratio of 5.0), EX31C